

**Deep-sea sediment core and coral
reconstructions of the Late Quaternary
paleoceanography of the eastern Indian Ocean**

Anne Müller

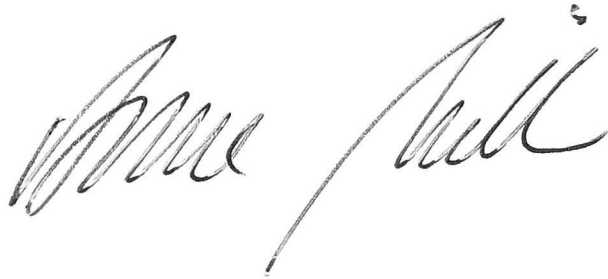
November 2002

A thesis submitted for the degree of Doctor of Philosophy of

The Australian National University

The data, interpretations and conclusions presented
in this thesis are my own unless stated otherwise.

Canberra, November 2002

A handwritten signature in cursive script, appearing to read "Anne Hill". The signature is written in dark ink on a white background.

Acknowledgments

Bradley N. Opdyke and Michael K. Gagan supervised the work presented in this thesis. Bradley N. Opdyke gave access to sediment cores and provided financial support for geochemical analyses. Michael K. Gagan gave access to coral cores and geochemical analyses and gave assistance during mass spectrometry. I am also grateful for scientific advice and discussions, which led to the publication of articles in *Paleoceanography* (Müller & Opdyke, Vol. 15. No. 1, Pages 85-94, February 2000) and *Geophysical Research Letters* (Müller, Gagan & McCulloch, Vol. 28. No. 23, Pages 4471-4474, December 2001) and to the submission of a third article to *Global Biogeochemical Cycles* (Müller, Gagan & Lough, revised and re-submitted in June 2003). Furthermore, the results of this thesis as published in these articles were presented at a number of conferences in co-authorship with Bradley N. Opdyke, Michael K. Gagan, Malcolm McCulloch and Janice M. Lough. These contributions as well as the complete references of the articles mentioned above are listed in the appendix of this thesis.

I am grateful to Janice Lough for discussions on coral ecology and climatology and for making density measurements possible. Also, David Barnes gave scientific input. Barry Tobin gave assistance during density measurements. Gary Meyers and Stuart Godfrey provided scientific advice on oceanography. Alan Pearce and Nick D'Adamo helped with regional knowledge on Ningaloo

Reef ecology and oceanography. Rob Allen gave information on climatological topics. Gail Craswell gave assistance in academic writing.

Patrick DeDeckker gave access to his micropaleontological laboratory, and Judith Shelley gave technical advise. Discussions with Ignacio Martinez on micropaleontological topics improved the quality of the work presented here. Malcolm McCulloch gave access to thermal ionization mass spectrometry. I am also very grateful for technical assistance during geochemical analyses from Joe Cali, Heather Scott-Gagan, Joan Cowley, Graham Mortimer and John Vickers. Ullrich Senff carried out XRF analyses.

Furthermore, I would like to thank all staff and students of the Department of Geology and the Research School of Earth Sciences at the Australian National University and at the Australian Institute of Marine Science who have contributed to the success of the work presented here.

This work was funded by a scholarship from the Australian National University and by an Overseas Postgraduate Research Scholarship.

Contents

	page
Abstract	8
1. Introduction – Paleoceanographic and paleoclimate reconstructions in the eastern Indian Ocean	11
2. Glacial-interglacial changes in paleoproductivity and nutrient utilization in the Indonesian Throughflow sensitive Timor Trough – paleoclimatic implications for the region of the easternmost Indian Ocean	
2.1. Introduction	19
2.2. Procedures	25
2.3. Results	29
2.4. Discussion	
2.4.1. Glacial-interglacial changes in paleoproductivity	34
2.4.1.1. Organic carbon, TOC/N ratios, and possible diagenetic imprints	34
2.4.1.2. Barium	37
2.4.1.3. Calcium carbonate	38
2.4.2. Glacial-interglacial changes in CO ₂ (aq) in surface waters	39
2.4.3. Changes in nutrient utilization in the surface waters	40
2.4.4. Fluctuations and lags in proxy records	46

2.5.	Conclusions	48
3.	Validity of paleoceanographic reconstructions from massive corals – Implications for sea surface temperature reconstructions for the Last Glacial Maximum and the Holocene	
3.1.	Introduction	51
3.2.	Procedures	53
3.3.	Results	56
3.4.	Discussion and conclusions	63
4.	Coral reconstructions of 20 th century changes in surface-ocean $^{13}\text{C} / ^{12}\text{C}$ and carbonate saturation state – Important tracers and potential errors	
4.1.	Introduction	68
4.2.	Carbonate geochemistry and coral calcification	71
4.3.	Procedures	74
4.4.	Results	75
4.5.	Discussion	79
4.6.	Conclusions	88
5.	Conclusions – Late Quaternary paleoceanography of the eastern Indian Ocean, implications for past climate	

reconstructions, and recommendations for future studies	91
References	98
Appendix	125

ABSTRACT

Geochemical records (TOC, N, CaCO_3 , K, Ba, Al, $\delta^{15}\text{N}$, $\delta^{13}\text{C}_{\text{TOC}}$, $\delta^{18}\text{O}$) of two marine sediment cores from the southern Timor Trough are presented for the past 80,000 years. These records reflect an El Niño-like mean oceanographic and climatic state during isotope stage 2 and, in particular, during the LGM. A comparison of the paleoceanography inferred from the paleodata with the modern-day analogue of an El Niño event suggests that, during the LGM, the Indonesian Throughflow (ITF) was restricted. The above results reinforce recent suggestions in the literature of an El Niño-Southern Oscillation (ENSO)-like equatorial climate mechanism operating at glacial-interglacial time scales in the tropical eastern Indian Ocean.

Improved understanding of the operation of the above mentioned equatorial climate mechanism in the tropical Indian Ocean in the past would greatly have benefited from a coral-based study of the operation of any modern equatorial climate mechanisms in the eastern Indian Ocean over the past few centuries. However, the scale of such a project would be such that it cannot be completed within the confines of a study of this type. Consequently, one goal of this thesis was to find a suitable site for pursuing the necessary coral-based high-resolution reconstructions in subsequent studies. Based on the results from measurements of growth characteristics and geochemical tracers of a number of coral cores from different sites, it was found that only one coral core from Ningaloo Reef was suitable for paleoceanographic reconstructions for the

region. Another core from the same reef was found to be unsuitable because of postdepositional alteration at the base of the core. The results of this thesis show that within Ningaloo Reef, Tantabiddi Bay appears to be a suitable site for the collection of coral-based paleoceanographic records.

The results of this thesis also contribute to the solution of some of the controversies currently found in paleodata bases. Differences found among the reconstructions of sea surface temperatures from different paleoproxies for adjacent sites can be explained by potential misinterpretations of values measured on coral material that may have been influenced by postdepositional alteration. The results also show that corals for which reconstructions of sea surface temperatures have been cross-checked with several tracers (e.g. $\delta^{18}\text{O}$, Sr/Ca) may not be reliable indicators of paleoceanographic conditions. They suggest that coral-based reconstructions of sea surface temperatures may have overestimated cooling of the tropical Indian Ocean in the past. Furthermore, the $\delta^{13}\text{C}$ values and the growth characteristics (density, growth rates, calcification rates) measured on pristine and altered coral material, help clarify the reasons for opposing findings in the current literature of past and recent changes in calcification in the tropical surface ocean in response to changes in atmospheric CO_2 levels. For example, a decrease in calcification seen in many coral records during the 20th century may not have been caused by changes in the carbonate saturation state of the tropical surface ocean. Instead, postdepositional addition of secondary aragonite has caused an apparent decrease in calcification rates

towards the present because of higher density values measured by coral densitometry at the base of the coral cores.

CHAPTER I

Introduction

—

Paleoceanographic and paleoclimate reconstructions in the eastern Indian Ocean

The eastern Indian Ocean is a key region for paleoclimate research (Thunell et al. 1994, Linsley 1996, Beaufort et al. 2001). Data on paleoceanography and paleoclimate are still lacking, however, for some of the significant parts of the region such as the Timor Sea off northwestern Australia and Ningaloo Reef Marine Park in Western Australia. Yet knowledge of paleoclimate variability in the region is of great importance for understanding the mechanisms behind tropical and global climate variability (e.g. Beaufort et al. 2001).

The region is influenced by the Indonesian Throughflow (ITF), which carries warm, low salinity water from the western Pacific into the eastern Indian Ocean (Godfrey and Golding 1981, Godfrey and Ridgway 1985). Because of this transport of warm water masses from the Western Pacific Warm Pool (WPWP), climate signals from the Pacific are transferred into the eastern Indian Ocean (Meyers 1996). As the warm water determines the degree of convection, the ocean currents strongly influence atmospheric circulation and precipitation patterns in the region (Nicholls 1989, Frederiksen and Balgovind 1994).

Recent studies have suggested that the eastern Indian Ocean is likely to be affected by an equatorial climate mechanism (Beaufort et al. 2001, De Garidel-Thoron et al. 2001). Such a mechanism has previously been suggested by Beaufort et al. (1997) for the western equatorial Indian Ocean, but its influence in the eastern Indian Ocean still needs further investigation. In the eastern Indian Ocean, this equatorial climate mechanism is believed to be directly related to insolation and to resemble the dynamics of the Southern Oscillation. It is thought to be independent of global ice volume variations and thus allows study of equatorial climate dynamics (Beaufort et al. 2001).

The hypothesis proposed by Beaufort et al. (2001) of the operation of an equatorial climate mechanism and resemblance of this climate mechanism to dynamics of the Southern Oscillation is quite revolutionary and represents considerable progress in the field of tropical paleoclimatology. No explanation of this mechanism, however, was offered in their paper. The authors merely state in their paper that contrasts in paleoceanographic features between interglacial and glacial times resemble the features typical of a contrast of the opposing phases of the El Niño-Southern Oscillation (ENSO), i.e. El Niño and La Niña. This statement is based solely on the observations of primary productivity in the surface ocean for areas of the Indian Ocean north of and close to the equator. Thus, the hypothesis of Beaufort et al. (2001) needs further proof from studies based on other proxies, covering different time scales and, in particular, for regions adjacent to the study area of Beaufort et al. (2001) in the eastern Indian

Ocean. The data of Beaufort et al. (2001) alone do not allow derivation of the character and the driving of their proposed climate mechanism.

Currently, the data base for the region with respect to this hypothesis is so sparse that no attempt can be made within a thesis project to prove the hypothesis by Beaufort et al. (2001). The existing data base needs to be considerably expanded to allow clear identification of a climate mechanism behind these large-scale oscillations over glacial and interglacial time scales.

Most of the data of Beaufort et al. (2001) from the eastern Indian Ocean have been collected north of or very close to the equator. Collection of data from regions located south of the equator in the eastern Indian Ocean is essential to fill the vacuum in the data base. The region of the eastern Indian Ocean stretching from the Timor Trough off the coast of northwestern Australia to Ningaloo Reef off the coast of Western Australia is one of the regions clearly understudied as scarce data exist. Along with data sets to be produced by other researchers, the new data presented in this study for this region may eventually contribute to a justification of the hypothesis proposed by Beaufort et al. (2001).

Expansion of the available data sets based on marine sediments in a key area south of the study area of Beaufort et al. (2001), i.e. the area of the southern Timor Trough in the eastern Indian Ocean south of the equator, was then a major goal of this project.

A second, original goal was to provide for the past 150 years a high-resolution oceanographic data set from coral for several relatively small time windows covering about 15 years. This goal was defined because the identification of past climate mechanisms clearly requires identification of and cross-checking with the modern mechanisms.

The majority of studies of modern climate variability in the Indian Ocean have focused on the forcing of such variability by ENSO occurring in the tropical Pacific Ocean. One recent study of sea-level variability in the Indian Ocean provided further evidence that interannual warming occurs in the Indian Ocean with a frequency similar to that of El Niño in the Pacific Ocean (Chambers et al. 1999). Furthermore, recent results from a 194-year annual record of skeletal $\delta^{18}\text{O}$ from a coral growing at Malindi, Kenya, suggest that the tropical Pacific Ocean imparts substantial decadal climate variability to the western Indian Ocean and, by implication, may force decadal variability in other regions with strong ENSO teleconnections (Cole et al. 2000).

The original intention of providing a small high-resolution oceanographic data set, as mentioned above, was to discriminate modern ENSO signals for the region for the past few centuries. It was during this work that, unexpectedly, it became evident that the studied region of the eastern Indian Ocean, reaching from the southern Timor Trough to Ningaloo Reef, appears in modern times to have not only been affected by the ENSO signals but possibly also by the Indian Ocean Dipole. The possible effect of the Indian Ocean Dipole in the

region was inferred because for some of the data variability in the coral studied by Kuhnert et al. (2000), no relation to ENSO was found and no sound explanation could be given.

The extent of the separate or combined influence of the two modern equatorial climate mechanisms believed to be operating in the eastern Indian Ocean, i.e. ENSO (Kuhnert et al. 2000) and the Indian Ocean Dipole (Saji et al. 1999) are currently not understood. Instrumental records, however, suggest that in 1994 both ENSO and Indian Ocean Dipole events may have occurred simultaneously in the equatorial eastern Indian Ocean north of Ningaloo Reef (cf Meyers 1996, Saji et al. 1999).

At present, the instrumental Indian Ocean dipole records available (cf Saji et al. 1999) are too short to allow identification of the degree and kinds of interference of the two mechanisms over the past 150 years. Also, no high-resolution coral-based data sets are available to allow extension of these instrumental records into the past. To date, the only high-resolution coral-based reconstruction including the Indian Ocean dipole has been done on coral from Christmas Island in the tropical Indian Ocean (Marshall and McCulloch 2001). However, this reconstruction is restricted to a 24-year period for which also blended ship and satellite data from the region are available. The results record unusual oceanographic conditions set up by the Indian Ocean Dipole, but do not extend far enough into the past to allow explanation of the driving forces of the

mechanism or comparative analysis of the overall impact of the Indian Ocean Dipole and ENSO signals.

Coral-based reconstruction of the Indian Ocean Dipole covering the past few centuries would require collection of a substantial amount of new data. The scale of this project is such that it cannot be completed within the confines of a single PhD thesis. One project currently being carried out at the Research School of Earth Sciences at the Australian National University is one of the first to have taken up the topic of the reconstruction of the Indian Ocean Dipole based on coral chemistry (Abram et al. 2003). The project focuses on the area off Sumatra which is a key site for a clear signal of the Indian Ocean Dipole (Stuart Godfrey, pers.comm. 2002). At present, the resolution of the above reconstruction is too low to allow identification of the degree and kinds of interference of the ENSO and Indian Ocean Dipole mechanisms in high-resolution oceanographic data sets from corals for the past 150 years.

Due to the lack of long-term data series of the Indian Ocean Dipole, the original second goal of this current project to produce reliable high-resolution paleoceanographic reconstructions based on geochemical data from coral for the area of Ningaloo Reef in the eastern Indian Ocean had to be abandoned. However, the results of the initial preliminary bulk analysis already performed on coral samples revealed another important finding. They showed that the data collected at different sites in Ningaloo Reef proved not to be representative for the entire area.

This finding led to a redefinition of the second goal of this thesis: to find a suitable site for pursuing the necessary coral-based high-resolution reconstructions in subsequent studies. Among a larger number of coral cores from different sites, only two coral cores from Ningaloo Reef initially appeared suitable for paleoceanographic reconstructions based on geochemical coral data for the region. Only for these two sites were coral growth rates found to be sufficiently large to exclude vital and kinetic effects on geochemical tracers due to a variation in growth rates. Further geochemical analysis conducted on 5-year-increments of the complete cores revealed that, of these two cores, only one was suitable for high-resolution studies. The other core proved unsuitable because, as shown in chapters III and IV, the formation of secondary aragonite after coral deposition obscured the results of measurements of growth parameters and geochemical tracers in this coral.

Recognition of the above deviations of growth parameters and geochemical values also drew attention to the potential of the results to help resolve controversies currently found in paleodata bases regarding the interpretation of sea surface temperatures, salinities and the carbonate saturation state of the ocean in the past. Consequently, the third goal of this project was to show that some of the current controversies in paleodata bases such as differences found among the reconstructions (e.g. sea surface temperature) from different paleoproxies for adjacent sites can be explained by potential misinterpretations of values measured on coral material which may have been influenced by

postdepositional alteration such as early marine diagenesis. Given the data presented in chapter III it can be inferred that fossil corals for which reconstructions of sea surface temperatures have been cross-checked with the two presumably independent tracers $\delta^{18}\text{O}$ and Sr/Ca (Guilderson et al. 1994, Beck et al. 1997) may not be reliable indicators of paleoceanographic conditions. This would imply that some of the above coral reconstructions of sea surface temperatures may have overestimated cooling of the tropical ocean in the past. Furthermore, the results and interpretations given in chapter IV clearly contribute to the solution of current controversies concerning possible effects of changes of the carbonate saturation state of the surface ocean in response to changes in atmospheric CO_2 levels. The geochemical data presented for pristine and altered material in chapter IV offer possible explanations for the opposing findings currently available in the literature of past and recent changes in calcification in the tropical surface ocean.

CHAPTER II

Glacial-interglacial changes in nutrient utilization and paleoproductivity in the Indonesian Throughflow sensitive Timor Trough

—

Paleoclimatic implications for the region of the easternmost Indian Ocean

2.1. Introduction

The Western Pacific Warm Pool (WPWP, Fig.2.1) is characterized by waters with mean sea surface temperatures (SSTs) exceeding 28°C. Its importance for climate dynamics has been recognized in recent studies, as has the need to understand long-term variations of primary production in low latitudes (e.g. Thunell et al. 1994, Ahmad et al. 1995, Linsley 1996, Beaufort et al. 2001, De Garidel-Thoron et al. 2001). Knowledge of past variation in primary production and nutrient utilization may contribute to the understanding of past changes in the thermal structure in the region. In the Timor Trough (Fig.2.2), which is situated at the southern edge of the WPWP, variations of primary production are poorly documented.

At present, the study area is strongly influenced by the Indonesian Throughflow

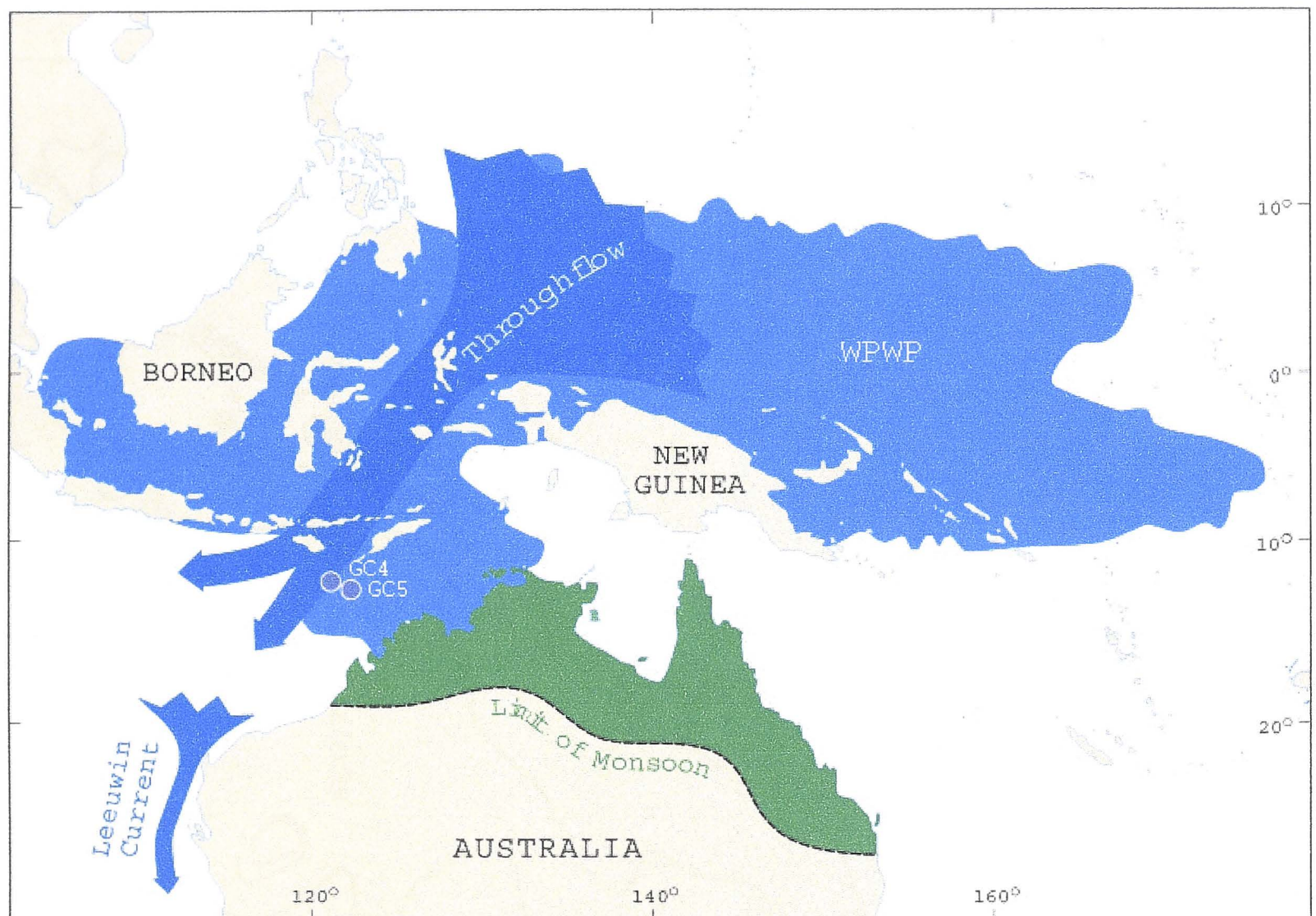


Figure 2.1. Physiographic map showing the location of the study site, the Western Pacific Warm Pool (WPWP) and schematic ocean circulation patterns.

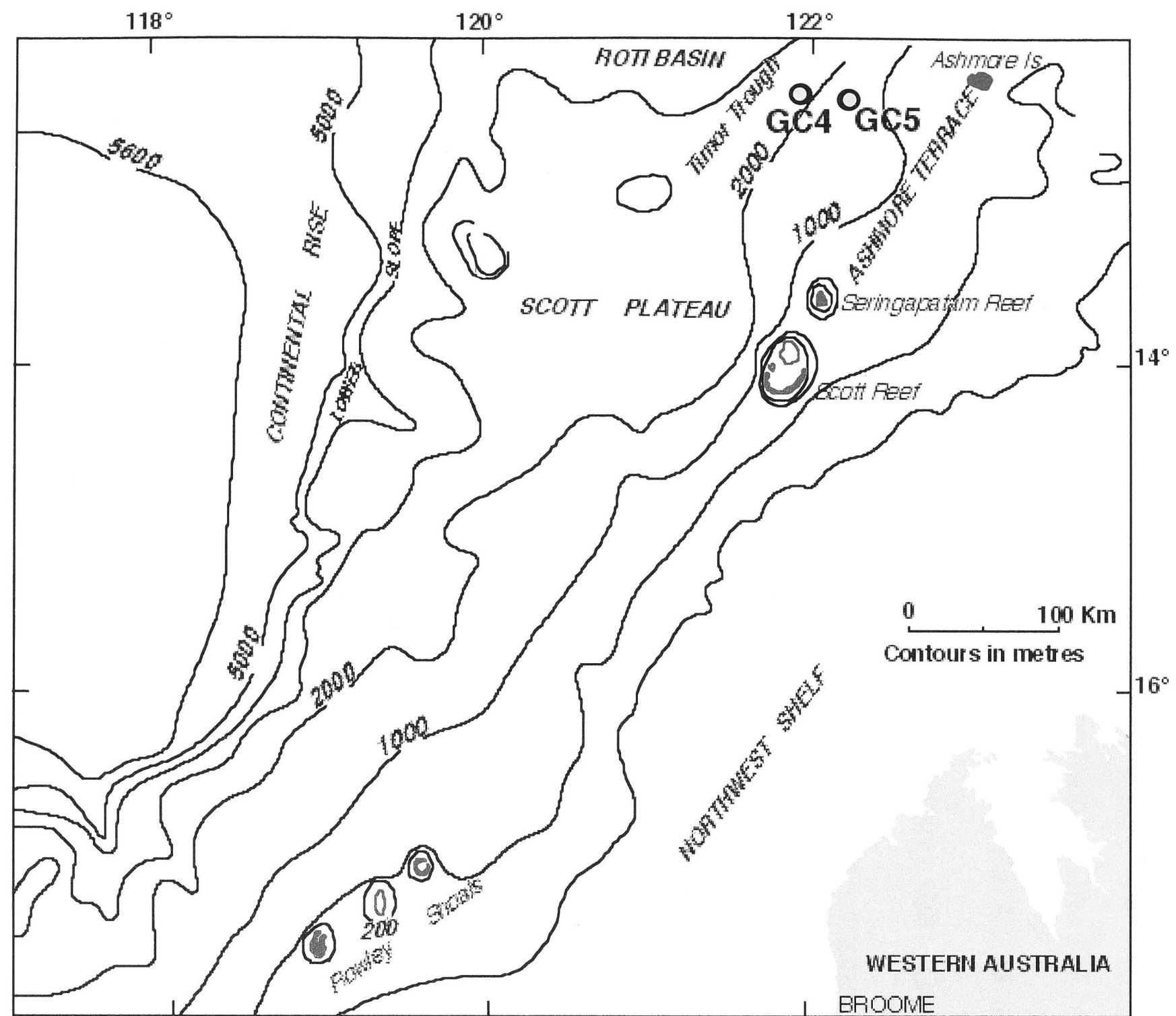


Figure 2.2. Bathymetric map showing the study sites.

(ITF). The ITF (Fig. 2.1) enters the Indian Ocean as a narrow band of low-salinity water, with a maximum water transport estimated in the range of 7-18 Sv (Gordon and Fine 1996). It is strongest in austral winter. The ITF represents the interocean transport of excess freshwater from the Pacific to the Indian Ocean through the Indonesian Seas (Godfrey and Golding 1981, Godfrey and Ridgway 1985). This is caused by the necessity to maintain constant pressure around islands, such as the island continent Australia (Godfrey 1989). Water that passes the ITF flows into the Indian Ocean as the west flowing South-Java and the South Equatorial Currents and as the south flowing Leeuwin Current (Godfrey and Ridgway 1985). The latter is maintained because of the lower steric height further south along the coast off Western Australia. Southward flow is accompanied by surface cooling, and surface cooling produces continuous southward flow (Tomczak and Godfrey 1994).

The dynamics of this eastern boundary current along the Western Australian coast are thus different from those of the Pacific and Atlantic Oceans. In these oceans, equatorward winds produce equatorward surface current flow, poleward undercurrents, and coastal upwelling along the eastern boundaries of the ocean basins. Along the Western Australian coast, however, annual mean winds do blow toward the equator, but at the surface a strong poleward flow runs against the wind, and the undercurrent is equatorward. The poleward flow is strong enough to override the wind-driven equatorward current, and the onshore geostrophic flow is strong enough to override the offshore Ekman flow.

Hence the upwelling that one might expect from the equatorward winds along the Western Australian coast is overwhelmed by an onshore geostrophic drift (Smith 1992, Tomczak and Godfrey 1994).

At present, no significant upwelling occurs in the study area (Tomczak and Godfrey 1994). However, because the pressure difference from the Pacific to the Indian Ocean is the driving force for through flow (Wyrski 1987), both the volume transport of through flow and the thermal structure in the area are expected to vary during the El Niño-Southern Oscillation (ENSO) cycle. Larger than normal transport is expected during the La Niña phase, when strong easterlies along the equatorial Pacific build up a high sea level in the western Pacific (Clarke and Liu 1994). Conversely, during an El Niño event, Pacific equatorial winds are anomalously westerly, and the western Pacific sea level falls. This low sea level is transferred to the coast northwest of Australia (Clarke and Liu 1994, Potemra and Lukas 1999). As a consequence, the baroclinic pressure gradient between northwestern Australia and Java decreases (Clarke and Liu 1994), resulting in a weakening of the ITF (Clarke and Liu 1994, Potemra 1999).

The alternation of easterly and westerly wind stress anomalies during an ENSO cycle is accompanied by a weaker reversal of anomalies in the eastern Pacific and in the equatorial Indian Ocean. The winds over the equatorial Indian Ocean determine the thermal structure on the Indonesian coast. During ENSO, when Pacific wind anomaly is westerly, Indian Ocean anomaly is easterly, resulting in

a shallow thermocline along the coast of Java. This has been observed to occur simultaneously with extremely cold SST, suggesting that upwelling contributes to the formation of a "cold spot". This SST temperature anomaly is widespread during some ENSO events, extending from Timor along Java and Sumatra (Meyers 1996).

During the Last Glacial Maximum (LGM), the circulation patterns in the Indian Ocean were significantly different from those of today. It has been suggested that a northflowing West Australian Current, associated with a weaker or absent Leeuwin Current linked to a reduced WPWP (Martinez 1994) and thereby weaker ITF, led to increased productivity and coastal upwelling at higher latitudes off Western Australia (McCorkle et al. 1994, Wells et al. 1994). As well, the Westerlies may have been compressed, and thus more intense, and moved north during the LGM. Part of the West Wind Drift was deflected equatorward by Australia. Thus, in contrast to the modern pattern of weak, seasonally reversing flow, the West Australian Current was a significant eastern boundary current. This current transported cooler waters equatorward all year-round (Prell et al. 1980).

In this chapter, geochemical results are presented from two sediment cores from the continental margin off northwestern Australia to show past changes in productivity and nutrient utilization, which may be related to changes in the ITF and thermal structure in the area. The chapter focuses on Holocene/LGM contrasts because for these time periods ^{14}C dating (B.N. Opdyke, unpublished

data) is available in addition to the $\delta^{18}\text{O}$ record of *Globigerinoides ruber*. Signals observed during isotope stages 3 and 4 for which an age model based on the $\delta^{18}\text{O}$ record of *Globigerinoides ruber* has been established will be pointed out, but they will not be discussed in detail due to the lack of results from additional dating.

4.4. Procedures

Two gravity cores, GC4 (12°17.48 S, 121°56.01 W, water depth 2069 m) and GC5 (12°22.3 S, 122°12.03 W, water depth 1462 m), were taken during a R.V. Franklin cruise in 1996 (Fig. 2.2). Two series of 3cm³ syringe samples were taken at 10-cm intervals for each core. To establish a foraminiferal $\delta^{18}\text{O}$ record, organic matter was removed from the samples of one series by treatment with 5% hydrogen peroxide solution (H_2O_2). The size fraction >150 μm was separated by wet sieving. Foraminiferal specimens of *Globigerinoides ruber* were hand picked from the >150 μm size fraction, washed in alcohol and placed in an ultrasonic cleaner for less than 5 seconds. 10-15 clean specimens (with a total weight between 150 and 200 μg) were selected for stable isotope analysis. Isotope analysis was carried out using an automated individual carbonate-reaction (Kiel) device coupled with a Finnigan-MAT 251 mass spectrometer. The $\delta^{18}\text{O}$ values were calculated as per mil (‰) deviations relative to PDB, and were calibrated via the NBS-19 standard ($\delta^{18}\text{O}=-2.20\text{‰}$). Average reproducibility for a typical 150- μg sample was 0.05‰.

The chronostratigraphy of the cores was based on the $\delta^{18}\text{O}$ records for *Globigerinoides ruber*, applying the SPECMAP time scale (Imbrie et al. 1984, Martinson et al. 1987, Fig. 2.3). An interpolation was made between $\delta^{18}\text{O}$ -age tie points, and linear sedimentation rates were derived.

For all following analyses, the samples of the second series were freeze dried, crushed and homogenized. For stable isotope analysis ($\delta^{13}\text{C}_{\text{TOC}}$ and $\delta^{15}\text{N}$) carbonate was removed from the sediment samples by adding 2% hydrochloric acid to sediment subsamples (20 mg aliquots). This was repeated until formation of CO_2 bubbles ceased. The samples were then dried at 60 °C, and combusted with a CHN-analyzer (ANCA/SL) coupled to a 20/20 mass spectrometer (Europa Scientific Ltd, UK). Pure CO_2 and N_2 gases from tanks calibrated as a standard against carbonate (NBS-22) and atmospheric nitrogen (Mariotti 1983) respectively, were used as reference gases. Isotope ratios were calculated using the following equation,

$$\delta X (\text{‰}) = \left(R_{\text{sample}} / R_{\text{reference}} - 1 \right) * 10^3.$$

where X and R are ^{13}C (or ^{15}N) and $^{13}\text{C}/^{12}\text{C}$ (or $^{15}\text{N}/^{14}\text{N}$), respectively.

Two secondary standards, flour for N and beet sugar for C, calibrated against IAEA-NI $(\text{NH}_4)_2\text{SO}_4$ and IAEA reference standard NBS-22 respectively, were included in the sample batch after every 8th sample. Values were reported relative to air nitrogen and relative to PDB. Analytical variability was checked

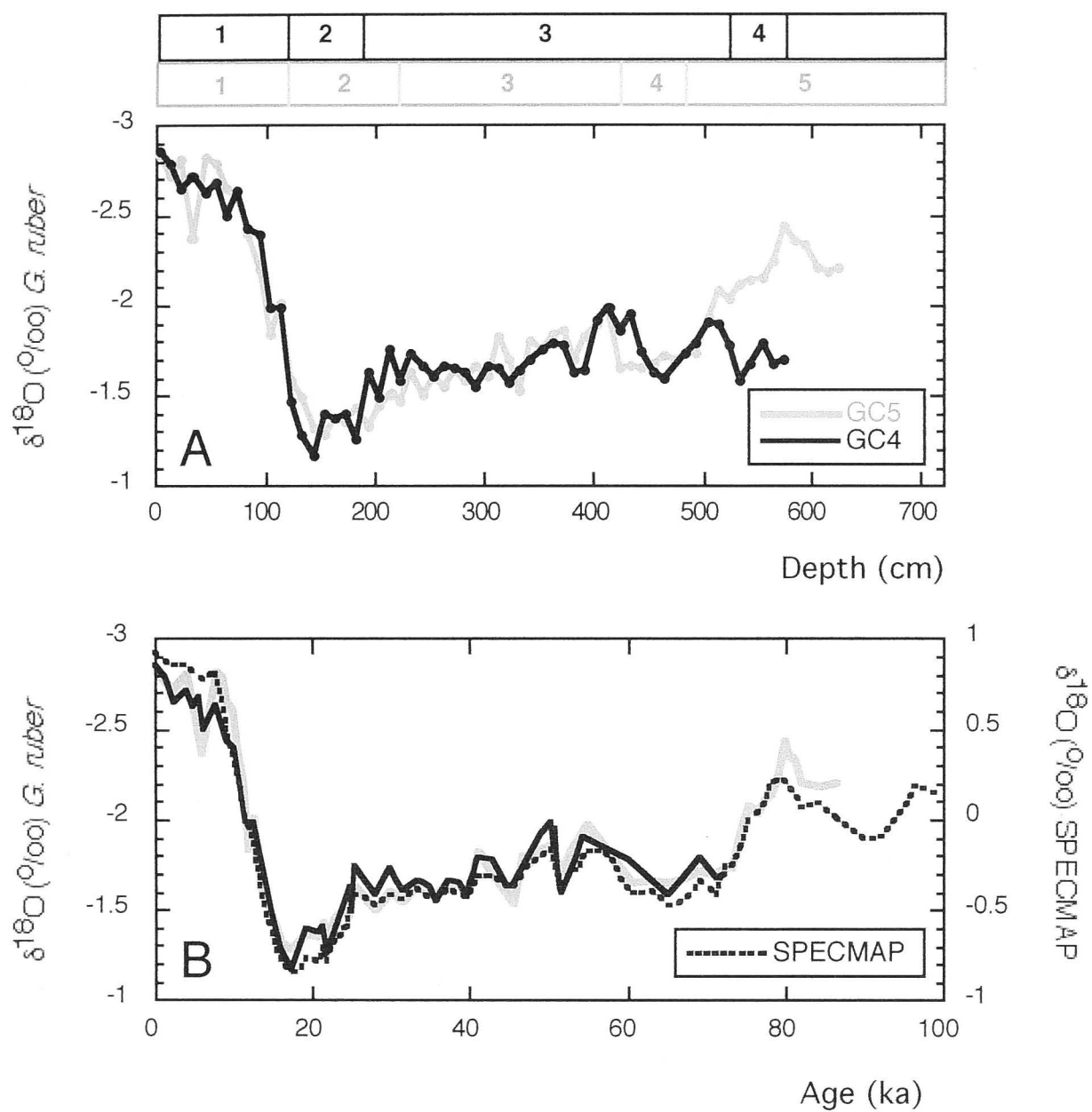


Figure 2.3. (a) Plot of $\delta^{18}\text{O}$ records of *Globigerinoides ruber* versus depth of cores GC4 (black) and GC5 (gray). Major isotopic events identified in the cores are indicated. (b) Plot of $\delta^{18}\text{O}$ stratigraphies of cores GC4 and GC5 compared to the SPECMAP $\delta^{18}\text{O}$ record (dotted line).

again using a soil, homogenized as an internal standard, as a sample after every reference standard. Throughout the analysis of sets of up to 50 samples, the test standard (flour) analysed in this way gave a standard deviation of 0.16‰ on a measured mean $\delta^{15}\text{N}$ of 3.87‰, and similar precision was obtained for the reference soil ($16.56 \pm 0.33\text{‰}$). Variation between duplicates was less than 0.2‰. The precision of $\delta^{13}\text{C}$ analysis was better than 0.22‰, and variation between duplicates was less than 0.3‰. Total organic carbon (TOC) and total nitrogen (N) values were determined simultaneously when measuring the isotope ratios, with the test standard showing a standard deviation of 0.009% for C and 0.001% for N, with duplicates having a variation less than 0.08% and 0.009% for C and N respectively.

Total carbon was measured on 2-mg aliquots, weighed in aluminum capsules, with a NA 1500 NC Fisons Analyzer at 1020°C. Together with the samples, urea, soil and one sediment sample were measured as internal standards after every 6th sample. From these measurements, the reproducibility appeared to be better than 0.06%. Here, mean values of duplicate measurements are reported, with the standard deviation usually better than $\pm 0.2\%$. Inorganic carbon content was derived from the difference between total carbon and organic carbon, and calcium carbonate content was calculated from inorganic carbon values by multiplying the inorganic carbon content by a factor of 8.33.

For major element determination (BaO , Al_2O_3 , K_2O) samples were prepared as glass discs following the method of Norrish and Hutton (1969), with the

exception that the flux used consisted of 12 parts lithium metaborate. These glass discs were measured on a PW2400 wavelength dispersive X-ray fluorescence (XRF) spectrometer. The precision of these measurements was better than 0.002% for BaO, 0.03% for Al₂O₃ and 0.05% for K₂O. Total barium was corrected for the nonbiogenic barium fraction using the Al content of the sediments, where Al is used as a measure of aluminosilicate contribution (Calvert 1976, Shimmield 1992). Total barium content was normalized using the equation given in Dymond et al. (1992): $Ba_{excess} = Ba_{tot} - (Al \times 0.0075)$.

The correction factor in the equation refers to the global Ba/Al aluminosilicate ratio of crustal rocks. Like in Francois et al. (1995), ranges for biogenic Ba fluxes have been estimated which refer to the extrema in the range of Ba/Al of $0.01 < Ba/Al < 0.005$ for crustal rocks as reported by Taylor and McLennan (1985). There is, however, a measure of imprecision with this method depending on the magnitude of the terrigenous barium fraction (Dymond et al. 1992). Because much of the terrigenous barium may be contained within feldspar, Ba/K ratios were also calculated to normalize for variations in feldspar contents (Schneider et al. 1997).

2.3. Results

Linear sedimentation rates range from 3.5 to 15.3 cm/kyr (Fig. 2.4). Values are higher during the LGM than the Holocene in the shallow core GC5, but not in core GC4. It is possible that the values are influenced by syndepositional

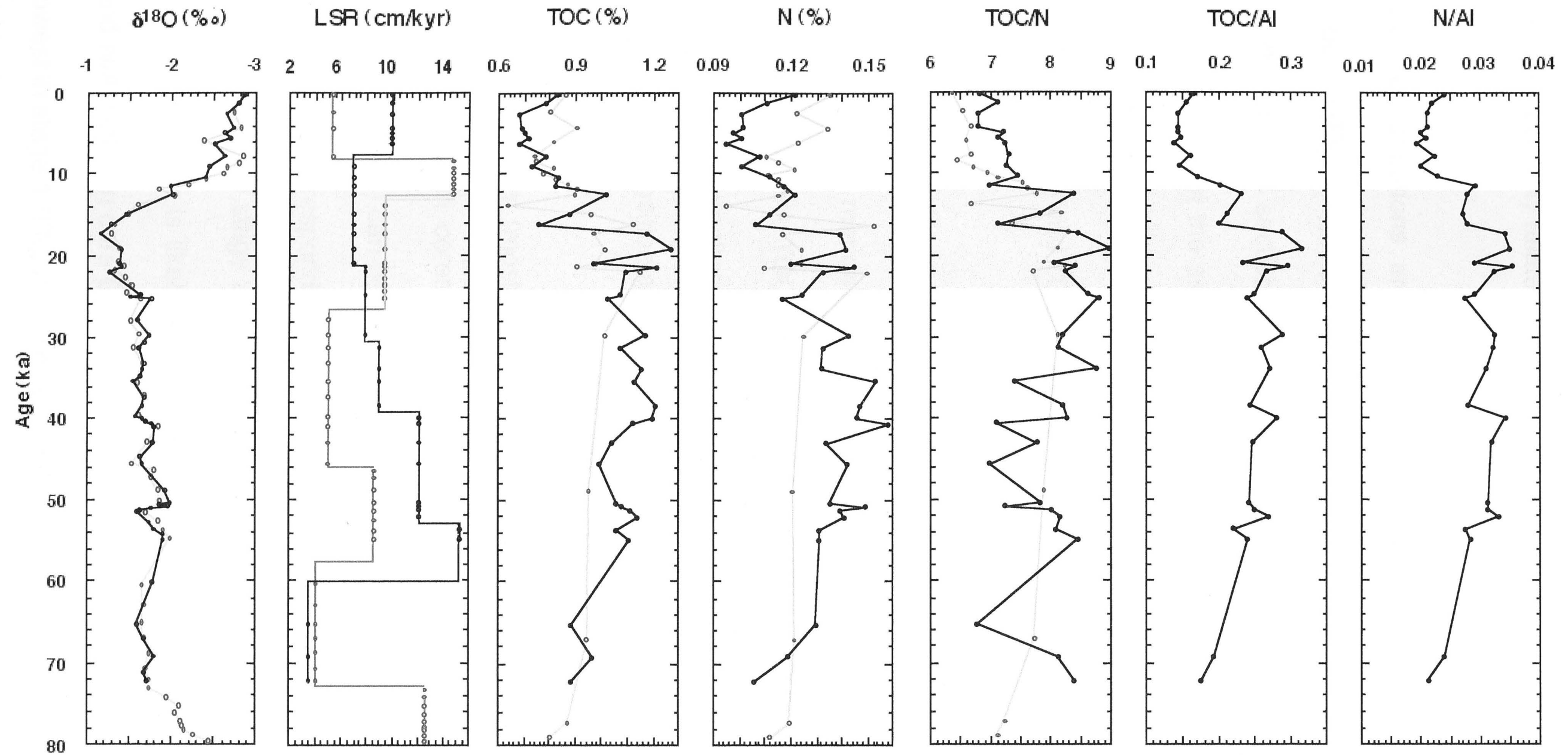


Figure 2.4. Linear sedimentation rates (LSR), concentrations of total organic carbon (TOC) and nitrogen (N), and TOC/N, TOC/Al, and N/Al ratios in sediment cores GC4 (black) and GC5 (gray). The $\delta^{18}\text{O}$ values of *Globigerinoides ruber* are shown to allow the temporal comparison of the records. The trends of the concentrations of nitrogen closely follow those of organic carbon. Organic carbon and nitrogen concentrations are more elevated in stage 2 than stage 1. TOC/N ratios are higher in stages 2, 3, and 4 compared with those of stage 1. The TOC/Al and N/Al ratios show similar trends. They are highest in stage 2 and lowest in stage 1.

redistribution of the sediments, which may result from changes in downslope transport, possibly related to changes in sea level.

TOC concentrations are higher in the sediments from the LGM than the Holocene (Fig. 2.4), implying higher productivity during the LGM. The LGM falls into the shaded section covering isotope stage 2 in the figure. The organic matter fraction of the sediments is predominantly of marine origin, although a minor terrigenous component may be present. Evidence for this is given by the TOC/N, $\delta^{13}\text{C}_{\text{TOC}}$ and TOC/Al and N/Al values (Fig. 2.4 and 2.5).

The TOC/N ratios in the sediments are relatively low and point toward the dominance of a marine organic matter fraction (Fig. 2.4., cf Müller 1977 and references therein). TOC/N ratios are higher during isotope stages 2 and 3. For the sediments from these stages, terrigenous input cannot be ruled out from the elemental composition alone.

Low TOC content (mostly $<0.8\%$) associated with low TOC/N ratios (<7.5) can be seen for both cores in isotope stage 1. In contrast, relatively high TOC contents ($>0.8\%$) can be observed together with high TOC/N ratios (>7.5) in the core section corresponding to isotope stage 2. Unlike the sediments of stage 1, the sediments of stage 2 contain an inorganic nitrogen fraction in both sediment cores. The latter is likely to be bound to illite (cf Müller 1977). The TOC/Al and N/Al ratios in core GC4 show similar trends in being highest in stage 2 and lowest in stage 1 (Fig. 2.4). These changes occur almost simultaneously with

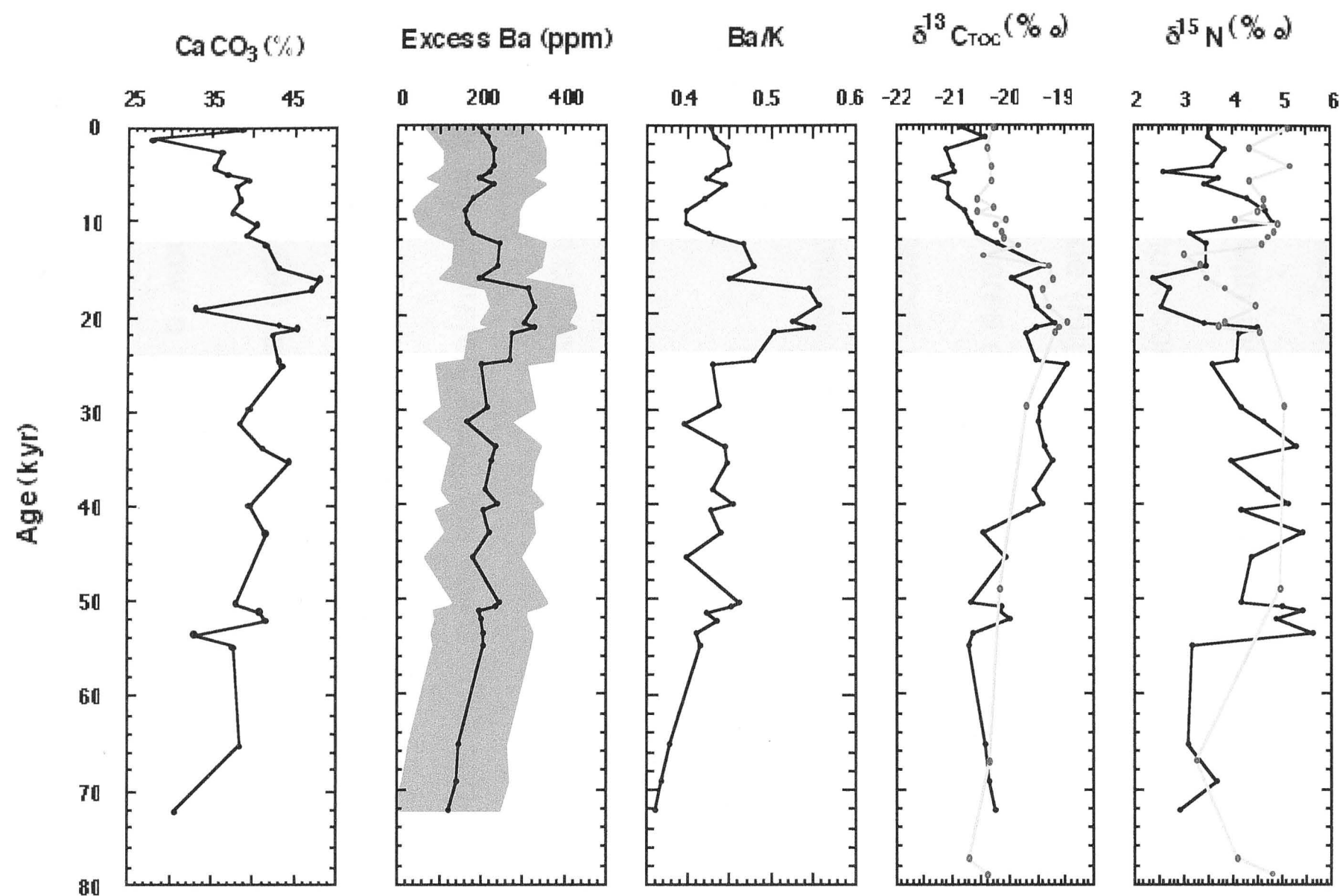


Figure 2.5. Calcium carbonate (CaCO_3) and excess barium (Ba) concentrations, Ba/K ratios, and stable isotope values of organic carbon ($\delta^{13}\text{C}$) and nitrogen ($\delta^{15}\text{N}$) (core GC4: black; core GC5: gray). The CaCO_3 concentrations reach maximum values in stage 2. Excess Ba concentrations in core GC4 are higher in stage 2 than stages 1 and 3. To account for a possible variation in the Ba/Al of aluminosilicates, we show the range of excess barium values (shaded) that would meet the values in the range of the Ba/Al ratios for crustal rocks given by Taylor and McLennan (1985). Ba/K ratios in core GC4 are clearly elevated during stage 2 compared with stage 1. The changes observed in the excess barium values and Ba/K ratios in core GC4 closely follow the variations in organic carbon (Figure 2.4) and calcium carbonate contents for stages 1 and 2. Periods of high organic carbon content also reveal high biogenic barium content. The $\delta^{15}\text{N}$ values in both cores are clearly lower during stage 2 than stages 1 and 3. The $\delta^{13}\text{C}_{\text{TOC}}$ values of cores GC4 and GC5 are lowest in stage 1 but are elevated in stages 2 and 3.

the transition from isotope stage 1 to isotope stage 2 and indicate the presence of two distinct sedimentological or stratigraphic units rather than continuous diagenetic alteration.

Higher CaCO_3 concentrations were observed in the sediments from the LGM compared with those from the Holocene (Fig. 2.5). As with the above values, excess barium concentrations and Ba/K ratios are higher during the LGM than the Holocene (Fig. 2.5), implying higher productivity. As TOC are relatively low in the study area compared with high productivity regions, it seems unlikely that barite undergoes significant diagenetic mobilization and reprecipitation due to anoxic conditions in the surface sediments (von Breymann et al. 1992, Torres et al. 1996).

The pattern of the records of the values above and those of $\delta^{13}\text{C}_{\text{TOC}}$ and $\delta^{15}\text{N}$ show similar trends along the cores. The sediments show clearly lower $\delta^{15}\text{N}$ and higher $\delta^{13}\text{C}_{\text{TOC}}$ values during the LGM than the Holocene (Fig. 2.5). The Holocene-LGM variations of TOC, $\delta^{13}\text{C}_{\text{TOC}}$, $\delta^{15}\text{N}$, Ba_{excess}, Ba/K and CaCO_3 records show a strong relationship with the planktonic foraminiferal $\delta^{18}\text{O}$ record. As a general trend, the Holocene is characterized by low TOC, CaCO_3 , Ba_{excess}, Ba/K, $\delta^{13}\text{C}_{\text{TOC}}$ and high $\delta^{15}\text{N}$ values, while the values from the LGM show the opposite. Apart from these general trends, the $\delta^{13}\text{C}_{\text{TOC}}$ and especially the $\delta^{15}\text{N}$ records appear to lag the $\delta^{18}\text{O}$, TOC, N, CaCO_3 and barium records, and reach maximum and minimum values a few years later. In

addition to the glacial/interglacial changes, higher-frequency fluctuations appear to be recorded in the sediment sequence. However, at this stage the resolution and the length of the data series is not sufficient to ensure that these fluctuations are not subject to noise. These high-frequency fluctuations using a longer time-series and a higher-resolution time-scale should be the subject of future studies.

2.4. Discussion

2.4.1. Glacial-interglacial changes in paleoproductivity

The combined use of paleoproductivity proxies in this chapter has proven useful in pointing out times of elevated productivity. This proxy comparison shows generally good agreement between three different paleoproductivity indicators. Given the uncertainty of any single proxy, simultaneous application of more than one tracer strengthens the interpretation of glacial/interglacial changes in paleoproductivity. However, the results also indicate that glacial productivity was increased only relative to the low productivity characteristics of this region in the modern ocean. In the following each proxy is discussed independently.

2.4.1.1. Organic carbon, TOC/N ratios and possible diagenetic imprints

Evidence of higher surface ocean productivity during the LGM is given by the TOC concentrations, which are higher in the sediments from the LGM than the Holocene (Fig. 2.4). In estimating changes in productivity from TOC values,

possible differences in organic matter preservation due to changes in the magnitude of the sedimentation rates (Heath et al. 1977, Müller and Suess 1979) have not been accounted for. They were not accounted for because TOC variations do not appear to show dependence on the sedimentation rates. In particular, higher TOC during the LGM are not always associated with higher sedimentation rates which could have supported preservation of organic matter.

As well, sediments from northwestern Australia do not appear to contain a significant input of terrigenous organic matter. This is because the $\delta^{13}\text{C}_{\text{TOC}}$ values of the sediments are high (Fig. 2.5), excluding significant input from C3 plant detritus. The only possible input of a terrigenous organic matter fraction would be from C4 plants. This cannot be excluded for the study area as palynological studies have shown that the climate was drier and grassland vegetation, characterized by C4 plants, was more prevalent during the LGM in northern Australia (van der Kaars 1991). Increased input of C4 plant detritus, associated with increased aridity during the LGM (Prell et al. 1980), could cause a shift to heavier $\delta^{13}\text{C}_{\text{TOC}}$ values in the sediments because C4 plants generally have a higher range of $\delta^{13}\text{C}$ values than C3 plants (Schidlowski et al. 1983). For example, Goñi et al. (1998) demonstrated in the Mississippi River drainage basin that when both C3 and C4 plant sources are equally important, land derived organic carbon ($\delta^{13}\text{C}_{\text{terr}} = -20$ to -22‰) can be isotopically indistinguishable from marine sources ($\delta^{13}\text{C}_{\text{mar}} = -19$ to -21‰).

However, at present the study area is not affected by large river inputs as is the case for the sites of Goñi et. al (1998). As well, dust input around Australia is smaller than during the LGM (Hesse 1994). During the Holocene, the ranges of the $\delta^{13}\text{C}_{\text{TOC}}$, TOC/N and $\delta^{15}\text{N}$ and the similar occurrence of higher C/N and lower $\delta^{13}\text{C}_{\text{TOC}}$ in GC4 than GC5 may reflect a terrigenous matter input from C3 plants, although the C/N values are too low to support the input having significant influence. Hydrodynamic transport patterns could be responsible for differences in the values between the cores from different water depths.

Due to the different geographical and climate conditions, increased input of terrigenous organic material from rivers and dust, in the form of C4 plant detritus, seems possible during the LGM. Although such an input cannot be excluded, it does not in itself appear significant enough to account for the magnitude of the shift in the TOC/N values and the isotope signals of bulk organic matter in the sediments. Therefore an increased input of C4 plants is not considered to have caused the observed shifts in the TOC/N and $\delta^{13}\text{C}_{\text{TOC}}$ values.

The cause of the glacial-interglacial variations in the TOC/N ratios may be attributed to variations in organic matter preservation rather than a source change. Variations in TOC/N ratios during diagenesis may be caused by variations in the organic matter/clay associations. This is because the sorption of organic matter to mineral surfaces (decreasing grain size meaning increasing specific surface area) in marine sediments stabilizes the component molecules

and slows remineralization rates (Keil et al. 1994). Most of the sediments from isotope stage 1 contain only small amounts of organic matter ($<0.8\%$ TOC) and consequently have low organic matter/clay mineral (TOC/Al) ratios (Fig. 2.4). In these sediments, the (mainly organic) nitrogen compounds protected within the interlayer spaces of clay minerals (e.g. Müller 1977) appear to primarily determine the lower TOC/N ratios.

In contrast, the diagenetic alteration in the sediment sequence of stage 2, with high TOC concentrations ($>0.8\%$) and higher TOC/N, is likely to be different from that occurring in the sediment sequence corresponding to isotope stage 1. This is because the effect of clay mineral assemblages on the TOC/N ratios may vary with the amount of organic matter in the sediments. Increasing TOC/N ratios are often accompanied by an increasing organic matter content (Müller 1977, Fontugne and Calvert 1992). In the stage 2 sequence, a higher organic matter/clay mineral ratio (TOC/Al) can be observed (Fig. 2.4), allowing a relatively smaller fraction of nitrogen to be preserved. It can be concluded that changes in the TOC/N ratios in the sediments of the study area are primarily controlled by organic matter preservation.

2.4.1.2. Barium

Ba_{excess} and Ba/K values are higher during the LGM than during the Holocene, suggesting elevated productivity. Barium is a highly refractive element in the water column, retaining a high proportion of the original

productivity signal relative to other common proxies like organic carbon and calcium carbonate (Dymond et al. 1992). It can be used as a paleoproductivity indicator because living plankton consists of a relatively large pool of labile barium, which is rapidly released during plankton decomposition. This pool of labile barium acts as the main source of barium for barite formation in supersaturated microenvironments. In addition to barite, biogenic barium occurs mainly as refractory organic barium (Ganeshram et al. 2003). Here, a comparison of biogenic (or excess) barium concentrations (Francois et al. 1997) and Ba/K ratios (Schneider et al. 1997) was done to obtain a reliable picture of productivity changes based on barium values. The similar glacial/interglacial trends of the Ba_{excess} and Ba/K ratios suggest that changes in terrigenous input do not mask the productivity signal reflected by the ratios.

2.4.1.3. Calcium carbonate

The CaCO₃ concentrations imply higher productivity during the LGM. Glacial-interglacial changes in CaCO₃ values have been interpreted in terms of variations in both CaCO₃ supply and dissolution intensity (Lyle et al. 1988, Farrell and Prell 1989, Archer and Maier-Reimer 1994). Carbonate dissolution varies as a function of water depth, bottom water chemistry and carbonate flux (Archer 1991). The possibility that the lower carbonate values in the Holocene section of the sediments reflect dissolution rather than low carbonate supply cannot be ruled out. However, the similarity of the CaCO₃ trends with those of TOC and barium (Fig. 2.4 and 2.5) suggests that changes in the rate of CaCO₃

supply, due to variations in productivity, drive the glacial/interglacial changes in CaCO_3 concentrations. All productivity proxies in this chapter show elevated values during the LGM, although the degree to which they are subject to dissolution or alteration may differ between proxies.

2.4.2. Glacial-interglacial changes in $[\text{CO}_2(\text{aq})]$ in surface waters

The changes in the $\delta^{13}\text{C}_{\text{TOC}}$ values in the sediments occur chronologically parallel to paleoproductivity changes documented by the organic carbon, calcium carbonate and barium data. The $\delta^{13}\text{C}_{\text{TOC}}$ values suggest CO_2 depletion in the surface waters, possibly as a result of enhanced productivity, during stage 2 and during the second half of stage 3. As has been shown, phytoplankton blooms can cause rapid lowering of surface water PCO_2 (e.g. Watson et al. 1991). Diagenetic alteration does not appear to have caused the change in the $\delta^{13}\text{C}_{\text{TOC}}$ values. The likelihood that a terrigenous organic matter fraction has influenced the $\delta^{13}\text{C}_{\text{TOC}}$ values of the sediment has also been excluded. Based on the assumption that changes in inorganic carbon $\delta^{13}\text{C}$ did not occur it was concluded that the shift from higher to lower marine sedimentary $\delta^{13}\text{C}_{\text{TOC}}$ across the Pleistocene/Holocene transition has resulted from an increase in ^{13}C discrimination by Holocene phytoplankton. This was associated with a widespread increase in relative $\text{CO}_2(\text{aq})$ availability and/or a decrease in phytoplankton carbon demand (cf Descolas-Gros and Fontugne 1985, Falkowski 1991, Rau et al. 1992). Alternatively, the elevated glacial

$\delta^{13}\text{C}_{\text{TOC}}$ values could reflect increased phytoplankton utilization of ^{13}C -rich HCO_3^- (relative to $\text{CO}_2(\text{aq})$) during that time, which could also be the result of increased productivity in the surface waters (Degens et al. 1968, Descolas-Gros and Fontugne 1985, Falkowski 1991).

This study documents past glacial/interglacial variations in plankton $\delta^{13}\text{C}_{\text{TOC}}$, and suggests that these variations have been caused by changes in surface water CO_2 concentrations as a result of variations in surface ocean productivity. In addition, the magnitude of change is in agreement with those reported in association with glacial/interglacial changes in surface ocean PCO_2 (cf Rau 1994). However, no empirical relationship between plankton $\delta^{13}\text{C}_{\text{TOC}}$ and $[\text{CO}_2(\text{aq})]$, and no detailed and sound paleo-SST estimates have been provided for the study area so far. That is why it is difficult to delineate local from global signals within the sedimentary record (cf Rau 1994), which may have been caused by lower atmospheric CO_2 levels during the LGM (Barnola et al. 1987).

2.4.3. Changes in nutrient utilization in the surface waters

Sedimentary nitrogen isotope ($\delta^{15}\text{N}$) records from a number of regions have been interpreted as reflecting changes in relative nitrate utilization (e.g. Farrell et al. 1995, Francois et al. 1997, Holmes et al. 1997). Thereby isotopically light particulate organic matter is produced during conditions of relative nutrient depletion (low relative nutrient utilization), whereas the opposite applies for

isotopically heavy organic matter (high relative nutrient utilization). As well, from several studies it is apparent that glacial/interglacial cycles have a strong effect on $\delta^{15}\text{N}$ values in many regions when climate induced changes in hydrography and/or upwelling intensity occur (e.g. Altabet et al. 1995, Farrell et al. 1995, Ganeshram et al. 1995).

$\delta^{15}\text{N}$ values in the sediments of the study area were measured in order to investigate changes in nutrient availability and productivity (Fig. 2.5). The following discussion shows that the values do reflect these specific changes rather than having been influenced by the factors of a terrigenous organic matter input, the degradation of sedimentary organic matter and the occurrence of denitrification in the water column of the study area.

The TOC/N and $\delta^{13}\text{C}_{\text{TOC}}$ data suggest that the input of terrigenous organic matter into the sediments was not significant. Therefore, a $\delta^{15}\text{N}$ signature of terrestrial matter in the sediments would be clearly overprinted by the signal of relative nitrate utilization. As well, it is assumed that the $\delta^{15}\text{N}$ signal has not been influenced by offsets between isotope ratios of particulate organic matter sinking through the water column and underlying sediments due to particle decomposition and trophic exchange of nitrogen. Although such offsets have been observed in similar settings with low TOC concentrations in sediments deposited under oxic conditions, their effects are usually constant and therefore not considered to be significant relative to the signals observed (Altabet and Francois 1994a).

In addition, the $\delta^{15}\text{N}$ values do not appear to be affected by the occurrence of denitrification in the water column of the study area. Evidence for this comes from several sources. First, the $\delta^{15}\text{N}$ values in the sediments do not exhibit a general elevation which would indicate the occurrence of denitrification (Cline and Kaplan 1975). As well, O_2 concentrations today do not drop below 0.2 ml/l (Wyrski 1988), the value that has been described for modern upwelling areas off Peru as being the threshold necessary for denitrification to occur (Packard et al. 1983). Moreover, if denitrification was an important factor affecting the $\delta^{15}\text{N}$ values in this area in the past, high sedimentary organic matter content should be associated with high sedimentary $\delta^{15}\text{N}$ values (e.g. Schäfer and Ittekkot 1993, Ganeshram et al. 1995). The highest $\delta^{15}\text{N}$ values are observed during the Holocene when TOC concentrations are low, and denitrification does not occur today. This indicates that denitrification has not occurred in the past either.

The results indicate that the sedimentary isotopic signal is primarily controlled by the degree of nutrient utilization in the surface waters and that, in this region, changes in relative nutrient utilization between the LGM and the Holocene determine the variation in the $\delta^{15}\text{N}$ signal in the sediments. During the Holocene, lower paleoproductivity was concurrent with higher $\delta^{15}\text{N}$ values, which suggests higher relative nitrate utilization. In contrast, the low $\delta^{15}\text{N}$ values suggest that nitrate was less depleted during the LGM when productivity

was high. Thus, although productivity was higher, relatively less of the available nitrate pool was utilized by the phytoplankton. Absolute nitrate concentrations must have been elevated to support the high rates of productivity.

Given the present day oceanography, one plausible explanation for the higher nutrient levels during the LGM involves nutrient supply to the surface waters being more efficient. This is because of a shallower thermocline, the restriction or the absence of the low-salinity cap of the ITF, and the occurrence of upwelling in the area. Upwelled water provides a large pool of nitrate which is available for uptake during photosynthesis, leading to lower planktonic $\delta^{15}\text{N}$ values than when nitrate is more limiting (Altabet and Francois 1994b, Holmes et al. 1996). Moreover, increased productivity, associated with the presence of upwelled nutrients, has been found to correlate with low $\delta^{15}\text{N}$ values in both sinking organic matter and sediments (Schäfer and Ittekkot 1993, Altabet and Francois 1994b). However, glacial productivity in the Timor Trough was high relative only to the low productivity characteristics of this region in the modern ocean. There is no evidence of strong upwelling of the magnitude of that observed in the modern ocean off the western coasts of Africa and South America.

In addition to the above interpretation for the LGM decline in the $\delta^{15}\text{N}$ values, other factors must have affected the sediment $\delta^{15}\text{N}$ record. This is because the $\delta^{15}\text{N}$ values of the sediment in the study area are very low compared to those from other study areas with similar settings for which total nitrate utilization and

diagenetic enrichment by $\sim 3\text{-}4\text{‰}$ has been considered. Similar to the study area, the latter areas are characterized by low TOC in the sediments as well as high O_2 in the water column (Altabet and Francois 1994a, Francois et al. 1997). If the values presented in this chapter showed such a diagenetic offset, they would reflect extremely low nitrate utilization.

Alternatively, the values could be explained by the removal of nitrate, not utilized by phytoplankton, from the surface waters, by physical processes like advection or mixing (Francois et al. 1997). At present there is strong evidence for tidal mixing in the study area (Godfrey and Mansbridge 2000). Another explanation could be that nitrogen (N_2) fixation was of importance. The $\delta^{15}\text{N}$ signature of newly fixed nitrogen is $\sim 0\text{‰}$, close to the isotopic composition of N_2 in air (Wada and Hattori 1979). N_2 fixing cyanobacteria of the genus *Trichodesmium* occur off northwestern Australia (Capone et al. 1997). N_2 fixation provides fixed N to compensate for the deficit in nitrate relative to phosphate that results from denitrification (Falkowski 1997).

The $\delta^{15}\text{N}$ values indicate that if N_2 fixation was of importance, it was more intense during the LGM than the Holocene. This could be for two reasons. First, the inflow of nitrate depleted surface waters from semi-enclosed basins of the Indonesian Seas into the study area may have occurred during the LGM. Inflow of oxygen-depleted waters has been reported for the Indonesian Throughflow sensitive northern Indian Ocean (Vénec-Peyré et al. 1995). At that time sea level was lower and denitrification was likely to occur in those semi-enclosed

basins in the Indonesian Seas, which were characterized by high productivity during the LGM (Linsley 1996, Ahmad et al. 1995). Haug et al. (1998) showed for the Cariaco Basin that denitrification resulted in the removal of nitrate from thermocline depths. This encouraged the growth of N_2 -fixing cyanobacteria when this nitrate deficit was transferred into the surface layer by mixing. A N_2 fixation response (Haug et al. 1998) to glacial/interglacial variations in denitrification on a global scale in the open ocean (Altabet et al. 1995, Ganeshram et al. 1995) is not likely to have occurred in the study area. The trend seen in the data does not accord with global trends of a glacial decrease in denitrification, accompanied by an increase in the oceanic nitrate reservoir, as the values suggest that N_2 fixation would have been more likely to occur during glacials in the Timor Trough.

Second, apart from the reported evidence for changes in the nutrient supply due to variations in the strength of the ITF, it cannot be excluded that changes in N_2 fixation may have been influenced by other factors. Besides phosphorus, N_2 -fixing cyanobacteria need trace elements, in particular iron and molybdenum (e.g. Capone et al. 1997). Given the lower sea level and the increase in dust flux to the study area during the LGM, metal input is likely to have been higher at that time and would not have inhibited higher levels of N_2 fixation. Further studies will be necessary to show the importance of N_2 fixation in the region.

There is still not enough information to unambiguously interpret these $\delta^{15}N$ records in more detail. However, the interpretation of upwelling in the region

during the LGM is derived from a combination of factors. Primarily, the increased productivity during the LGM suggests increased nutrient supply. Previous studies have also shown that during the LGM, the WPWP was reduced in size. Moreover, the present day oceanography favors the occurrence of a shallow thermocline and weak upwelling during El Niño events (Meyers 1996), when the WPWP is reduced in size (Yan et al. 1992).

2.4.4. Fluctuations and lags in proxy records

The TOC, CaCO_3 and $\delta^{13}\text{C}_{\text{TOC}}$ records and their correlation with the $\delta^{18}\text{O}$ record suggest that sea level variations have driven changes in the fertility of the surface waters of the study area. This is because variations in environmental parameters such as SSTs and surface ocean stratification can be expected to be linked to glaciation and sea level history. The parallel trend of the bulk sediment $\delta^{15}\text{N}$ variations suggests coincident changes in the nutrient cycling. However, the lag between $\delta^{15}\text{N}$ and sea level suggests that other factors were important.

The lag of the $\delta^{15}\text{N}$ record compared to the $\delta^{18}\text{O}$ record is of the magnitude of a few thousand years. Similar lags have been observed in other regions and were attributed to a significant $[\text{NO}_3]/[\text{PO}_4]$ change in the global ocean, which would take several thousand years, whereas changes on a regional scale would require less time (e.g. Haug et al. 1998). However, at present there is no proof of a global driving force for the $\delta^{15}\text{N}$ signals.

In addition to the glacial/interglacial changes, higher-frequency fluctuations appear to be recorded in the sediment sequence. Although the resolution and the length of the present data series is not sufficient to ensure that these fluctuations are not subject to noise, similar fluctuations have been observed in other areas of the northern Indian Ocean. Vénec-Peyré et al. (1995), based on correspondence analysis of foraminiferal and radiolarian assemblages, suggested short-term events (with a duration of <5 kyr); for example temporary deepenings of the mixed layer. These authors related these events to the rapid inflow of oxygen-depleted water through the Indonesian straits, as a result of the highest sea level rise during deglaciation. They suggested that the events reflected the reorganization of the oceanographic circulation, before the establishment of the regular interglacial Throughflow. Similar explanations of variable inflow by the ITF could apply in the study area.

The strong contrasts observed at isotope transition 2/1 can be considered to be the oceanic signature of the most rapid sea level rise, which caused an increased outflow of surface waters from the Indonesian basins. Similar contrasts were observed in the Indonesian Throughflow sensitive northern Indian Ocean (e.g. Vénec-Peyré et al. 1997). Evidence for highest sea level rise at that time has been given by reef terraces, which are presently emerged in the region of the Indo-Pacific Ocean (Chappell and Shackleton 1986). The results found in these reef terraces have recently been confirmed by investigations of

the siliciclastic system on the tectonically stable Sunda Shelf in Southeast Asia (Hanebuth et al. 2000).

The high $\delta^{13}\text{C}_{\text{TOC}}$, TOC and CaCO_3 in stage 3 prior to the clearly elevated values in stage 2 may indicate that a phytoplankton community was already established and then fertilized further. This was previously observed for the northern Indian Ocean, and was thought to be related to water stratification (Vénec-Peyré et al. 1995). The more elevated values in stage 2 are linked to lowest sea level which contributed further to shallow water, mixing and more efficient nutrient supply to the surface waters. This is reflected by the minima seen in the $\delta^{15}\text{N}$. Although a detailed interpretation cannot be offered here, the data suggest that the enhanced barium levels in stage 2, which do not occur in stages 3 and 4, are also linked to lowest sea level.

2.5. Conclusions

Glacial-interglacial changes in productivity and nutrient utilization in the Timor Trough in the eastern Indian Ocean appear to reflect changes in the activity of the ITF and sea level. Productivity appears to be inversely proportional to the strength of the ITF. On the basis of the present day oceanography it is inferred that during the Holocene, productivity has been inhibited by stratification of the water column, suppressed vertical mixing and low nutrient concentrations in surface waters. This is because of the narrow band of low salinity water that

moves through the Indonesian Archipelago and spreads out over the equatorial portions of the eastern Indian Ocean.

However, higher surface ocean productivity during the LGM than the Holocene can be inferred for this area; the surface waters being depleted in CO_2 and relative nitrate utilization lower. Covariation of the paleo- $\delta^{15}\text{N}$ signal with changes in paleoproductivity indicates the presence of a higher flux of nutrient-rich water to the surface during the LGM. This higher flux is the result of a shallower thermocline and weak upwelling in the region. The findings reflect the restriction or the absence of this low salinity "cap" of the ITF, which would be in agreement with previous suggestions of a considerably weaker ITF during the LGM. In addition, thermal structure appears to have been influenced by sea level changes in the region.

Apart from the reported evidence for changes in the nutrient supply due to variations in the depth of the thermocline, there is the suggestion that N_2 fixation may have contributed to the N nutrition of the surface waters. Further studies will be necessary, however, to show the importance of N_2 fixation in the region. The paleo-records do not appear to be influenced by changes in the nutrient reservoir in the global ocean, but reflect local changes in nutrient supply. The latter are likely to be caused by changes in sea level and the strength of the ITF.

While the paleorecords give a good indication of past climate change and the mechanisms behind this change, high-resolution studies are needed to fully understand the nature of the climate mechanism in the region of the eastern Indian Ocean. High-resolution studies can be performed using massive coral. However, the potential of massive coral from the region of the eastern Indian Ocean to act as paleoclimate proxies still needs extensive testing. The following two chapters test the potential of corals from Ningaloo Reef in Western Australia for paleoceanographic and paleoclimate studies for the region of the eastern Indian Ocean in the more recent past.

CHAPTER III

Validity of paleoceanographic reconstructions from massive corals

—

Implications for sea surface temperature reconstructions for the Last Glacial Maximum and the Holocene

3.1. Introduction

Sea surface temperatures (SSTs) are an important quantity for understanding past climate dynamics, and estimates of SSTs are an essential boundary condition used in general circulation models of past and future climate (Graham 1995, Bush 1999). Large negative SST anomalies of 4 to 6.5°C have been reconstructed for the last deglaciation and the Last Glacial Maximum (LGM) using $\delta^{18}\text{O}$ and Sr/Ca measurements in scleractinian corals (Guilderson et al. 1994, Beck et al. 1997). The tropical SSTs recorded from fossil coral for the LGM (Guilderson et al. 1994), however, are much lower than those recorded from other marine proxies. These proxies, which include foraminifera speciation (CLIMAP 1981, Mix et al. 1986), foraminiferal oxygen isotopes (Broecker 1986, Birchfield 1987) and alkenone results (Lyle et al. 1992, Rostek et al. 1993,

Sikes and Keigwin 1994), suggest a cooling of no more than 3°C. At present, it is not clear if this difference reflects regional differences in the extent of cooling, or if one group of proxies is misleading (Broecker 1996). Another surprising finding is the large warming and/or freshening trends for the ocean surface over the last 200 years indicated by many recent coral $\delta^{18}\text{O}$ records (reviewed by Gagan et al. 2000). These long-term trends generally exceed those of 20th century instrumental records (Cane et al. 1997) and suggest that tracers in corals may overestimate cooling of the ocean in the past.

Recent studies indicate that anomalously low SST estimates given by Sr/Ca thermometry may be produced by early marine diagenesis including recrystallization and secondary aragonite precipitation in live coral. Secondary inorganic aragonite has a significantly higher Sr/Ca ratio than primary coral aragonite (Enmar et al. 2000). Marine aragonite is more difficult to detect in coral skeletons than calcite but it may be common in corals that are only decades old. Few studies have investigated the geochemical implications of early marine diagenesis; thus the understanding of these for paleoenvironmental and paleoclimate reconstructions is limited.

A common approach used to address the issue of diagenesis is independent geochemical tracers to cross-check the results of coral records. For example, the large cooling for the LGM and the mid-stages of the last deglaciation has been justified because SST reconstructed from both coral $\delta^{18}\text{O}$ and Sr/Ca showed the same large negative temperature anomalies (Guilderson et al.

1994, Beck et al. 1997, McCulloch et al. 1999). In this chapter, it is shown that cool artefacts in coral records can be produced by early marine diagenesis because secondary aragonite is enriched in $\delta^{18}\text{O}$ and Sr/Ca relative to the coral skeleton. In the study area, the enrichment of $\delta^{18}\text{O}$ and Sr/Ca in the secondary aragonite is such that the cool artefacts given by $\delta^{18}\text{O}$ and Sr/Ca are identical in magnitude.

3.2. Procedures

Cores were drilled from live coral colonies at two different locations in Ningaloo Reef Marine Park, Western Australia. One was located in Tantabiddi Lagoon ($21^{\circ}54.3'\text{S}$, $113^{\circ}57.9'\text{E}$) and the other off South Muiron Island ($21^{\circ}41.9'\text{S}$, $114^{\circ}18.8'\text{E}$) (Fig. 3.1). During sampling, water depth to the top of the colony was 3 m and 1 m respectively.

The cores were mounted and sawn to remove slices that were 6-7 mm thick. X-ray diffraction was carried out to detect any secondary calcite with a Siemens D501 diffractor, using Cu $K\alpha$ radiation (40 kV, 40 mA), equipped with a curved graphite monochromator and a scintillation detector. The diffraction data were recorded over a range of 20 to 70 degrees 2θ using a step width of 0.02 degrees per minute at a scan speed of 0.5° per minute. The detection limit was 1%. Thin sections were prepared for different parts of the cores and investigated for the presence of early marine diagenesis, particularly aragonite.

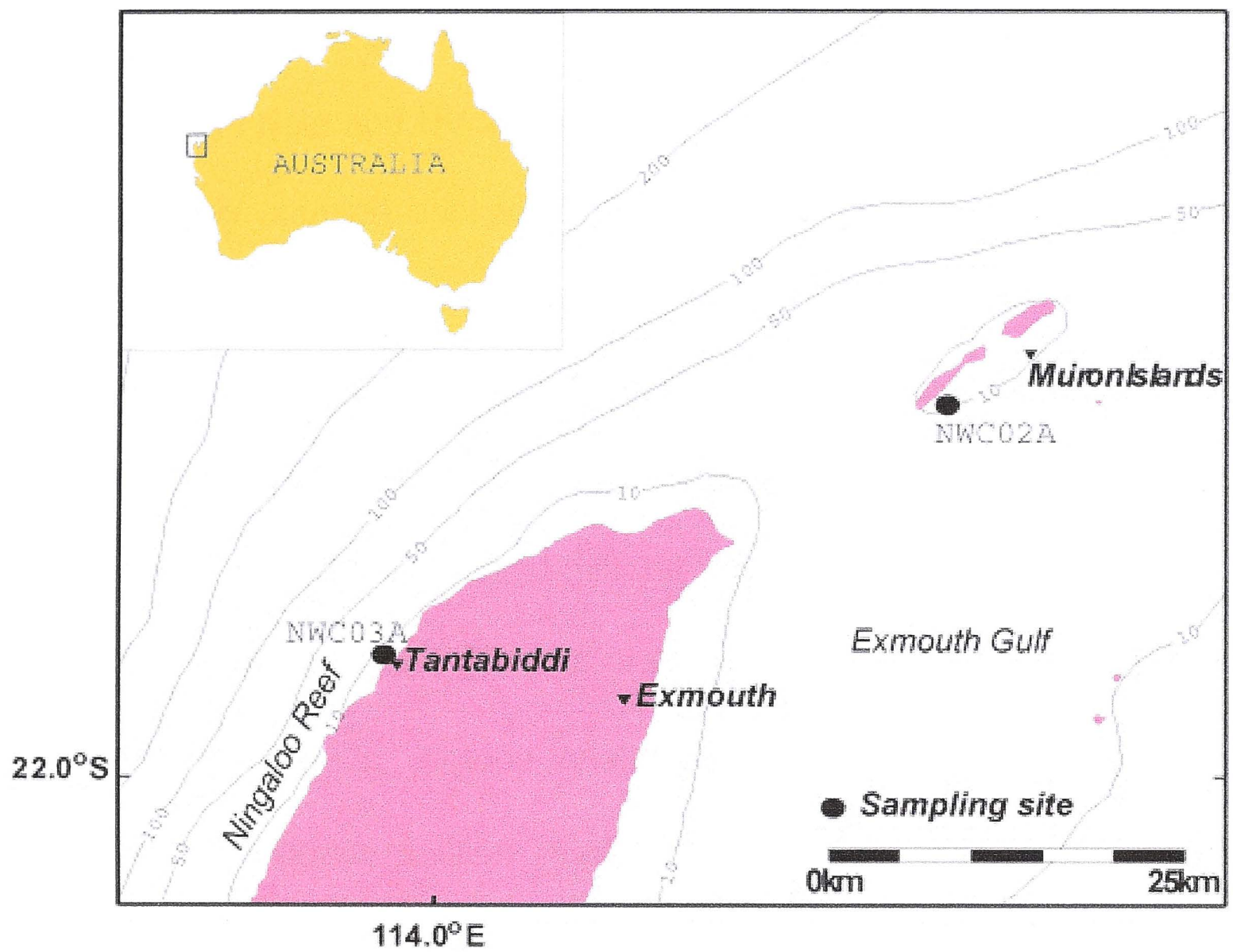


Figure 3.1. Location of the coral study sites at Tantabiddi and South Muiron Island, Ningaloo Reef Marine Park, Western Australia. Bathymetric lines show water depth in m.

Five-year sample increments were chosen using X-ray prints, gamma densitometry data and UV fluorescence light. Peaks in the density profiles were successively counted backwards from the last (outermost or youngest) peak. Surfaces of slabs were cleaned before sampling by removing 1 mm deep and 2 mm wide grooves cut continuously along the maximum growth axis. Five-year increments 2 mm wide and 2 mm deep were then milled within this groove using a 2 mm diameter end-mill bit rotating at 170 RPM. Every second increment was analyzed. Aliquots of powder were analyzed, some in duplicate, for $\delta^{18}\text{O}$ and Sr/Ca. Isotope analysis was carried out using an automated individual carbonate-reaction (Kiel) device coupled with a Finnigan-MAT 251 mass spectrometer. The $\delta^{18}\text{O}$ values were calculated as per mil (‰) deviations relative to VPDB, and were calibrated via the NBS-19 standard ($\delta^{18}\text{O} = -2.20\text{‰}$). Average reproducibility for a typical 150- μg sample was $\pm 0.04\text{‰}$ (2σ , $n=14$), which is equivalent to about $\pm 0.2^\circ\text{C}$ if $\delta^{18}\text{O}$ is controlled by temperature alone. Sr/Ca ratios were measured by isotope dilution on a Finnigan MAT 261 thermal ionisation mass spectrometer (TIMS), following the method described in Alibert and McCulloch (1997). About 80 to 150 μg of powdered coral was diluted in 0.775 ml of 0.5 N HCl. The volume equivalent of 4 μg Ca and one drop phosphoric acid were added to 4-5 drops of a ^{43}Ca - ^{84}Sr -spike solution. The solution was loaded onto a Ta filament and analysed. A power law was used to correct for the instrumental fractionation relative to $^{43}\text{Ca}/^{42}\text{Ca} = 0.960269$ (the spike composition) and $^{86}\text{Sr}/^{88}\text{Sr} = 0.1194$. Mixed solutions of the spike and a gravimetrically known standard were measured at regular intervals to monitor

spike concentration. The reproducibility of Sr/Ca was 0.00005 (2σ) which is equivalent to $<0.2^{\circ}\text{C}$.

3.3. Results

While the results of the XRD analysis show that the coral cores do not contain any detectable amounts of calcite, petrographic investigations indicate that secondary aragonite is present within the coral skeleton toward the base of core NWC02A (South Muiron Island) (Fig. 3.2.A). Abundant secondary aragonite fibres were observed in skeletal pores exposed in thin section. Secondary aragonite could not be seen in core NWC03A (Tantabiddi) (Fig. 3.2.B).

The formation of secondary aragonite fibers in coral, as seen in Fig. 3.2, has previously been suggested to occur under marine conditions (Sansone et al. 1988, Tribble et al. 1990). Generally, as with the coral of this project, cementation in shallow marine subtidal environments is believed to result from turbulent current conditions associated with the discontinuous flow of CaCO_3 saturated seawater through the coral skeletons (Tucker 1991).

The presence of the secondary aragonite is reflected by the dramatic shift in the $\delta^{18}\text{O}$ and Sr/Ca values toward the base of the core. The $\delta^{18}\text{O}$ and Sr/Ca values for the pristine coral show little change over time (Fig. 3.3.A). However, higher $\delta^{18}\text{O}$ and Sr/Ca values can be seen in the cemented bottom part of core NWC02A (South Muiron Island) and are linked to the presence of the

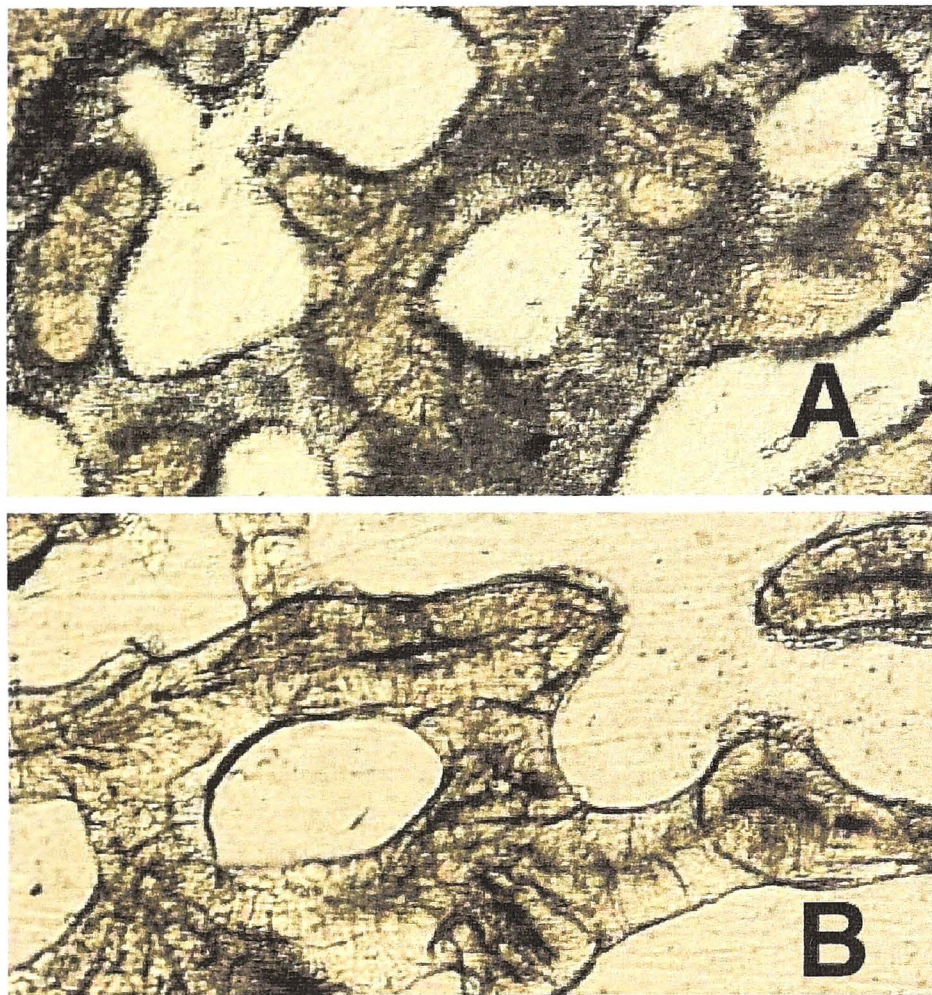


Figure 3.2. Microscopic images of coral cores:
(A) Diagenetically altered coral skeleton in basal part of core NWC02A at South Muiron Island. (B) Pristine coral aragonite of core NWC03A at Tantabiddi.

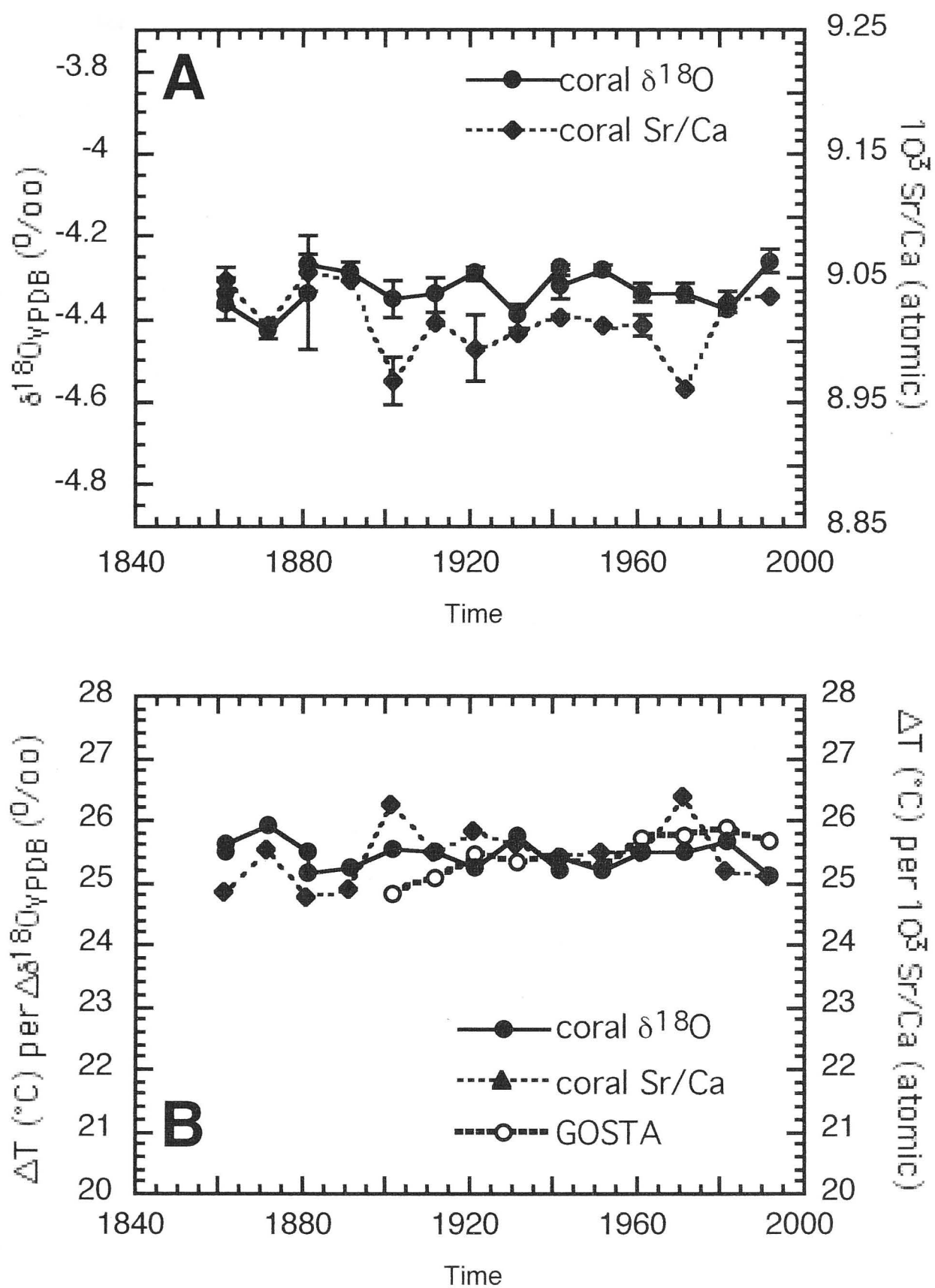


Figure 3.3. (A) $\delta^{18}\text{O}$ (circles) and Sr/Ca values (squares) in the pristine coral core NWC03A at Tantabiddi. Error bars show standard deviation (2σ) for duplicate measurements. (B) Sea surface temperature (SST) units reconstructed from $\delta^{18}\text{O}$ and Sr/Ca values using the mean slopes of five established relationships of temperature change per unit change in $\delta^{18}\text{O}$ (circles) and Sr/Ca (squares). The mean values of $\delta^{18}\text{O}$ and Sr/Ca calculated SST units have been aligned with the mean GOSTA values for the time period 1900-1994. The trends of the relative SST change reconstructed from the geochemical data agree with that of the GOSTA instrumental SST data set (open circles).

secondary aragonite (Fig. 3.4.A). The findings for Sr/Ca are in agreement with those of Enmar et al. (2000), who also reported higher Sr/Ca in early marine inorganic aragonite cements than in pristine *Porites* skeletons. Consequently, in the altered core, there is a trend to lower $\delta^{18}\text{O}$ and Sr/Ca values toward the present, due to the presence of decreasing amounts of this cement which is characterized by high $\delta^{18}\text{O}$ and Sr/Ca values. A change in growth rate does not account for the anomalous skeletal chemistry at the basal part of this core because extension rates were the same at the base of the core as those elsewhere. The results suggest that, in this case, the $\delta^{18}\text{O}$ and Sr/Ca values do not reflect the true SSTs for the altered coral core. SSTs were calculated from $\delta^{18}\text{O}$ using the mean slope of five established equations for the temperature dependence of oxygen isotope fractionation in coral aragonite (Fig. 3.3.B and 3.4.B): $T = (4.854 \pm 0.773)\delta^{18}\text{O}$ (McConnaughey 1989, Leder et al. 1996, Quinn et al. 1996, Wellington et al. 1996, Gagan et al. 1998). Similarly, the mean slope of five published Sr/Ca-SST relationships was used, which were established using TIMS measurements of Sr/Ca to calculate a change in degree Celsius ($^{\circ}\text{C}$) per unit change in Sr/Ca (Fig. 3.3.B and 3.4.B): $T = (17242 \pm 3506)\text{Sr/Ca}$ (Beck et al. 1992, Min et al. 1995, Shen et al. 1996, Alibert and McCulloch 1997, Gagan et al. 1998). To simplify these calculations and since only the slope of the relationship of each tracer to temperature is of interest, only the mean slope of the five equations considered for each tracer was used, and the offset was ignored. Consequently, rather than true SSTs, the relative SST changes per unit in $\delta^{18}\text{O}$ and Sr/Ca respectively were calculated. This

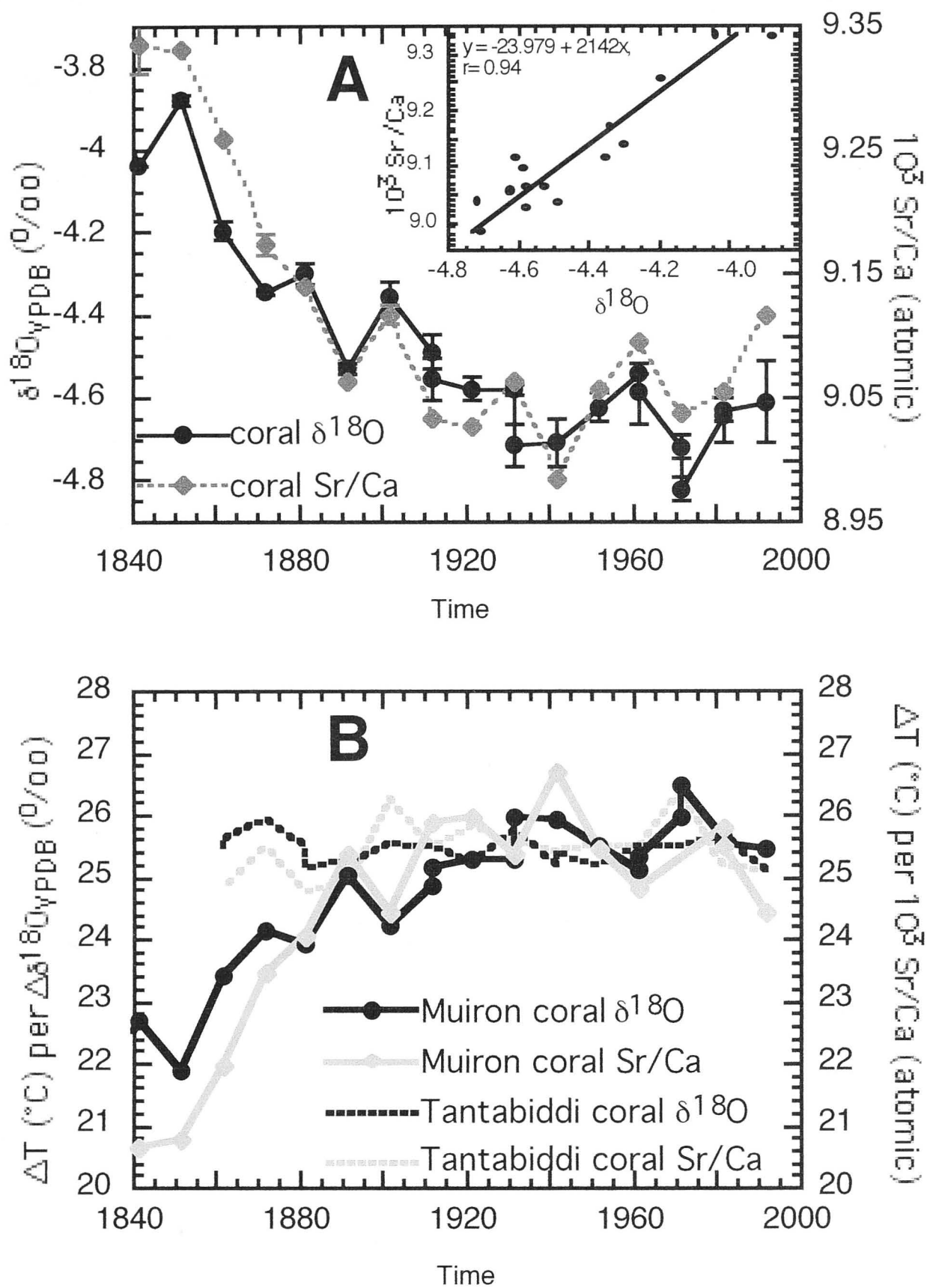


Figure 3.4. (A) $\delta^{18}\text{O}$ (circles) and Sr/Ca values (squares) in the diagenetically altered coral core NWC02A at South Muiron Island. Error bars show standard deviation (2σ) for duplicate measurements. Secondary aragonite toward the base of the altered core causes a shift to higher $\delta^{18}\text{O}$ and Sr/Ca values. Linear regression plots of $\delta^{18}\text{O}$ and Sr/Ca (insert) show good correlation of the two tracers. (B) Reconstructed sea surface temperature (SST) units, calculated from $\delta^{18}\text{O}$ and Sr/Ca as described in Figure 3.3. In this plot, the GOSTA aligned reconstructed SST unit data from both coral cores were compared. This approach was chosen to eliminate the influence of differences in chemistry between the two coral cores in the absence of diagenesis. Because of the high geochemical values of the secondary aragonite present at the base of the South Muiron Island core, the values show a difference in SST between the pristine and the altered coral core of 4-5°C before 1900.

simplification is possible because the least-square approximation for these linear equations shows that the slope would be the same whether the offset was included or not (Fig. 3.5).

For both cores, the means of the reconstructed $\delta^{18}\text{O}$ -SST and Sr/Ca-SST unit values have been aligned with the mean value of the GOSTA instrumental SST data (Parker et al. 1995) for the period 1900-1994 AD (Fig. 3.3.B and 3.4.B). A comparison of the SST unit data with the GOSTA data shows that the $\delta^{18}\text{O}$ and Sr/Ca based SST trends in the pristine coral core correspond reasonably well with those of the GOSTA instrumental SST data set (Fig. 3.3.B). A comparison of the aligned SST unit data from the pristine and the altered core, however, indicates a large difference of 4-5°C in the data from the basal parts of the two cores (Fig. 3.4.B). Both the $\delta^{18}\text{O}$ and Sr/Ca based values record cooler temperatures for the altered core. Interestingly, the coral shows a similar magnitude of decrease in SSTs for $\delta^{18}\text{O}$ and Sr/Ca based reconstructions. The trend for $\delta^{18}\text{O}$ to rise from older to younger regions of the core resembles that of other records that were interpreted to reflect warming/freshening trends of the ocean (Gagan et al. 2000). In contrast, no such trend of decreasing $\delta^{18}\text{O}$ can be seen in the pristine core. There is a strong correlation of $\delta^{18}\text{O}$ and Sr/Ca in the altered core NWC02A off South Muiron Island ($r=0.94$, $n=16$) (insert in Fig. 3.4.A). This indicates simultaneous enrichment of $\delta^{18}\text{O}$ and Sr/Ca, as determined by kinetic behaviour, with the addition of secondary aragonite. The relationship between $\delta^{18}\text{O}$ and Sr/Ca in this core is such that it

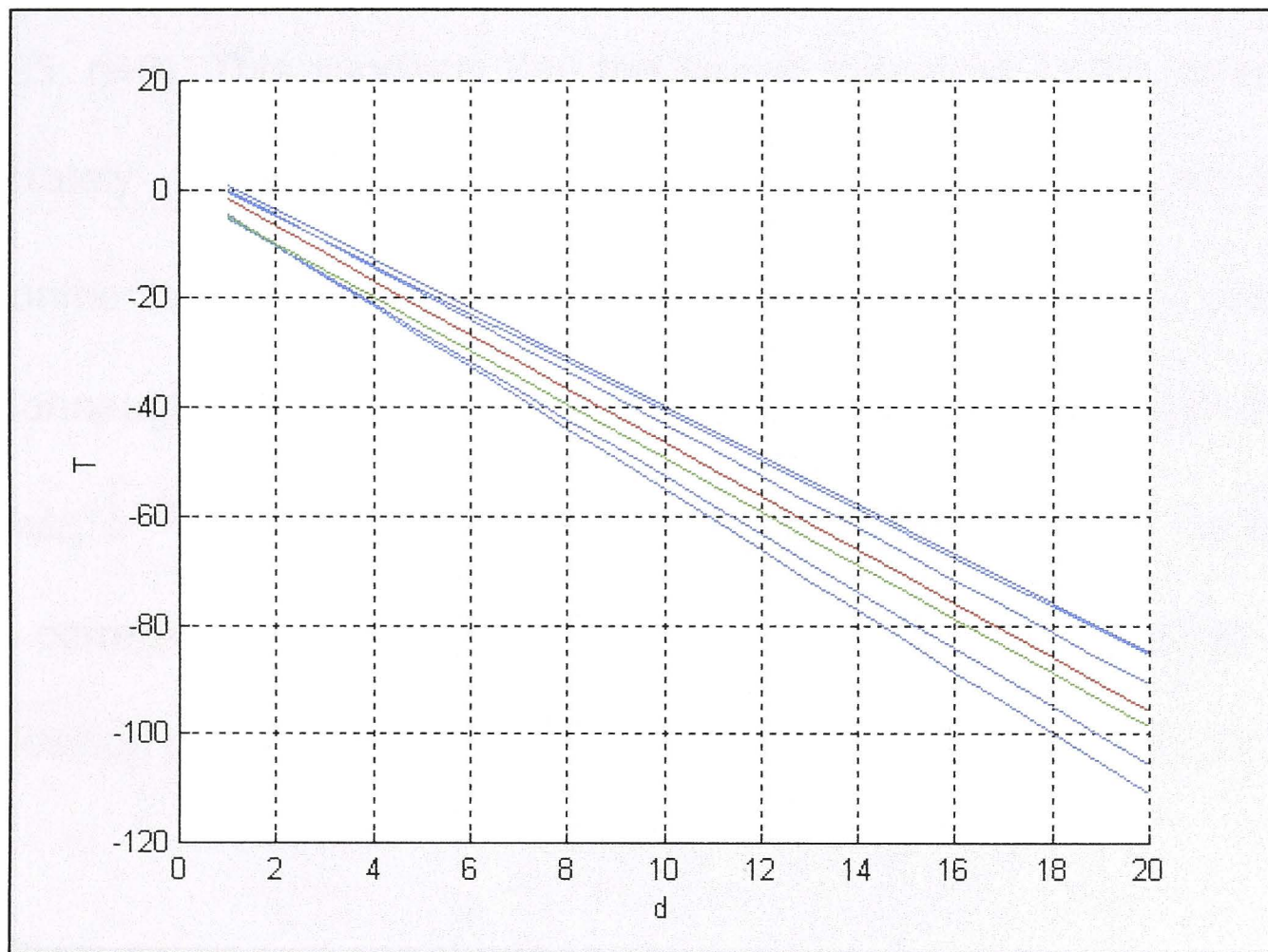


Figure 3.5. Linear curves: The blue curves are the five original curves from the set of published equations $T = 4.76 - 4.79d$, $T = 5.33 - 4.52d$, $T = 0.02 - 5.28d$, $T = 3.97 - 4.48d$, $T = 0.82 - 5.59d$. The red curve is the least-squares-error estimated curve and the green curve is the least-squares-error estimated curve when only the slope is considered. For the red curve, $a = -4.93$ and $b = 2.98$.

yields nearly equal SST changes for both tracers regardless of the degree of diagenesis. The slope of the regression line shows that a change in $\delta^{18}\text{O}$ of 0.2‰ (equal to a change of 1°C) would be accompanied by a change in Sr/Ca of 0.8 (equal to a change of 1.3°C). The correlation coefficient in the unaltered upper half of the core is lower ($r=0.57$, $n=8$) than in the altered lower half ($r=0.95$, $n=8$). This suggests that the kinetic behaviour in the coral skeleton is moderately masked by environmental conditions, such as changes in environmental temperature and composition, which can modify $\delta^{18}\text{O}$ (McConnaughey 1989) and Sr/Ca values (Alibert and McCulloch 1997). In contrast, $\delta^{18}\text{O}$ and Sr/Ca values in the unaltered core from Tantabiddi show poor correlation ($r=0.34$, $n=14$), most likely due to changes in isotopic composition of sea water because of high rates of evaporation in the lagoon.

3.4. Discussion and conclusions

Both the skeletal aragonite and the secondary aragonite compositions deviate from equilibrium in that they show depleted compositions in ^{18}O (McConnaughey 1989) and Sr (cf Kinsman and Holland 1969). The cement shows values closest to what would represent equilibrium carbonate precipitation. The correlation in the altered coral core, and particularly in its basal part, suggests a simultaneous depletion of $\delta^{18}\text{O}$ and Sr/Ca for the cement. The simultaneous depletion of ^{18}O and Sr/Ca relative to equilibrium reflects the kinetic effects which have been previously credited with much of the

^{13}C depletion and all of the ^{18}O depletion, relative to isotopic equilibrium (McConnaughey 1989).

As expected, the same temperatures were reconstructed from $\delta^{18}\text{O}$ and Sr/Ca values at the top of the core (Fig. 3.4.B). This was because the $\delta^{18}\text{O}$ and Sr/Ca equations were used which have been set up for pristine coral from known seawater temperatures and isotopic compositions. These calibrations consider the specific departure of coral from equilibrium (McConnaughey 1989).

It was not, however, expected that both tracers would show the same temperature at the base of the core, which proved to be the case (Fig. 3.4.B). In the coral both tracers show a downcore change in the status of kinetic disequilibrium with seawater, with the cement having a different kinetic disequilibrium status than the coral skeleton. The difference in kinetic disequilibrium can be caused by differences in the composition of the solution from which the aragonite crystals of the coral and the cement were precipitated. Another reason for the difference could be a difference in precipitation rate of the aragonite crystals. It might be expected from this difference in kinetic disequilibrium that the temperature equations would not be applicable to the cement and that temperature reconstructions based on these equations would result in different temperatures being reconstructed from each tracer.

The offset between the pristine top and the altered base of the core in Fig. 3.4.B is 4-5°C SST units for both $\delta^{18}\text{O}$ and Sr/Ca. This simultaneous anomaly can be

explained by mechanisms of crystal growth. Contrary to what would be expected, in the secondary aragonite of the coral, both distribution coefficient of Sr and isotope fractionation of ^{18}O are a function of the rate of crystal growth as well as the composition of the layer of solution in the vicinity of the crystal surface. It has previously been shown experimentally that the distribution coefficient of Sr can be a function of the composition of this layer of solution (Kinsman and Holland 1969). This study showed that coprecipitation of Sr^{2+} with aragonite can depend upon surface phenomena rather than upon equilibrium between the solution and the interior of aragonite crystals. The value of the distribution coefficient for Sr would depend upon surface phenomena under certain conditions. One such condition is a high rate of crystal growth. The rate of crystal growth needs to be greater than the rate of diffusion of Sr^{2+} and Ca^{2+} between the solution and the interior of growing aragonite crystals. A second condition is that the rate of crystal growth is sufficiently slow to allow the Sr/Ca ratio in the younger regions of the crystal to adjust itself accordingly by reaction with the solution. In this situation the growth region of the crystal is moved away from older regions before the older regions have time to equilibrate with the precipitating solution. The younger regions have time to equilibrate with the solution. It then follows that the offset is similar for both $\delta^{18}\text{O}$ and Sr/Ca because their distribution in both the coral skeleton and the secondary aragonite is largely controlled by kinetic effects, which are determined by similar mechanisms of crystal growth controlled by surface phenomena.

The covariation in $\delta^{18}\text{O}$ and Sr/Ca in the coral shows that these two measurements do not give an independent evaluation of SSTs and that they cannot reliably be used as cross checks. This implies that chemical cross checks with two tracers may not be sufficient to verify coral records and that textural studies using petrographic observations or scanning electron microscopy must be included to detect potential secondary overgrowths.

The finding of cold Sr/Ca artefacts produced by diagenesis adds to previous suggestions of potential misinterpretations of SST reconstructions from coral Sr/Ca. For example, it has also been shown that increases in the Sr/Ca ratio of seawater due to large shelf recrystallization fluxes during glacial maxima would produce up to 1.5° errors in paleotemperatures calculated from Sr/Ca ratios in *Porites* since the LGM (Stoll and Schrag 1998).

The magnitude of the "temperature" drop observed in the altered coral is nearly 5°C. This cold artefact is larger than that observed in previous investigations of diagenetic effects on Sr/Ca (Enmar et al. 2000). The magnitude of the decrease in temperature in the coral exceeds that of some observed differences in reconstructed SSTs among different paleo-proxies, as pointed out earlier. Consequently, secondary aragonite in fossil corals must be carefully considered for records suggesting SSTs are cooler than today. Diagenesis can also potentially cause other misinterpretations. When seasonal variations are identifiable (e.g. Guilderson et al. 1994), there would appear to be no diagenetic

bias in the geochemical values. However, diagenesis can change the amplitude even when a seasonal signal is evident (Enmar et al. 2000), thus giving false temperature. As well, interpretation of warming or freshening trends in coral records can be affected by early marine diagenesis. Nearly all published coral $\delta^{18}\text{O}$ records show warming/freshening trends toward the present over the last 200 years. It is possible that many of these trends are in fact related to secondary aragonite accumulating over 10s of years, beginning at the older base of the corals. Clearly, these trends have to be critically assessed, and care taken in drawing conclusions from $\delta^{18}\text{O}$ trends on the role of the tropical oceans in the hydrological cycle.

Other trends important involve changes in surface-ocean $^{13}\text{C}/^{12}\text{C}$, surface-ocean carbonate saturation state and coral reef growth as a response to global climate change. The reconstruction of these changes from massive coral is addressed in the following chapter.

CHAPTER IV

Coral reconstructions of 20th century changes in surface-ocean

$^{13}\text{C} / ^{12}\text{C}$ and carbonate saturation state

—

Important tracers and potential errors

4.1. Introduction

Recent research suggests that future decreases in the aragonite saturation state of surface seawater associated with the projected build-up of atmospheric CO_2 could cause a global decline in coral reef-building capacity (Gattuso et al. 1999, Kleypas et al. 1999a, Langdon et al. 2000, Leclercq et al. 2000). Whether significant reductions in coral calcification are underway is a matter of considerable debate.

Studies of environmental proxies in massive coral skeletons have provided evidence for changes in coral reef growth over the past few centuries. For example, a combined record from 35 long coral cores from the Great Barrier Reef (GBR) showed a significant decline in skeletal density and calcification but not linear extension rate over the common period 1934-1982 (Lough and Barnes 1997). Analyses of several of the longest coral cores suggest, however, a significant increase in calcification rate in the late 20th century on the GBR

(Lough and Barnes 2000) compared with the previous two centuries. Analysis of a long coral core from French Polynesia also shows increased calcification through time (Bessat and Buiges 2001). Both these studies attributed the rise in calcification rate to increased sea water temperatures. Lough and Barnes (1997) did, however, note a tendency for skeletal density to decline through time in the majority of the 35 coral cores examined with ages varying from 49 to 507 years. The average skeletal density in 60% of the long coral cores was significantly higher in the oldest 30 years compared with the youngest 30 years. There were no significant changes in linear extension or calcification rates over the same periods.

In addition to changes in coral growth parameters, several studies report a decrease in coral skeleton $\delta^{13}\text{C}$ values at tropical sites during the 20th century (Carriquiry et al. 1994, Swart et al. 1996a, 1996b, Quinn et al. 1996a, 1996b, 1998, Wellington and Dunbar 1995, Roulier and Quinn 1995, Felis et al. 1998). The slopes of these trends vary. Although a number of the trends have been attributed to geomorphological development of reefs or building activities next to the reef, most studies suggest the decrease in coral $\delta^{13}\text{C}$ is due to changes in seawater carbonate chemistry. A decrease in $\delta^{13}\text{C}$ is considered to result from a decline in photosynthesis or a change in the dissolved inorganic carbon concentration (DIC).

Changes in seawater carbonate chemistry may have several implications for rates of photosynthetic CO_2 fixation (photosynthesis) and CaCO_3 precipitation

(calcification) of marine organisms and ecosystems. Photosynthesis and calcification in coral reefs depend on seawater chemistry. An increase of DIC concentrations and a reduction in pH lowers aragonite saturation levels and results in lower rates of photosynthesis and calcification (Spero et al. 1997, Smith and Buddemeier 1992). Gattuso et al. (1998) provided experimental evidence for a nonlinear increase in calcification rate as a function of aragonite saturation levels. This dependence of calcification on the carbonate saturation state occurs both at the organism and ecosystem scale (Mann 1986). It has been suggested that a decreased saturation state will result in reduced coral calcification rates, a shift toward calcite secretors, or a competitive advantage for noncalcifying reef organisms (Smith and Buddemeier 1992, Buddemeier 1994).

Experimental and modeling studies have suggested that rates of coral calcification have declined since the late 19th century. These studies also project significant decreases into the future as a result of the decrease in the saturation levels due to the anthropogenic release of CO₂ into the atmosphere (Gattuso et al. 1999, Kleypas et al. 1999a, Langdon et al. 2000, Leclercq et al. 2000, Marubini et al. 2001). Recent estimates suggest that the global ocean presently increases its storage of CO₂ by 1.7 +/- 0.9 Pg C yr⁻¹ (Keeling et al. 1996) because of this anthropogenically induced increase of atmospheric CO₂ partial pressure and pCO₂ equilibration across the air-sea interface (Houghton et al. 1996). As significant acclimation of coral to a reduced saturation state is not expected, it is estimated that a 40% decline in saturation state from 1880 to

2065 will occur due to the effect of rising CO_2 and temperature on saturation state (Langdon et al. 2000). Estimates of tropical sea surface carbonate saturation levels under conditions of a doubling of the preindustrial pCO_2 are about 14 to 28% (Kleypas et al. 1999a) or two-thirds of present values (Smith and Buddemeier 1992).

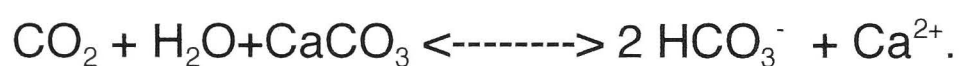
In this chapter it is shown that there may be a diagenetic tendency toward lower skeletal density and calcification rates toward the youngest part of large coral colonies. This tendency could lead to erroneous interpretation of past trends of reef growth and reef composition. Any evidence for reduced coral calcification in recent decades must be supported by evidence that early marine diagenesis is not present in the coral cores. Furthermore, the results show that artefacts of high $\delta^{13}\text{C}$ in coral records can be produced by early marine diagenesis because secondary aragonite is enriched in $\delta^{13}\text{C}$ relative to the coral skeleton. The enrichment of $\delta^{13}\text{C}$ in the secondary aragonite is such that the productivity artefacts given by $\delta^{13}\text{C}$ and calcification rates show the same trends. This can lead to incorrect conclusions on reduced calcification, aragonite saturation state of the ocean and, consequently, past and future trends in atmospheric pCO_2 .

4.2. Carbonate geochemistry and coral calcification

The addition of fossil fuel CO_2 decreases surface-ocean pH and thus the carbonate ion concentration $[\text{CO}_3^{2-}]$ in seawater, which can be explained as follows. In seawater, DIC occurs in three basic forms: CO_2^* ($\text{CO}_2(\text{aq}) + \text{H}_2\text{CO}_3$),

HCO_3^- , and CO_3^{2-} . When CO_2 dissolves in seawater, most dissociates into HCO_3^- and CO_3^{2-} , and less than 1% remains as CO_2^* . Under normal seawater conditions of pH 8.0-8.2, (HCO_3^-) is about 6 to 10 times (CO_3^{2-}).

So while the addition of CO_2 to seawater enhances CaCO_3 dissolution, the removal of CO_2 would result in increased CaCO_3 precipitation. This seawater-mediated interaction of CO_2 and calcium carbonate is described by the equation:



The acid formed by dissolution of CO_2 in seawater lowers the pH, so that, according to the equation, some CO_3^{2-} will combine with H^+ to form HCO_3^- to achieve a new equilibrium. Consequently, CO_2 uptake by surface seawater, which is associated with pCO_2 equilibration across the air-sea interface under conditions of increased atmospheric CO_2 partial pressure, increases the concentration of DIC and decreases pH.

Decreasing pH results in a decrease of the aragonite saturation state. Generally, the saturation of seawater with respect to calcium carbonate (calcite and aragonite) is defined as the ratio of the ion activity product to the stoichiometric solubility product (Morse and Mackenzie 1990). The calcium carbonate saturation state is largely determined by CO_3^{2-} because Ca^{2+} is near

conservative in seawater (Broecker and Peng 1982). If the saturation equals 100%, the solid and solution are in equilibrium.

Increased DIC concentrations and reduced pH result in lower rates of photosynthesis and calcification. Photosynthesis appears to elevate skeletal $\delta^{13}\text{C}$ in most calcareous groups (Weber and Woodhead 1970, Goreau 1977, Swart 1983, McConnaughey 1989, Grottoli 2002). There are, however, suggestions that photosynthesis reduces skeletal $\delta^{13}\text{C}$ (Erez 1978, Erez and Honjo 1981, Williams et al. 1981 a, b), because it increases the efficiency with which ^{13}C depleted respired CO_2 is fixed into the skeleton. These suggestions, however, are not widely accepted because they do not offer any explanation for the physiology of such a phenomenon. Furthermore, it is likely that these studies did not appreciate the separate influence of kinetic effects. An apparent negative modulation of skeletal $\delta^{13}\text{C}$ by photosynthesis involves an association between kinetic disequilibria and rapid skeletal growth. The kinetic depletion of ^{13}C sometimes overpowers the photosynthetic (metabolic) ^{13}C increase, causing negative correlation between photosynthesis and skeletal $\delta^{13}\text{C}$ (McConnaughey 1989). Here the interpretation of $\delta^{13}\text{C}$ values is based on the model that increased rates of photosynthesis increase $\delta^{13}\text{C}$ values in the coral skeleton. Consequently, low rates of photosynthesis and calcification due to increased DIC levels and reduced pH as a result of anthropogenic release of CO_2 into the atmosphere will lead to lower $\delta^{13}\text{C}$ values in the coral skeleton.

4.3. Procedures

The two coral cores from Ningaloo Reef Marine Park in Western Australia (Fig. 3.1) were further investigated in this chapter. Density was measured directly on coral slices using gamma densitometry (Chalker and Barnes 1990). Peaks in density defining annual growth increments were successively counted backwards from the outermost (youngest) peak. The following time series were obtained from the density measurements for each core: (1) mean annual density ($\text{g}\cdot\text{cm}^{-3}$); (2) annual extension rate as the distance between high-density peaks ($\text{cm}\cdot\text{yr}^{-1}$); and (3) annual calcification rate as the product of mean annual density and annual extension ($\text{g}\cdot\text{cm}^{-2}\cdot\text{yr}^{-1}$).

The mean value for calcification rates before 1880 was calculated as an estimate of 'pre-industrial' calcification. This value has been considered equal to 100% calcification for preindustrial times. Based on this value the percentages of calcification after 1880 have been calculated. For the altered core NWC02A (South Muiron Island) a mean of 1.4985 was used from 1830 to 1879 (there was no value for 1880). For the pristine core NWC03A (Tantabiddi) the mean was 1.6577 for the time period 1857-1880, including 1880. A second order polynomial curve fit was then plotted for these percentages to make the trend of coral calcification clearer.

In contrast to Chapter III where only every second aliquot from 5-year sample increments was used, the complete series of aliquots of coral powder was analyzed in this chapter. Isotope analysis of $\delta^{18}\text{O}$ and $\delta^{13}\text{C}$ was carried out as described for $\delta^{18}\text{O}$ in Chapter III. The $\delta^{13}\text{C}$ values were calculated as per mil (‰) deviations relative to VPDB, and were calibrated via the NBS-19 standard ($\delta^{13}\text{C} = 1.95\text{‰}$). Average reproducibility of duplicate 150- μg samples (2σ , $n = 14$) was $\delta^{18}\text{O}$ and $\pm 0.04\text{‰}$ for $\delta^{13}\text{C}$.

4.4. Results

While no secondary aragonite was seen in core NWC03A (Tantabiddi) (Fig. 3.2.A), secondary aragonite needles filled the skeletal pores almost completely in some areas at the base of core NWC02A (South Muiron Island) (Fig. 3.2.B) and accounted for 30% of the total aragonite (primary and secondary aragonite).

The density for the pristine coral did not show significant change over time (Fig. 4.1.A). This coral shows a decline in extension rate toward the present (Fig. 4.2.A), resulting in a slight decline in calcification rates toward the present. Such a change in extension is likely to reflect a true change in photosynthesis and/or calcification (Kleypas et al. 1999b). As with density, the $\delta^{13}\text{C}$ and $\delta^{18}\text{O}$ values did not show significant change over time (Fig. 4.3.A). In contrast, for the altered core higher skeletal density was measured in the altered coral sections where secondary aragonite filled the pores of the original coral skeleton and

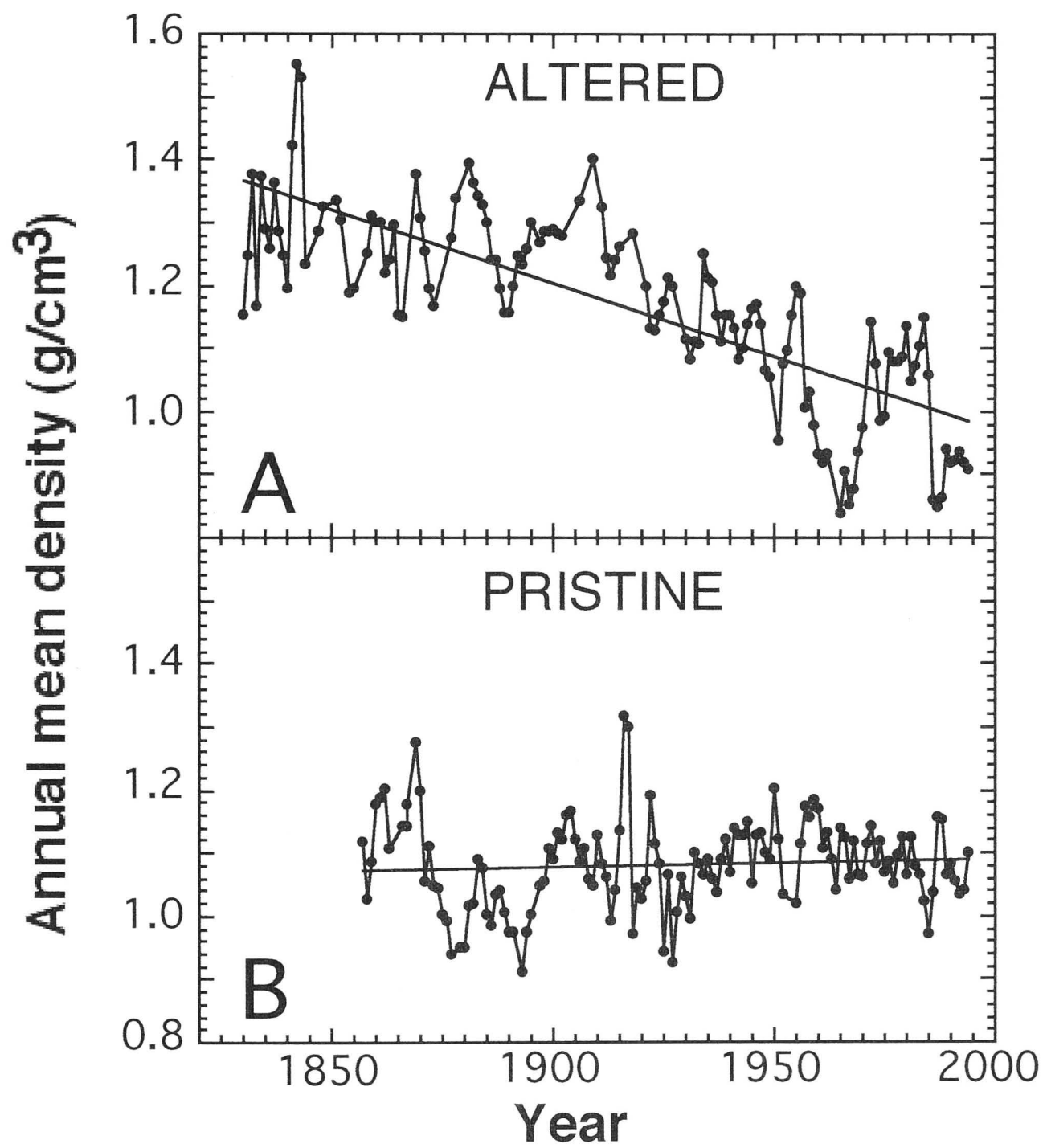


Figure 4.1. Mean density values for (A) pristine and (B) diagenetically altered coral.

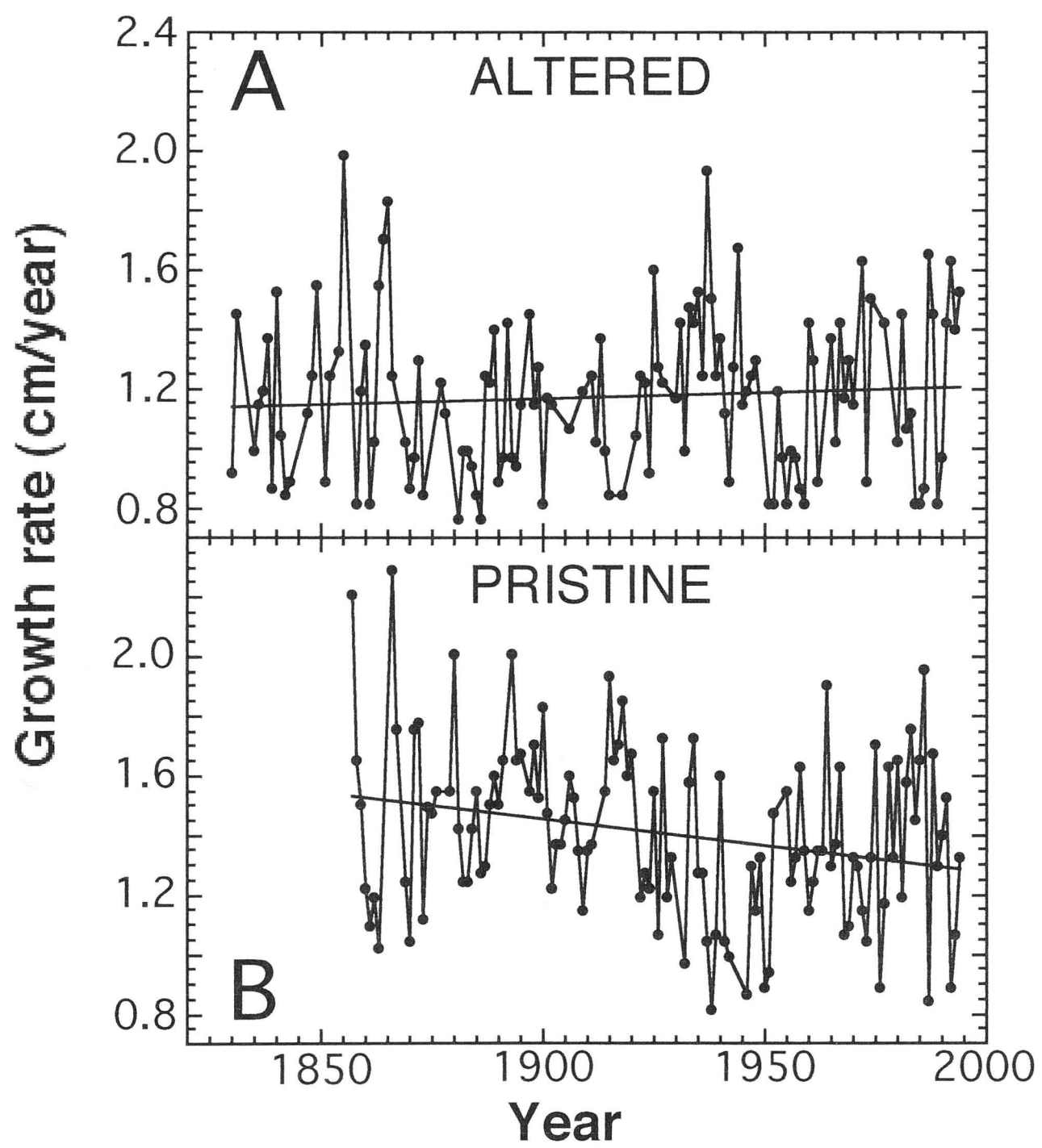


Figure 4.2. Coral growth rates for (A) for pristine and (B) diagenetically altered coral.

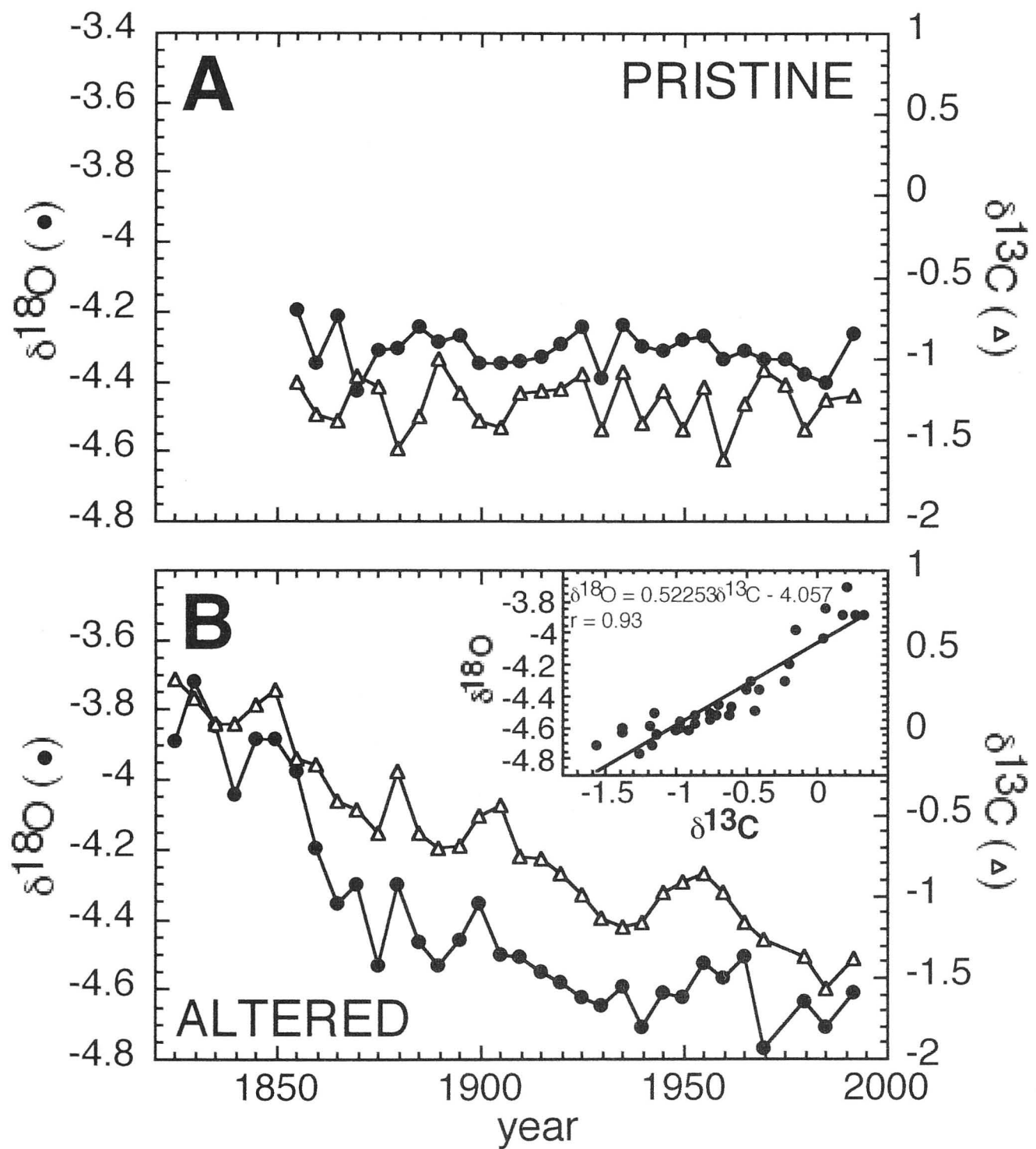


Figure 4.3. $\delta^{18}\text{O}$ and $\delta^{13}\text{C}$ data for (A) pristine coral and (B) diagenetically altered coral. The $\delta^{18}\text{O}$ values correlate with the $\delta^{13}\text{C}$ values in the diagenetically altered coral. Furthermore, the altered base of the core shows $\delta^{18}\text{O}$ representative of cooler SST, giving the impression of a warming trend of the surface ocean towards the present.

there was a significant decrease in skeletal density through time (Fig. 4.1.B). Linear extension rates (Fig. 4.2) were not affected by the cementation, because the annual density peaks were not overprinted by the presence of the cement. Since calcification rates are a product of mean density and linear extension rate, the trend of decreasing values through time seen in the density values was also evident in the calcification rates. As secondary aragonite was present in the older part of the core, the calcification rate, the $\delta^{13}\text{C}$ and $\delta^{18}\text{O}$ showed declining trends toward the youngest part of the coral core (Fig. 4.3.B). The decline in $\delta^{13}\text{C}$ values was as large as 1.7‰.

There was no significant correlation between the $\delta^{13}\text{C}$ and $\delta^{18}\text{O}$ in the pristine core NWC03A. In contrast, the $\delta^{13}\text{C}$ values of the altered core NWC02A showed good agreement with the $\delta^{18}\text{O}$ ($r=0.93$, $n=33$, Fig. 4.3.B).

4.5. Discussion

The results of this chapter demonstrate that a long-term decline in skeletal density and calcification rate over the life of a coral colony may be purely an artefact of early marine diagenesis in the oldest part of the coral skeleton. This may be especially relevant to previous ecological studies, which traditionally tend not to include mineralogical and petrographical investigation of the coral material. Yet, many of these studies are used to provide basic information for deriving conclusions on long-term and/or regional changes in reef growth (e.g. Lough and Barnes 1997, Lough and Barnes 2000).

The findings of higher $\delta^{13}\text{C}$ in the cemented part are in agreement with those of Gonzáles and Lohmann (1985), who also reported higher $\delta^{13}\text{C}$ values in early marine inorganic aragonite cements than in pristine *Porites* skeletons. Thus, diagenesis can seriously affect paleoceanographic reconstructions from $\delta^{13}\text{C}$ and calcification. There are a number of possible interpretations for the trend in $\delta^{13}\text{C}$ seen in the altered coral core (Fig. 4.3.B) if diagenesis remains undetected. First, in the context of previous observations, the trend in the $\delta^{13}\text{C}$ time series in the altered core would suggest dramatic changes in DIC because some of the trends to lighter $\delta^{13}\text{C}$ values toward the present have been interpreted to reflect the isotopic composition of DIC (reviewed by Swart 1983). This composition is believed to be influenced by the CO_2 concentration of the atmosphere, where the increased input of ^{12}C from the burning of fossil fuel dilutes ^{13}C (Keeling et al. 1989). However, this is incorrect as the values are influenced by the presence of secondary aragonite. This suggests that, similarly, the differing gradients of published coral $\delta^{13}\text{C}$ time series may be caused by alteration of coral cores rather than biological overprints or changes in DIC.

A second possible interpretation of the $\delta^{13}\text{C}$ trend is that photosynthesis slowed down toward the present resulting in lower $\delta^{13}\text{C}$ values together with lower calcification rates. If the diagenetic alteration were overlooked, the variation in the $\delta^{13}\text{C}$ values in the altered coral core would appear to be due to

metabolic isotope effects, caused by variations in the $\delta^{13}\text{C}$ of the DIC reservoir due to photosynthesis and respiration (McConnaughey 1989). High photosynthesis rates cause a depletion of the coral's internal reservoir of inorganic carbon in ^{12}C , resulting in an enrichment of the coral skeleton in ^{13}C (reviewed by Swart 1983).

A third possibility is that the values could reflect a lower ratio of photosynthesis to respiration (P/R) in the younger part of the coral. Conversely to photosynthesis, respiration lowers the $\delta^{13}\text{C}$ of the inorganic carbon reservoir because biomass is depleted in ^{13}C . So, as with a low photosynthesis rate, a low P/R ratio results in low $\delta^{13}\text{C}$ in coral skeletons, because of the excess of respired CO_2 that is incorporated into the skeleton at reduced photosynthesis (McConnaughey 1989). However, in contrast to other calcifying organisms, the respiratory effect on the skeletal $\delta^{13}\text{C}$ in coral is believed to be small compared to the photosynthesis effect (McConnaughey 1989). The trend in the $\delta^{13}\text{C}$ values would therefore be attributed to a change in the rate of photosynthesis. Such an interpretation would lead us to the conclusion that photosynthesis of the coral has slowed down during this century. If the $\delta^{13}\text{C}$ trends of other studies were to be taken into account, it would mistakenly be concluded that photosynthesis of many reefs in the world has slowed down during this century.

Covariation of the carbon and oxygen isotopic compositions, as seen in the altered coral, has been shown in previous investigations of Holocene reef

carbonates (González and Lohmann 1985). Such a covariation has also been seen in a Permian Reef complex (Given and Lohmann 1985). It appears that this covariation is an expression of cemental carbonate precipitation occurring close to equilibrium. This is supported by the magnitude of the values, which shows that the cement is the component with the most enriched isotopic compositions, i.e. closest to what would represent equilibrium carbonate precipitation. Furthermore, although marine carbonate components have been shown to exhibit apparent disequilibrium relative to predicted compositions, no mechanism for producing enrichment in both carbon and oxygen in normal marine, non-evaporative settings has been postulated so far (González and Lohmann 1985). Disequilibrium compositions occur because of biological fractionation or “vital effects” or because of kinetic fractionation related to rates of precipitation. Either process, however, would result in depleted rather than enriched compositions (cf McConnaughey 1989).

The change in calcification rate over time in the pristine coral (Fig. 4.4.A) resembles the trend of atmospheric $p\text{CO}_2$ data for the past 160 years (Fig. 4.4.B). These data have been compiled from Law Dome ice core data in East Antarctica (Etheridge et al. 1998) and, for the last 40 years, from instrumental measurements at Mauna Loa, Hawaii (Keeling et al. 1995). The trend seen in the coral is caused by a change in extension rates over time, which may be caused by changes in water depth relative to the top of the coral colony. It becomes clear that the trend in calcification rates is not related to changes in atmospheric CO_2 when $\delta^{13}\text{C}$ values of the pristine coral (Fig. 4.5.A) are

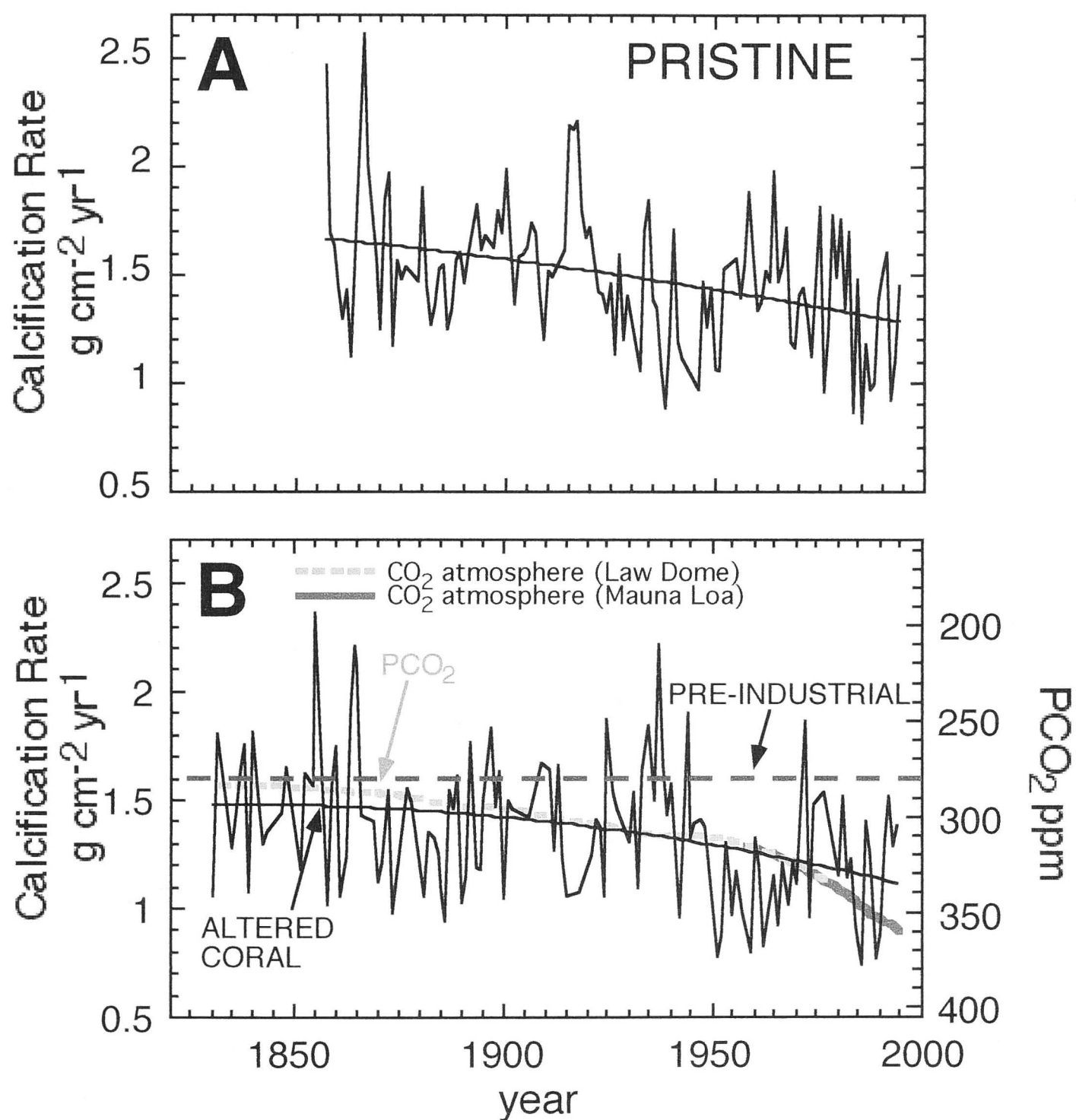


Figure 4.4. Calcification rates for (A) pristine coral and (B) diagenetically altered coral, and second order polynomial curve fits. The curve fit for the diagenetically altered coral (B) follows the trend of atmospheric CO₂ levels derived from ice core (20 year smoothed data, Etheridge et al. 1998) and instrumental data (Keeling et al. 1995). The CO₂ ice core data overlap with the record from direct atmospheric measurements for up to 20 years. The dotted line shows pre-industrial pCO₂ levels of 280 ppm.

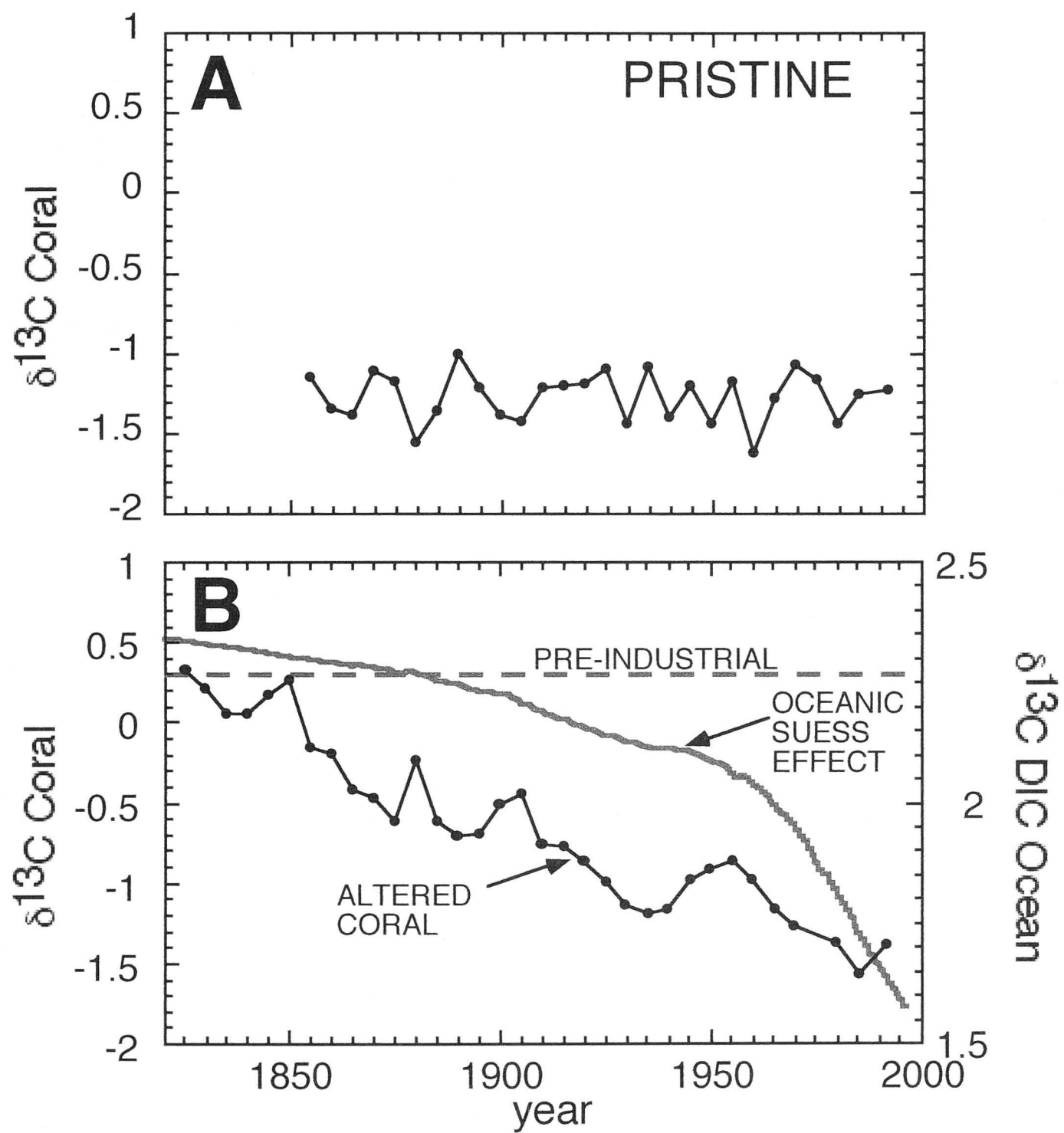


Figure 4.5. $\delta^{13}\text{C}$ data for (C) pristine coral and (D) diagenetically altered coral. The $\delta^{13}\text{C}$ values for the diagenetically altered coral (D) follow the trend of $\delta^{13}\text{C}$ of dissolved inorganic carbon (DIC) caused by the Suess effect for the surface ocean.

compared to the trend of $\delta^{13}\text{C}$ of DIC (Fig. 4.5.B). Since there appears to be no link between the $\delta^{13}\text{C}$ of coral and DIC, the magnitude of which is influenced by the oceanic Suess effect, calcification appears not to reflect atmospheric or oceanic CO_2 trends either.

The changes in calcification observed in the altered coral due to the presence of diagenesis appear to track changes in pCO_2 of the atmosphere (Fig. 4.4.B). The similar trend of coral calcification rates and atmospheric CO_2 levels is supported by the changes in $\delta^{13}\text{C}$. These changes, which are due to diagenesis, appear to track the change in $\delta^{13}\text{C}$ of DIC due to the oceanic Suess effect. The secondary inorganic aragonite is enriched in ^{13}C , relative to coral aragonite, resulting in a 1.7‰ decrease in $\delta^{13}\text{C}$ toward the present, which is similar to the decrease expected from the oceanic Suess effect (Gruber et al. 1999). Taken together, the effect of diagenesis could be misinterpreted to reflect reduction in calcification due to the effect of atmospheric CO_2 on aragonite saturation state of the surface ocean. It is evident from the comparison of the diagenetically altered coral and the pristine coral, however, that the changes in calcification seen in the diagenetically altered coral are not the result of the response of the coral to changes in aragonite saturation of the ocean caused by atmospheric CO_2 . Instead the changes are caused by diagenesis. Furthermore, the $\delta^{13}\text{C}$ values are not a result of a change in $\delta^{13}\text{C}$ of DIC due to the oceanic Suess effect but are a result of diagenesis also.

A comparison of the trend of decline in coral calcification of the diagenetically altered coral with that of experimental and modeling studies (Gattuso et al. 1999, Kleypas et al. 1999a, Leclercq et al. 2000, Langdon et al. 2000) shows that the trend of the calcification rates calculated for the altered coral core would appear to confirm the declining trends calculated by experimental and modeling studies (Fig. 4.6). The slope of the trend and the absolute decline agrees closest with the experimental study of Langdon et al. (2000), who suggest a decline in coral reef calcification between the years 1880 and 2065 A.D. by 40% due to the effect of a changed calcium carbonate saturation state as a result of increased atmospheric CO₂ levels.

Furthermore, the decline in $\delta^{18}\text{O}$ of 1.055‰ in the altered coral (Fig. 4.3.B) would correspond to a warming trend of sea surface temperatures of the ocean of 4-5°C towards the present if the mean slope of five established equations for the temperature dependence of oxygen isotope fractionation in coral aragonite ($T = 4.854 \pm 0.773\delta^{18}\text{O}$) was used to calculate a change in degree °C per unit change in $\delta^{18}\text{O}$ (Chapter 3.3.). The trend of reduced calcification towards the present corresponds with the warming trend. This would appear to contradict the finding that with the initial rise in water temperatures due to an enhanced greenhouse effect, there will be a corresponding increase in coral calcification (Lough and Barnes 2000, Bessat and Buiges 2001).

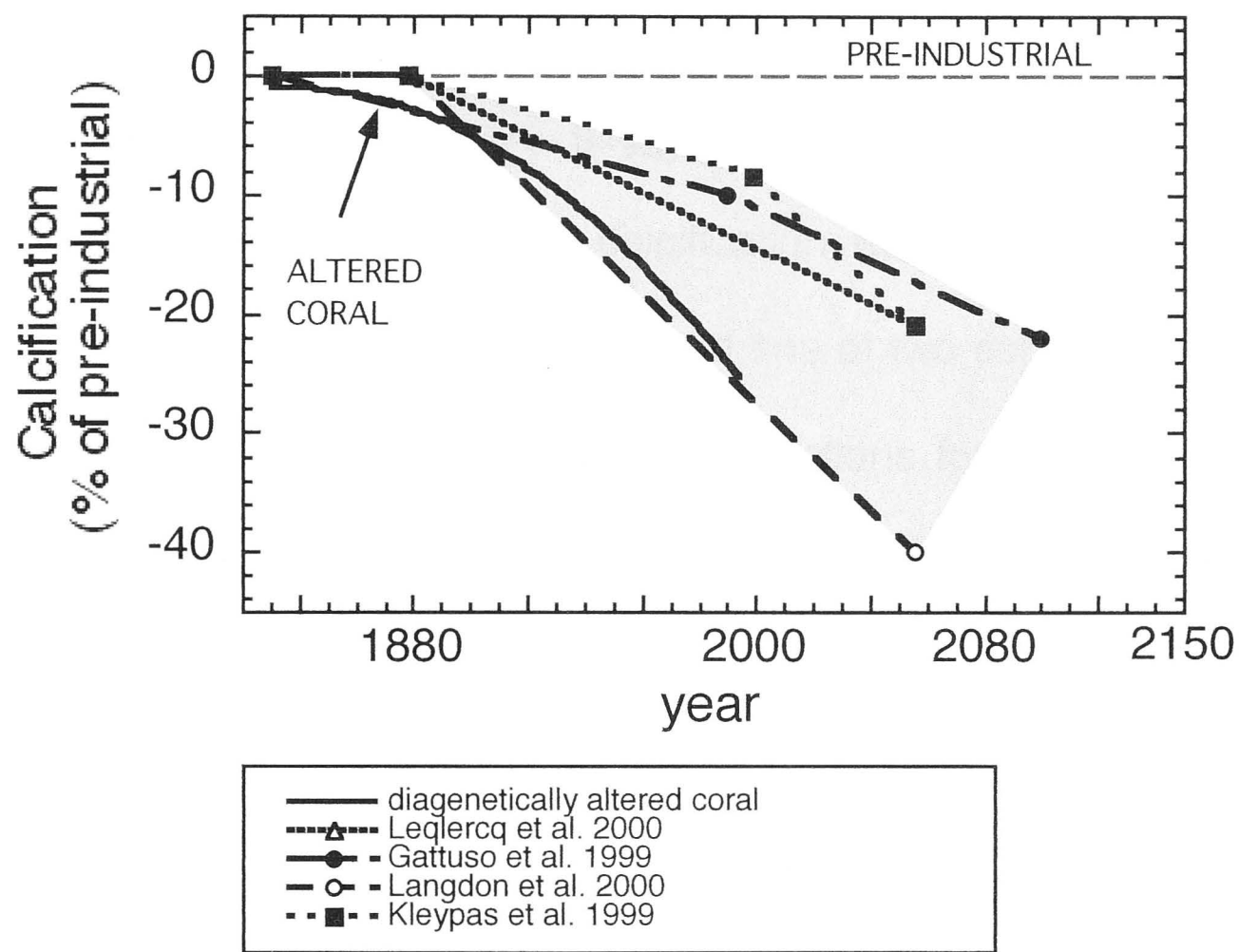


Fig.4.6. Second order polynomial curve fit for calcification rates in % of pre-industrial values (decrease in % after 1880, i.e. compared to pre-industrial values) for the diagenetically altered coral at Muiron Island. This line has been compared to the trends of decline in coral calcification suggested by experimental and modeling studies of Gattuso (1999), Kleypas et al. (1999a), Leclercq et al. (2000) and Langdon et al. (2000).

4.6. Conclusions

An important question for the future of the world's coral reefs concerns the effect of increasing atmospheric CO_2 on coral calcification rates. Experimental and modeling studies have suggested that increased atmospheric CO_2 will result in a decrease of coral calcification rates due to reduced tropical sea surface carbonate saturation levels. In one of two corals examined here, a 30% cementation was estimated from thin sections for the older part of the coral. This cementation and resultant increased skeletal density in the older part of the coral resulted in the coral appearing to show a decrease in calcification through time. The magnitude of this decrease matched modeling and experimental studies of the effects of enhanced atmospheric CO_2 on coral reef calcification. This shows that diagenesis can seriously affect reconstructions of coral reef growth, saturation state of the ocean and atmospheric CO_2 from calcification rates. Furthermore, even small postdepositional alteration of coral skeleton can significantly alter geochemical signals from paleoceanographic tracers.

Contamination of records of coral growth and geochemical composition by early marine diagenesis has significant implications for an understanding of past climate. First, reduced calcification in the younger parts of the coral might be attributed to a reduced aragonite saturation state of the ocean due to increasing atmospheric CO_2 . Second, increased temperatures as derived from

diagenetically altered $\delta^{18}\text{O}$ would reflect warming of the ocean, possibly due to the enhanced greenhouse effect due to increased CO_2 .

Diagenesis, however, can be diagnosed if one or a combination of the following indicators are considered. First, thin section analysis is a strong indicator of diagenesis. Second, comparison of the magnitudes of density and geochemistry changes can also help to detect diagenesis. Third, calcification rates in combination with $\delta^{13}\text{C}$ values allow identification of diagenetic alteration in recent corals.

Correlations of $\delta^{13}\text{C}$ and $\delta^{18}\text{O}$ may also be an indicator of early marine diagenesis in coral. And lastly, the combined use of density, linear extension rates and calcification rates allows differentiation between pristine and diagenetically altered corals. A change in density and calcification values at constant extension rates can be an indicator of diagenesis. In contrast, if extension rate varies in addition to density and/or calcification rates, this variation is likely to reflect a true change in photosynthesis and/or calcification rates. This finding is in agreement with biological studies.

Investigators should be aware that there might be a diagenetic tendency toward lower density toward the younger parts of long coral cores. Evidence for reduced coral calcification in recent decades must be supported by evidence that the coral has not been modified by early diagenesis. If diagenesis remains undetected, the impression is that dramatic changes in calcification rates have

occurred. These suspected calcification rates are then used as boundary conditions in modeling studies on geochemical consequences of increased atmospheric carbon dioxide levels on coral reefs. Models of this type lead to far-reaching conclusions on drastically declining reef-building capacities. These conclusions, however, rely on the application of incorrect boundary conditions.

CHAPTER V

Conclusions

—

Late Quaternary paleoceanography of the eastern Indian Ocean, implications for past climate reconstructions, and recommendations for future studies

The geochemical data of marine sediments and corals presented in this thesis fill an important gap in the observational paleoceanographic data base for the region of the eastern Indian Ocean. The data are essential for the reinforcement of an earlier observation and a first suggestion (Beaufort et al. 2001) of ENSO-like climate variability in the tropical Indian Ocean. They also provide a sound basis for directions of future work aimed at further improvement of the data base. Studies identifying the mechanisms behind ENSO-like climate variability at different time scales in the region depend on such improvement.

As shown in Chapter II, two marine sediment cores from the Indonesian Throughflow sensitive Timor Trough indicate distinct glacial-interglacial contrasts in paleoceanography and paleoclimatology. Elevated biogenic barium, organic carbon, calcium carbonate and $\delta^{13}\text{C}_{\text{TOC}}$ values reflect increased surface ocean productivity during the Last Glacial Maximum (LGM) in the

region. Low $\delta^{15}\text{N}$ values at this time show that such productivity was due to the occurrence of upwelling in the Timor Sea.

The geochemical data records of the sediment cores evidence an El Niño-like mean oceanographic and climatic state during isotope stage 2 and, in particular, during the LGM. A comparison with the modern-day analogue of an El Niño event suggests that, during the LGM, the Indonesian Throughflow (ITF) was suppressed.

Since $\delta^{18}\text{O}$ records are a function of both salinity and temperature, elevated foraminiferal $\delta^{18}\text{O}$ values in the sediment cores point towards lower sea surface temperatures (SSTs) during the LGM as a consequence of upwelling and/or towards higher salinity. Both of these possible interpretations reflect a suppressed ITF. Consequently, both interpretations would confirm the conclusions given above on a suppressed ITF. In order to establish the amount of cooling observed during the LGM, other temperature proxies such as Mg/Ca values of planktonic foraminifera will need to be considered in future research.

An El Niño-like climate state during the LGM would have considerable consequences for precipitation and hydrological balance in the area. As with modern El Niño events, the climate would have been affected by reduced precipitation and stronger winds over the mainland of Australia. New results from modeling studies (P.Hope, pers. comm, 2002) suggest that precipitation was indeed reduced and that stronger zonal (e.g. East-West) winds were

prevalent over Australia during the LGM. While this study allowed reconstruction of the paleoceanography, such as the variability of the ITF over the past 80,000 years, the variability of wind and precipitation patterns over this time period needs further investigation.

The results of analysis of sediments from the eastern Indian Ocean south of the equator reinforce recent suggestions derived from studies of marine sediments in the Indian Ocean north and close to the equator of an El Niño-Southern Oscillation (ENSO)-like equatorial climate mechanism operating at glacial-interglacial time scales in the tropical eastern Indian Ocean.

The contrast observed in this thesis between isotope stages 1 and 2 in the strength of the ITF is clearly an expression of contrasts in mean climate states that occurred during each isotope stage and have been transferred into the eastern Indian Ocean from the equatorial Pacific. Although the data discussed in this thesis evidence contrasts in mean climate stages similar to those of the mean climate states occurring during the opposite phases of ENSO, they do not allow for analysis of oscillations in climate similar to the analysis of Beaufort et al. (2001). In order to determine a possible resemblance of the dynamics of past climate variations in the eastern Indian Ocean south of the equator and those of the Southern Oscillation, the approach of this study needs to be extended further into the past, i.e. beyond the past 80,000 years currently covered in this thesis.

A focus of future studies should not only be the expansion in time and the frequency analysis of existing and future data series for the study area of this thesis. New data series should also extend beyond the time period of the past 250,000 years of Beaufort et al. (2001) both for the study area of this thesis and the study area of Beaufort et al. (2001). Ideally, these new data series should cover time periods including several glacial-interglacial cycles and they should be collected at the same or a higher resolution than those of Beaufort et al. (2001). As the studies of Beaufort et al. (2001) and De Garidel-Thoron et al. (2001) have shown, reliable frequency analysis of these new data series will depend on precise dating of the sediments. Consequently, a larger number than currently available of accelerator mass spectrometer (AMS) ^{14}C ages for the sediment cores of the study area will be required. The proposed future studies are essential for derivation of the true character and driving forces of the equatorial climate mechanism proposed to be responsible for climate variability in the eastern Indian Ocean.

A thorough understanding of an ENSO-like climate mechanism at glacial-interglacial cycles also requires a detailed understanding of the observation of this mechanism in modern times. Although recent studies offer observations of climate variability in the tropical Pacific and the eastern Indian Oceans, attempts to achieve such a detailed understanding have been restricted by the limitation of instrumental data available to study ENSO variability.

Values of $\delta^{18}\text{O}$ and Sr/Ca in massive coral of the eastern Indian Ocean have the potential to augment existing data series on sea surface temperatures and salinities for the region. However, suitable sites for paleoceanographic reconstructions in this region need to be chosen carefully as local reef morphology and environmental conditions at many sites obscure the large-scale paleoceanographic signals linked to climate variability.

The results of this study show that Tantabiddi Bay at Ningaloo Reef is a suitable site for paleoceanographic reconstructions for the region. The coral at this site appears to be a reliable recorder of ENSO variability in the eastern Indian Ocean. As demonstrated in Chapter III, long-term trends of SSTs reconstructed from $\delta^{18}\text{O}$ and Sr/Ca for a well-preserved coral at Tantabiddi Bay correlate strongly with instrumental SST records spanning the 20th century. This shows that the geochemical values of the coral at this site clearly reflect temperature trends. As Ningaloo Reef is strongly influenced by the Leeuwin Current, temperature trends seen in the coral are expected to be influenced by the ENSO dynamics in the western Pacific via the ITF, which feeds the Leeuwin Current. However, it cannot be excluded that the site is also significantly influenced by the Indian Ocean Dipole. Future studies will need to focus on identification of the separate influences of each of the two climate mechanisms and their interference at the study site. Little influence on $\delta^{18}\text{O}$ trends is to be expected from evaporation at Tantabiddi Bay, as increased evaporation occurs simultaneously to higher SSTs in the area. Consequently, evaporation may alter the magnitude of the $\delta^{18}\text{O}$ values at this site, but it does not obscure the long-

term climate trends recorded in the coral of ENSO variability in the eastern Indian Ocean.

The coral data presented in both Chapters III and IV shows that deviations in coral growth parameters and chemistry caused by local reef morphology and environmental conditions obscure reconstructions of the large-scale paleoceanographic signals linked to climate variability such as ENSO. For example, specific forms of reef morphology and local environmental conditions, such as fringing reef environments affected by turbulent water flow, may cause early marine diagenesis in corals that are only decades old. The $\delta^{18}\text{O}$ and Sr/Ca for a diagenetically altered coral from Ningaloo Reef give identical cool SST anomalies of 4-5°C, as a consequence of the addition of secondary aragonite enriched in ^{18}O and Sr. The results indicate that cross-checking of paleoclimate reconstructions with two supposedly independent paleothermometers may not be valid, and that coral records showing cooler SSTs in the past need to be interpreted with caution. Furthermore, modern coral records with long-term trends in $\delta^{18}\text{O}$ indicating recent warming and freshening of the ocean can potentially be explained by early marine diagenesis.

Moreover, taken together, the diagenetic changes in coral calcification rate and skeletal $\delta^{13}\text{C}$, which are presented in Chapter IV for one site at Ningaloo Reef, could be misinterpreted to reflect changes in surface-ocean aragonite saturation state driven by the 20th century build-up of atmospheric CO_2 . If undetected, such

diagenetic changes can lead to erroneous conclusions concerning the oceanic Suess effect as the increased cementation in the older part of a coral can result in an apparent decrease in ^{13}C towards the present. If undetected, such diagenesis can also lead to erroneous conclusions concerning a changing aragonite saturation state due to increasing atmospheric CO_2 as the increased cementation in the older part of a coral can result in an apparent decrease in coral calcification rate towards the present.

The results presented in Chapters III and IV show that correct interpretation of long-term trends in coral growth, isotopic and geochemical tracers must be supported by evidence that the coral skeleton has not been diagenetically altered. With this proviso the records contained in massive coral skeletons can make a significant contribution to understanding and detecting climate change.

References

Abram, N.J., Gagan, M.K., McCulloch, M.T., Chappell, J. and W.S. Hantoro, Coral reef death during the 1997 Indian ocean dipole linked to Indonesian wildfires, *Science* 301, 952-955.

Ahmad, S.M., Guichard, F., Hardjawidjaksana, K., Adisaputra, M.K. and L.D. Labeyrie, Late Quaternary paleoceanography of the Banda Sea, *Marine Geology* 122, 385-397, 1995.

Alibert, C. and M.T. McCulloch, Strontium/calcium ratios in modern Porites corals from the Great Barrier Reef as a proxy for sea surface temperature: Calibration of thermometer and monitoring of ENSO, *Paleoceanography* 12, 345-363, 1997.

Altabet, M.A. and R. Francois, Sedimentary nitrogen isotopic ratio as a recorder for surface ocean nitrate utilization, *Global Biogeochemical Cycles* 8, 103-116, 1994a.

Altabet, M.A. and R. Francois, The use of nitrogen isotopic ratio for reconstruction of past changes in surface ocean nutrient utilization, in *Carbon Cycling in the Glacial Ocean*, edited by R. Zahn, T.F. Pedersen, M. Kaminski, and L. Labeyrie, pp. 281-306, *NATO ASI Series I* 17, 1994b.

Altabet, M.A., Francois, R., Murray, D.W. and W.L. Prell, Climate-related variations in denitrification in the Arabian Sea from sediment $^{15}\text{N}/^{14}\text{N}$ ratios, *Nature* 373, 506-509, 1995.

Archer, D., Equatorial Pacific calcite preservation cycles: production or dissolution, *Paleoceanography* 6, 561-571, 1991.

Archer, D. and E. Maier-Reimer, Effect of deep-sea sedimentary calcite preservation on atmospheric CO_2 concentration, *Nature* 367, 260-263, 1994.

Barnola, J.M., Raynaud, D., Korotkevich, D.Y.S. and C. Lorius, Vostok ice core provides 160,000-year record of atmospheric CO_2 , *Nature* 329, 408-414, 1987.

Beck, J.W., Edwards, R.L., Ito, E., Taylor, F.W., Recy, J., Rougerie, F., Joannot, P. and C. Henin, Sea surface temperature from coral skeletal strontium/calcium ratios, *Science* 257, 644-647, 1992.

Beck, J.W., Récy, J., Taylor, F.W., Edwards, R.L. and G. Cabioch, Abrupt changes in early tropical sea surface temperature derived from coral records, *Nature* 385, 705-707, 1997.

Beaufort, L., Lancelot, Y., Camberlin, P., Cayre, O., Vincent, E., Bassinot, F. and L. Labeyrie, Insolation cycles as a major control of equatorial Indian Ocean primary production, *Science* 278, 1451-1454, 1997.

Beaufort, L., de Garidel-Thoron, T., Mix, A.C. and N.G. Pisias, ENSO-like forcing on oceanic primary production during the Late Pleistocene, *Science* 293, 2440-2444, 2001.

Bessat, F. and D. Buiges, Two centuries of variation in coral growth in a massive *Porites* colony from Moorea (French Polynesia): a response of ocean-atmosphere variability from south central Pacific. *Palaeogeography, Palaeoclimatology, Palaeoecology* 175, 381-392, 2001.

Birchfield, G.E., Changes in deep-ocean water $\delta^{18}\text{O}$ and temperature from the Last Glacial Maximum to the present, *Paleoceanography* 2, 431-442, 1987.

Broecker, W.S., Oxygen isotope constraints on surface ocean temperatures, *Quaternary Research* 26, 121-134, 1986.

Broecker, W.S., Glacial climate in the tropics, *Science* 272, 1902-1904, 1996.

Broecker, W.S. and T.-H. Peng, *Tracers in the Sea*, Lamont-Doherty Geological Observatory, Columbia University, Palisades, New York, 690 p., 1982.

Buddemeier, R.W., Symbiosis, calcification, and environmental interactions, *Bull. Inst. Oceanogr., no. spec. 13*, 119-131, 1994.

Bush, A.B.G., Assessing the impact of mid-Holocene insolation on the atmosphere-ocean system, *Geophysical Research Letters* 26, 99-102, 1999.

Calvert, S.E., The mineralogy and geochemistry of nearshore sediments, in *Treatise on Chemical Oceanography*, Vol. 6, edited by J.P. Riley and R. Chester, pp. 187-280, Academic Press, San Diego, 1976.

Cane, M.A., Clement, A.C., Kaplan, A., Kushnir, Y., Murtugudde, R., Podzdnayakov, D., Seager, R. and S.E. Zebiak, 20th century sea surface temperature trends, *Science* 275, 957-960, 1997.

Capone, D.G., Zehr, J.P., Paerl, H.W., Bergman, B. and E.J. Carpenter, *Trichodesmium*, a globally significant marine cyanobacterium, *Science* 276, 1221-1229, 1997.

Carriquiry, J.D., Risk, M.J. and H.P. Schwarcz, Stable isotope geochemistry of corals from Costa Rica as proxy indicator of the El Niño/Southern Oscillation (ENSO), *Geochimica et Cosmochimica Acta* 58, 335-351, 1994.

Chalker, B.E. and D.J. Barnes, Gamma densitometry for the measurement of coral skeletal density, *Coral Reefs* 4, 95-100, 1990.

Chambers, D.P., Tapley, B.D. and R.H. Stewart, Anomalous warming in the Indian Ocean coincident with El Niño, *Journal of Geophysical Research-Oceans* 104 (C2), 3035-3047, 1999.

Chappell, J. and N.J. Shackleton, Oxygen isotopes and sea level, *Nature* 324, 137-140, 1986.

Clarke, A.J. and X. Liu, Interannual sea level in the northern and eastern Indian Ocean, *Journal of Physical Oceanography* 24, 1224-1235, 1994.

CLIMAP project members, Seasonal reconstructions of the Earth's surface at the last glacial maximum, *Geol.Soc.Am. Map chart ser. MC36*, 1-18, 1981.

Cline, J.D. and I.R. Kaplan, Isotopic fractionation of dissolved nitrate during denitrification in the Eastern Tropical North Pacific Ocean, *Marine Chemistry* 3, 271-299, 1975.

Cole, J.E., Dunbar, R.B., McClanahan, T.R. and N.A. Muthiga, Tropical Pacific forcing of decadal SST variability in the western Indian Ocean over the past two centuries, *Science* 287, 617-619, 2000.

De Garidel-Thoron, T., Beaufort, L., Linsley, B.K. and S. Dannemann, Millennial-scale dynamics of the East Asian winter monsoon during the last 200,000 years, *Paleoceanography* 16, 1-12, 2001.

Degens, E.T., Guillard, R.R.L., Sackett, W.M. and J.A. Hellebust, Metabolic fractionation of carbon isotopes in marine plankton - I. Temperature and respiration experiments, *Deep-Sea Research* 15, 1-9, 1968.

Descolas-Gros, C. and M.R. Fontugne, Carbon fixation in marine phytoplankton: carboxylase and paleoclimatological aspects, *Marine Biology* 87, 1-6, 1985.

Dymond, J., Suess, E. and M. Lyle, Barium in deep-sea sediment: a geochemical proxy for paleoproductivity, *Paleoceanography* 7, 163-181, 1992.

Enmar, R., Stein, M., Bar-Matthews, M., Sass, E., Katz, A. and B. Lazar, Diagenesis in live corals from the Gulf of Aqaba.I. The effect on paleo-oceanography tracers, *Geochimica et Cosmochimica Acta* 64, 3123-3132, 2000.

Erez, J., Vital effect on stable isotope composition seen in foraminifera and coral skeletons, *Nature* 273, 199-202, 1978.

Erez, J. and S. Honjo, Comparison of isotopic composition of planktonic foraminifera in plankton tows, sediment traps, and sediments, *Palaeogeography, Palaeoclimatology, Palaeoecology* 33, 129-156, 1981.

Etheridge, D.M., Steele, L.P., Langenfelds, R.L., Francey, R.J., Barnola, J.-M. and V.I. Morgan, Historical CO₂ records from the Law Dome DE08, DE08-2, and DSS ice cores, in *Trends: A Compendium of Data on Global Change*, Carbon Dioxide Information Analysis Center, Oak Ridge National Laboratory, U.S. Department of Energy, Oak Ridge, Tenn., 1998.

Falkowski, P.G., Species variability in the fractionation of ¹³C and ¹²C by marine phytoplankton, *Journal of Plankton Research* 13, 21-28, 1991.

Falkowski, P.G., Evolution of the nitrogen cycle and its influence on the biological sequestration of CO₂ in the ocean, *Nature* 387, 272-275, 1997.

Farrell, J.W. and W.L. Prell, Climatic change and CaCO₃ preservation: an 800,000 year bathymetric reconstruction from the central equatorial Pacific Ocean, *Paleoceanography* 4, 447-466, 1989.

Farrell, J.W., Pedersen, T.F., Calvert, S.E. and B. Nielsen, Glacial-interglacial changes in nutrient utilization in the equatorial Pacific Ocean, *Nature* 377, 514-517, 1995.

Felis, T., Pätzold, J., Loya, Y. and G. Wefer, Vertical water mass mixing and plankton blooms recorded in skeletal stable carbon isotopes of a Red Sea coral, *Journal of Geophysical Research-Oceans* 103 (C13), 30731-30739, 1998.

Fontugne, M.R. and S.E. Calvert, Late Pleistocene variability of the carbon isotopic composition of organic matter in the eastern Mediterranean: Monitor of changes in carbon sources and atmospheric CO₂ concentrations, *Paleoceanography* 7, 1-20, 1992.

Francois, R., Honjo, S., Manganini, S.J. and G.E. Ravizza, Biogenic barium fluxes to the deep sea: implications for paleoproductivity reconstruction, *Paleoceanography* 9, 289-303, 1995.

Francois, R., Altabet, M.A., Yu, E.-F., Sigman, D.M., Bacon, M.P., Frank, M., Bohrmann, G., Bareille, G. and L.D. Labeyrie, Contribution of Southern Ocean surface-water stratification to low atmospheric CO₂ concentrations during the last glacial period, *Nature* 389, 929-935, 1997.

Frederiksen, C.S. and R.C. Balgovind, The influence of the Indian Ocean/Indonesian SST gradient on the Australian winter rainfall and circulation in an atmospheric GCM. *Q.J.R.Meteorol.Soc.* 120, 923-952, 1994.

Gagan, M.K., Ayliffe, L.K., Hopley, D., Cali, J.A., Mortimer, G.E., Chappell, J. and M.J. Head, Temperature and surface-ocean water balance of the mid-Holocene tropical western Pacific, *Science* 279, 1014-1018, 1998.

Gagan, M.K., Ayliffe, L.K., Beck, J.W., Cole, J.E., Druffel, E.R.M., Dunbar, R.B. and D.P. Schrag, New views from tropical paleoclimates from corals. *Quaternary Science Reviews* 19, 45-64, 2000.

Ganeshram, R.S., Pedersen, T.F., Calvert, S.E. and J.W. Murray, Large changes in oceanic nutrient inventories from glacial to interglacial periods, *Nature* 376, 755-758, 1995.

Ganeshram, R.S., Francois, R., Commeau, J. and S.L. Brown-Leger, An experimental investigation of barite formation in seawater, *Geochimica et Cosmochimica Acta* 67, 2599-2605, 2003.

Gattuso, J.-P., Frankignoulle, M., Bourge, I., Romaine, S. and R.W. Buddemeier, Effect of calcium carbonate saturation of seawater on coral calcification, *Global and Planetary Change* 18, 37-46, 1998.

Gattuso, J.-P., Allemand, D. and M. Frankignoulle, Photosynthesis and calcification at cellular, organismal and community levels in coral reefs: A review on interactions and control by carbonate chemistry, *American Zoologist* 39, 160-183, 1999.

Given, R.K. and K.C. Lohmann, Isotopic evidence for the early meteoric diagenesis of the reef facies, Permian reef complex of west Texas and New Mexico, *Journal of Sedimentary Petrology* 56, 183-193, 1985.

Godfrey, J.S., A Sverdrup model of the depth-integrated flow for the world ocean allowing for island circulations, *Geophys. Astrophys. Fluid Dyn.* 45, 89-112, 1989.

Godfrey, J.S. and T.J. Golding, The Sverdrup relation in the Indian Ocean, and the effect of Pacific-Indian Ocean throughflow on Indian Ocean circulation and on the East Australian Current, *Journal of Physical Oceanography* 11, 771-779, 1981.

Godfrey, J.S. and J.V. Mansbridge, Ekman transports, tidal mixing, and the control of temperature structure in Australia's northwest waters, *Journal of Geophysical Research-Oceans* 105 (C10), 24,021-24,044, 2000.

Godfrey, J.S. and K.R. Ridgway, The large-scale environment of the poleward-flowing Leeuwin Current, Western Australia: Longshore steric height gradients, wind stresses and geostrophic flow, *Journal of Physical Oceanography* 15, 481-495, 1985.

Goñi, M.A., Ruttenberg, K.C. and T.I. Eglinton, A reassessment of the sources and importance of land-derived organic matter in surface sediments from the Gulf of Mexico, *Geochimica et Cosmochimica Acta* 62, 3055-3075, 1998.

González, L.A. and K.C. Lohmann, Carbon and oxygen isotopic composition of Holocene reefal carbonates, *Geology* 13, 811-814, 1985.

Gordon, A.L. and R.A. Fine, Pathways of water between the Pacific and Indian oceans in the Indonesian seas, *Nature* 379, 146-149, 1996.

Goreau, T.J., Carbon metabolism in calcifying and photosynthetic organisms: Theoretical models based on stable isotope data, *Proc. 3rd Intl. Coral Reef Symp., Miami 2*, 395-401, 1977.

Graham, N.E., Simulation of recent global temperature trends, *Science* 267, 666-671, 1995.

Grottoli, A.G., Effect of light and brine shrimp on skeletal $\delta^{13}\text{C}$ in the Hawaiian coral *Porites compressa*: a tank experiment, *Geochimica Cosmochimica Acta* 66, 1955-1967, 2002.

Gruber, N., Keeling, C.D., Bacastow, R.B., Guenther, P.R., Lueker, T.J., Wahlen, M., Meijer, H.A.J., Mook, W.G. and T.F. Stocker, Spatiotemporal patterns of carbon-13 in the global surface oceans and the oceanic Suess effect, *Global Biogeochemical Cycles* 13, 307-335, 1999.

Guilderson, T.P., R.G. Fairbanks and J.L. Rubenstone, Tropical temperature variations since 20,000 years ago: Modulating interhemispheric climate change, *Science* 263, 663-665, 1994.

Hanebuth, T., Stattegger, K. and P.M. Grootes, Rapid flooding of the Sunda Shelf: A late-glacial sea-level record, *Science* 288, 1033-1035, 2000.

Haug, G.H., Pedersen, T.F., Sigman, D.M., Calvert, S.E., Nielsen, B. and L.C. Peterson, Glacial/interglacial variations in production and nitrogen fixation in the Cariaco Basin during the last 580 kyr, *Paleoceanography* 13, 427-432, 1998.

Heath, G.R., Moore, T.C. and J.P. Dauphin, Organic carbon in deep-sea sediments, in *The Fate of Fossil Fuel CO₂ in the Oceans*, edited by R.N. Anderson and A. Malahoff, pp. 605-625, New York, Plenum, 1977.

Hesse, P.P., The record of continental dust from Australia in Tasman Sea sediments, *Quaternary Science Reviews* 13, 257-272, 1994.

Holmes, M.E., Müller, P.J., Schneider, R.R., Segl, M., Pätzold, J. and G. Wefer, Stable nitrogen isotopes in Angola Basin surface sediments, *Marine Geology* 134, 1-12, 1996.

Holmes, M.E., Schneider, R.R., Müller, P.J., Segl, M. and G. Wefer, Reconstruction of past nutrient utilization in the eastern Angola Basin based on sedimentary $^{15}\text{N}/^{14}\text{N}$ ratios, *Paleoceanography* 12, 604-614, 1997.

Houghton, J.T., Meira Filho, L.G., Callander, B.A., Harris, N., Kattenberg, A. and K. Maskell, *Climate change 1995. The Science of Climate Change*, Cambridge University Press, Cambridge, 572 p., 1996.

Huber, M. and L.S. Sloan, Climatic responses to tropical sea surface temperature changes on a „greenhouse“ Earth, *Paleoceanography* 15, 443-450, 2000.

Imbrie, J., Hays, J.D., Martinson, D.G., McIntyre, A., Mix, A., Morley, J.J., Pisias, N.G., Prell, W.L. and Shackleton, N.J., The orbital theory of Pleistocene climate: Support from a revised chronology of the marine ^{18}O record, in *Milankovitch and Climate*, Part I., edited by A.L. Berger, J. Imbrie, J.D. Hays, J. Kukla and J. Saltzman, pp. 269-305, Reidel, Hingham, Mass., 1984.

Keeling, C.D., Bacastow, R.B., Carter, A.F., Piper, S.C., Whorf, T.P., Heimann, M., Mook, W.G. and H. Roeloffzen, A three dimensional model of atmospheric CO_2 transport based on observed winds: 1. Analysis of observational data, in *Aspects of climate variability in the Pacific and western Americas*, edited by D.H. Peterson, *Geophys. Monogr.* 55, AGU, 165-236, 1989.

Keeling, C.D., Whorf, T.P., Wahlen, M. and J. van der Plicht, Interannual extremes in the rate of rise of atmospheric carbon dioxide since 1980, *Nature* 375, 666-670, 1995.

Keeling, R.F., Piper, S.C. and M. Heimann, Global and hemispheric CO₂ sinks deduced from changes in atmospheric O₂ concentration, *Nature* 381, 218-221, 1996.

Keil, R.G., Montluçon, D.B., Prahl, F.G. and J.I. Hedges, Sorptive preservation of labile organic matter in marine sediments, *Nature* 370, 549-552, 1994.

Kinsman, D.J.J. and H.D. Holland, The co-precipitation of cations with CaCO₃ - IV. The co-precipitation of Sr²⁺ with aragonite between 16°C and 96°C, *Geochimica et Cosmochimica Acta* 33, 1-17, 1969.

Kleypas, J.A., Buddemeier, R.W., Archer, D., Gattuso, J.-P., Langdon, C. and B.N. Opdyke, Geochemical consequences of increased atmospheric carbon dioxide on coral reefs, *Science* 284, 118-120, 1999a.

Kleypas, J.A., McManus, J.W. and L.A.B. Menez, Environmental limits to coral reef development: Where do we draw the line ?, *American Zoologist* 39, 146-159, 1999b.

Kuhnert, H., Pätzold, J., Wyrwoll, K.H. and G. Wefer, Monitoring climate variability over the past 116 years in coral oxygen isotopes from Ningaloo Reef, Western Australia, *International Journal of Earth Sciences* 88, 725-732, 2000.

Langdon, C., Takahashi, T., Sweeney, C., Chipman, D. and J. Goddard, Effect of calcium carbonate saturation state on the calcification rate of an experimental coral reef, *Global Biogeochemical Cycles* 14, 639-654, 2000.

Leder, J.J., Swart, P.K., Szmant, A. and R.E. Dodge, The origin of variations in the isotopic record of scleractinian coral: I. Oxygen. *Geochimica et Cosmochimica Acta* 60, 2857-2870, 1996.

Leclercq, N., Gattuso, J.P. and J. Jaubert, CO₂ partial pressure controls the calcification rate of a coral community, *Global Change Biology* 6, 329-334, 2000.

Linsley, B.K., Oxygen-isotope record of sea level and climate variations in the Sulu Sea over the past 150,000 years, *Nature* 380, 234-237, 1996.

Lough, J.M. and D.J. Barnes, Several centuries of variation in skeletal extension, density and calcification in massive *Porites* from the Great Barrier Reef: a proxy for seawater temperature and a background of variability against which to identify unnatural change, *Journal of Experimental Marine Biology and Ecology* 211, 29-67, 1997.

Lough, J.M. and D.J. Barnes, Environmental controls on growth of the massive coral *Porites*, *Journal of Experimental Marine Biology and Ecology* 245, 225-243, 2000.

Lyle, M., Murray, D.W., Finney, B.P., Dymond, J., Robbins, J.M. and K. Brooksforce, The record of Late Pleistocene biogenic sedimentation in the eastern tropical Pacific ocean, *Paleoceanography* 3, 39-59, 1988.

Lyle, M.W., Prahl, F.G., and M.A. Sparrow, Upwelling and productivity changes inferred from a temperature record in the central equatorial Pacific, *Nature* 355, 812-815, 1992.

Mann, S., Biomineralization in lower plants and animals – chemical perspectives, in *Biomineralization in Lower Plants and Animals*, edited by B.S.C. Leadbeater and R. Riding, pp. 39-54, Clarendon, Oxford, 1986.

Mariotti, A., Atmospheric nitrogen is a reliable standard for natural ^{15}N abundance measurements, *Nature* 303, 680-683, 1983.

Marshall, J.F. and M.T. McCulloch, Evidence of El Niño and the Indian Ocean Dipole from Sr/Ca derived SSTs for modern corals at Christmas Island, Eastern Indian Ocean, *Geophysical Research Letters* 28, 3453-3456, 2001.

Martinez, J.I., Late Pleistocene palaeoceanography of the Tasman Sea: implications for the dynamics of the warm pool in the western Pacific, *Palaeogeography, Palaeoclimatology, Palaeoecology* 112, 19-62, 1994.

Martinson, D.G., Pisias, N.G., Hays, J.D., Imbrie, I., Moore, T.C. and N.J. Shackleton, Age dating and the orbital theory of the ice-ages: development of a high-resolution 0 to 300,000-year chronostratigraphy, *Quaternary Research* 27, 1-29, 1987.

Marubini, F., Barnett, H., Langdon, C. and M.J. Atkinson, Dependence of calcification on light and carbonate ion concentration for the hermatypic coral *Porites compressa*, *Marine Ecology Progress Series* 220, 153-162, 2001.

McConnaughey, T.A., ^{13}C and ^{18}O isotopic disequilibrium in biological carbonates, I. Patterns, *Geochimica et Cosmochimica Acta* 53, 151-162, 1989.

McCorkle, D.C., Veeh, H.H. and D.T. Heggie, Glacial-Holocene paleoproductivity off Western Australia: a comparison of proxy records, in *Carbon Cycling in the Glacial Ocean*, edited by R. Zahn, T.F. Pedersen, M. Kaminski and L. Labeyrie, pp. 443-479, *NATO ASI Series I* 17, 1994.

McCulloch M.T., Tudhope, A.W., Esat, T.M., Mortimer, G.E., Chappell, J, Pillans, B. and A.R. Chivas, A. Omura, Coral record of equatorial sea-surface

temperatures during the penultimate deglaciation at Huon Peninsula, *Science* 283, 202-204, 1999.

Meyers, G., Variation of Indonesian throughflow and the El Niño - Southern Oscillation, *Journal of Geophysical Research-Oceans* 101 (C5), 12,255-12,263, 1996.

Min, R.G., Edwards, R.L., Taylor, F.W., Recy, J., Gallup, C.D. and J.W. Beck, Annual cycles of U/Ca in coral skeletons and U/Ca thermometry, *Geochimica et Cosmochimica Acta* 59, 2025-2042, 1995.

Mix, A.C., Ruddiman, W.F. and A. McIntyre, Late Quaternary paleoceanography of the tropical Atlantic, 2; The seasonal cycle of sea surface temperatures, 0-20,000 years B.P., *Paleoceanography* 1, 339-353, 1986.

Morse, J.W. and F.T. Mackenzie, *Geochemistry of Sedimentary Carbonates*. Elsevier, Amsterdam 707 p., 1990.

Müller, P.J., C/N ratios in Pacific deep-sea sediments: effect of inorganic ammonium and organic nitrogen compounds sorbed by clays, *Geochimica et Cosmochimica Acta* 41, 765-776, 1977.

Müller, P.J. and E. Suess, Productivity, sedimentation rate and organic matter in the oceans. - I. Organic carbon preservation, *Deep-Sea Research* 26, 1347-1362, 1979.

Nicholls, N., Sea surface temperatures and Australian winter rainfall. *J. Climate* 2, 965-973, 1989.

Norrish, K. and J.T. Hutton, An accurate X-ray spectrographic method for the analysis of a wide range of geological samples, *Geochimica et Cosmochimica Acta*, 33, 431 - 453, 1969.

Packard, T.T., Garfield, P.C. and L.A. Codispoti, Oxygen consumption and denitrification below the Peruvian upwelling, in *Coastal Upwelling, Its Sediment Record*, Part A, edited by J. Thiede and E. Suess, pp. 365-398, Plenum, New York, 1983.

Parker, D.E., Jackson, M. and E.B. Horton, The GISST2.2 sea surface temperature and sea-ice climatology, *CRTN63*, Hadley Centre, Met. Office, Bracknell, U.K., 35 pp., 1995.

Potemra, J.T., Seasonal variations of upper ocean transport from the Pacific to the Indian Ocean via Indonesian straits, *Journal of Physical Oceanography* 29, 2930-2944, 1999.

Potemra, J.T. and R. Lukas, Seasonal to interannual modes of sea level variability in the western Pacific and eastern Indian Oceans, *Geophysical Research Letters* 26, 365-368, 1999.

Prell, W.L., Hutson, W.H., Williams, D.F., Be, A.W.H., Geitzenauer, K. and B. Molino, Surface circulation of the Indian Ocean during the Last Glacial Maximum, approximately 18,000 yr BP, *Quaternary Research* 14, 309-336, 1980.

Quinn, T.M., Taylor, F.W., Crowley, T.J. and S.M. Link, Evaluation of sampling resolution in coral stable isotope records: A case study using records from New Caledonia and Tarawa, *Paleoceanography* 11, 529-542, 1996a.

Quinn, T.M., Crowley, T.J. and F.W. Taylor, New stable isotope results from a 173-year coral from Espiritu Santo, Vanuatu, *Geophysical Research Letters* 23, 3413-3416, 1996b.

Quinn, T.M., Crowley, T.J., Taylor, F.W., Henin, C., Joannot, P. and Y. Join, A multicentury stable isotope record from a New Caledonia coral: Interannual and decadal sea surface temperature variability in the southwest Pacific since 1657 A.D., *Paleoceanography* 13, 412-426, 1998.

Rau, G.H., Takahashi, T., Des Marais, D.J., Repeta, D.J. and J.H. Martin, The relationship between $\delta^{13}\text{C}$ of organic matter and $[\text{CO}_2(\text{aq})]$ in ocean surface

water: Data from a JGOFS site in the northeast Atlantic Ocean and a model, *Geochimica et Cosmochimica Acta* 56, 1413-1419, 1992.

Rau, G.H., Variations in sedimentary organic $\delta^{13}\text{C}$ as a proxy for past changes in ocean and atmospheric CO_2 concentrations, in *Carbon Cycling in the Glacial Ocean*, edited by R. Zahn, T.F. Pedersen, M. Kaminski and L. Labeyrie, pp. 307-321, *NATO ASI Series I* 17, 1994.

Rostek F., Ruhland, G., Bassinot, F.C., Müller, P.J., Labeyrie, L.D., Lancelot, Y. and E. Bard, Reconstructing sea surface temperature and salinity using $\delta^{18}\text{O}$ and alkenone records, *Nature* 364, 319-321, 1993.

Roulier, L.M. and T.M. Quinn, Seasonal- to decadal-scale climatic variability in southwest Florida during the middle Pliocene: Inferences from a coralline stable isotope record, *Paleoceanography* 10, 429-443, 1995.

Saji, N.H. & Goswami, B.N., Vinayachandran, P.N. & Yamagata, T., 1999: A dipole mode in the tropical Indian Ocean. *Nature* 401, 360-363.

Sansone, F.J., Tribble, G.W., Andrews, C.C. and J.P. Cajnton, Anaerobic diagenesis within Recent, Pleistocene, and Eocene marine carbonate frameworks, *Sedimentology* 37, 887-1009, 1988.

Schäfer, P. and V. Ittekkot, Seasonal variability of $\delta^{15}\text{N}$ in settling particles in the Arabian Sea and its palaeogeochemical significance, *Naturwissenschaften*, 80, 511-513, 1993.

Schidlowski, M., Hayes, J.M. and I.R. Kaplan, Isotopic inferences of ancient biochemistries: carbon, sulfur, hydrogen, and nitrogen, in *Earth's Earliest Biosphere, its Origin and Evolution*, edited by J.W. Schopf, pp. 149-186, Princeton, 1983.

Scheider, R.R., Price, B., Müller, P.J., Kroon, D. and I. Alexander, Monsoon related variations in Zaire (Congo) sediment load and influence of fluvial silicate supply on marine productivity in the east equatorial Atlantic during the last 200,000 years, *Paleoceanography* 12, 463-481, 1997.

Shen, C.-C., Lee, T., Chen, C.-Y., Wang, C.-H., Dai, C.-F. and L.-A. Li, The calibration of δ [Sr/Ca] versus sea surface temperature relationship for Porites corals, *Geochimica et Cosmochimica Acta* 60, 3849-3858, 1996.

Shimmield, G.B., Can sediment geochemistry record changes in coastal upwelling paleoproductivity ? Evidence from northwest Africa and the Arabian Sea, in *Upwelling Systems: Evolution Since the Early Miocene*, edited by C. Summerhayes, W. Prell and K.-C. Emeis, pp. 29-46, *Geol. Soc. Spec. Publ.* 64, 1992.

Sikes, E.L. and L.D. Keigwin, Equatorial Atlantic sea surface temperature for the last 30-kyr – a comparison of Uk^{37} , $\delta^{18}O$ and foraminiferal assemblage temperature, *Paleoceanography* 9, 31-45, 1994.

Smith, R.L., Coastal upwelling in the modern ocean, in *Upwelling Systems: Evolution Since the Early Miocene*, edited by C.P. Summerhayes, W.L. Prell and K.-C. Emeis, pp. 9-28, *Geol. Soc. Spec. Publ.* 64, 1992.

Smith, S.V. and R.W. Buddemeier, Global change and coral reef ecosystems, *Ann.Rev.Ecol.Syst.* 23, 89-118, 1992.

Spero, H.J., Bijma, J., Lea, D.W. and B.E. Bemis, Effect of seawater carbonate concentration of foraminiferal carbon and oxygen isotopes, *Nature* 390, 497-500, 1997.

Stoll, H.M. and D.P. Schrag, Effects of Quaternary sea level cycles on strontium in seawater, *Geochimica et Cosmochimica Acta* 62, 1107-1118, 1998.

Swart, P., Carbon and oxygen fractionation in Scleractinian corals: A review, *Earth Science Reviews* 19, 51-80, 1983.

Swart, P.K., Healy, G.F., Dodge, R.E., Kramer, P., Hudson, J.H., Halley, R.B. and M.B. Robblee, The stable oxygen and carbon isotopic record from a coral growing in Florida Bay: a 160 year record of climatic and anthropogenic

influence, *Palaeogeography, Palaeoclimatology, Palaeoecology* 123, 219-237, 1996a.

Swart, P.K., Dodge, R.E. and H.J. Hudson, A 240-year stable oxygen and carbon isotopic record in a coral from South Florida: implications for the prediction of precipitation in southern Florida, *PALAIOS* 11, 362-375, 1996b.

Taylor, R.S. and S.M. McLennan, *The Continental Crust: Its Composition and Evolution.*, 312 p., Blackwell Scientific, Boston, Mass, 1985.

Thunell, R., Anderson, D., Gellar, D. and Q. Miao, Sea-surface temperature estimates for the tropical western Pacific during the last glaciation and their implications for the Pacific Warm Pool, *Quaternary Research* 41, 255-264, 1994.

Tomczak, M. and J.S. Godfrey, *Regional Oceanography: an Introduction*, 422 p., Pergamon, Oxford, 1994.

Torres, M.E., Brumsack, H.J., Bohrmann, G. and K.-C. Emeis, Barite fronts in continental margin sediments: a new look at barium remobilization in the zone of sulfate reduction and formation of heavy barites in diagenetic fronts, *Chemical Geology* 127, 125-139, 1996.

Tribble, G.W., Sansone, F.J. and S.V. Smith, Stoichiometric modeling of carbon diagenesis within a coral reef framework, *Geochimica et Cosmochimica Acta* 54, 2439-2449, 1990.

Tucker, M., *Sedimentary Petrology: an introduction to the origin of sedimentary rocks*, 2nd. edition Blackwell, Oxford, 260 pp, 1991.

van der Kaars, W.A., Palynology of eastern Indonesian marine piston-cores. A Late Quaternary vegetational and climatic record for Australasia, *Palaeogeography, Palaeoclimatology, Palaeoecology* 117, 55-72, 1991.

Vénec-Peyré, M.-T., Caulet, J.P. and C.V. Grazzini, Paleohydrographic changes in the Somali Basin (5°N upwelling and equatorial areas) during the last 160 kyr, based on correspondence analysis of foraminiferal and radiolarian assemblages, *Paleoceanography* 10, 473-491, 1995.

Vénec-Peyré, M.-T., Caulet, J.P. and C.V. Grazzini, Glacial/interglacial changes in the equatorial part of the Somali Basin (NW Indian Ocean) during the last 355 kyr, *Paleoceanography* 12, 640-648, 1997.

von Breymann, M.T., Emeis, K.-C. and E. Suess, Water depth and diagenetic constraints on the use of barium as a palaeoproductivity indicator, in *Upwelling Systems: Evolution since the early Miocene*, edited by C.P. Summerhayes, W.L. Prell and K.-C. Emeis, pp. 273-284, *Geol. Soc. Spec. Public*, 64, 1992.

Wada, E. and A. Hattori, Natural abundances of ^{15}N in particulate organic matter in the North Pacific Ocean, *Geochimica et Cosmochimica* 40, 249-251, 1979.

Watson, A.J., Robinson, C., Robinson, J.E., Williams, P.J. and M.J.R. Fasham, Spatial variability in the sink for atmospheric carbon dioxide in the North Atlantic, *Nature* 350, 50-53, 1991.

Weber, J.N. and P.M.J. Woodhead, Carbon and oxygen isotope fractionation in the skeletal carbonate of reef-building corals. *Chemical Geology* 6, 93-117, 1970.

Wellington, G.M. and R.B. Dunbar, Stable isotopic signature of El Niño-Southern Oscillation events in eastern tropical Pacific reef corals, *Coral Reefs* 14, 5-25, 1995.

Wellington, G.M., Dunbar, R.B. and G. Merlen, Calibration of stable oxygen isotope signatures in Galapagos corals, *Paleoceanography* 11, 467-480, 1996.

Wells, P.E., Wells, G.M., Cali, J. and A. Chivas, Response of deep-sea foraminifera to Late Quaternary climate changes, southeast Indian Ocean, offshore Western Australia, *Marine Micropaleontology* 23, 185-229, 1994.

Williams, D.F., Be, A.W.H. and R.G. Fairbanks, Seasonal stable isotopic variations in living planktonic foraminifera from Bermuda plankton tows, *Palaeogeography, Palaeoclimatology, Palaeoecology* 33, 71-102, 1981a.

Williams, D.F., Rottger, R., Schmaljohann, R. and L. Keigwin, Oxygen and carbon isotopic fractionation and algal symbiosis in the benthic foraminifera *Heterostigina depressa*, *Palaeogeography, Palaeoclimatology, Palaeoecology* 33, 231-251, 1981b.

Wyrtki, K., Indonesian throughflow and the associated pressure gradient, *Journal of Geophysical Research-Oceans* 92, 12,941-12,946, 1987.

Wyrtki, K., *Oceanographic atlas of the International Indian Ocean Expedition*, 531 p., National Science Foundation, Washington D.C., 1988.

Yan, X.-H., Ho, C.-R., Zheng, Q. and V. Klemas, Temperature and size variabilities of the Western Pacific Warm Pool, *Science* 258, 1643-1645, 1992.

APPENDIX

Parts of this thesis have been published in journal articles and presented at conferences. The following articles and conference contributions are based on the contents of this thesis:

Journal papers

Müller, A., Gagan, M.K. & Lough, J.M., 2002: Effect of early marine diagenesis on coral reconstructions of 20th century changes in surface-ocean carbonate saturation state. *Global Biogeochemical Cycles (submitted/ revised)*.

Müller, A., Gagan, M.K., McCulloch, M.T., 2001: Early marine diagenesis in coral and geochemical consequences of paleoceanographic reconstructions. *Geophysical Research Letters Vol. 28, No.23, 4471-4474*.

Müller, A. & Opdyke, B.N., 2000: Glacial-interglacial changes in nutrient utilization and paleoproductivity in the Indonesian Throughflow sensitive Timor Trough, easternmost Indian Ocean. *Paleoceanography 15, 85-94*.

Conference contributions

Müller, A., Gagan, M.K. & Lough, J.M., Effect of early marine diagenesis on coral reconstructions of 20th century changes in surface-ocean carbonate

saturation state. Australian Coral Reef Society, Annual meeting, Stradbroke, November 2002.

Müller, A., Gagan, M.K. & Lough, J.M., Early marine diagenesis in corals and consequences for paleo-reconstructions of carbonate saturation state in coral reefs and atmospheric CO₂. European Meeting of the International Society for Reef Studies, Cambridge, September 2002.

Müller, A. & Gagan, M.K., Geochemical expressions of early marine diagenesis in corals. 12th Goldschmidt conference, Davos, August 2002.

Müller, A. & Gagan, M.K., Early marine diagenesis in corals and geochemical consequences for sea surface temperature reconstructions. European Geophysical Union, XVII. General Assembly, Nice, April 2002.

Müller, A. & Gagan, M.K., Validity of paleoceanographic reconstructions from corals for the last interglacial. Stage 5 deposits in Europe in the context of global climate evolution First Workshop of the DEKLIM-EEM project: Climate Change at the Very End of a Warmstage, Leipzig, March 2002.

Müller, A. & Gagan, M.K., Past sea surface temperature reconstructions from massive coral: Important tracers and potential errors. Australian Meteorological and Oceanographic Society, Annual Conference, Melbourne, February 2002.

Müller, A. & Gagan, M.K., Early marine diagenesis in coral and geochemical consequences for paleoceanographic reconstructions. VIIth International Conference on Paleoceanography, Sapporo, Japan, September 2001.

Müller, A. & Gagan, M.K., A re-evaluation of sea surface temperature reconstructions from coral. Australian Marine Geoscience Conference, Hobart, June 2001.

Müller, A.: Sedimentological response to climatic change off northwest Australia. Australian Meteorological and Oceanographic Society, Annual Conference, Hobart, February 2001.

Müller, A. & B.N. Opdyke, B.N.: Variations in biogenic and terrigenous inputs in the easternmost Indian Ocean during the past 80 kyr - paleoceanographic and paleoclimate implications. Australian Marine Sciences Association, Annual Conference, Western Australia, Perth, April 2000.

Müller, A., Gagan, M.K., McCulloch, M.T.: Systematics of $\delta^{13}\text{C}$, $\delta^{18}\text{O}$, and Sr/Ca ratios in Ningaloo Reef coral, Western Australia. AUStralian COral REcords (AUSCORE) workshop. Canberra, February 2000.

Müller, A. and Opdyke, B.N.: Past changes in productivity and nutrient utilization off NW Australia - evidence for a restricted Indonesian throughflow

during the LGM ? Fourth Australian Marine Geoscience Conference, Exmouth, September/October 1999.

Müller, A., Gagan, M.K., McCulloch, M.T.: Systematics of $\delta^{13}\text{C}$, $\delta^{18}\text{O}$, and Sr/Ca ratios in relation to environmental parameters in Ningaloo Reef coral, Western Australia. Australian Marine Sciences Association Annual Conference, Melbourne, July 1999.

Müller, A., Lough, J.M. & Gagan, M.K.: Storage and recovery of environmental information in coral skeletons from Ningaloo Reef, Western Australia. 6th International Conference on Paleoceanography, Lisbon, August 1998.

Glacial-interglacial changes in nutrient utilization and paleoproductivity in the Indonesian Throughflow sensitive Timor Trough, easternmost Indian Ocean

Anne Müller¹ and Bradley N. Opdyke

Department of Geology, Australian National University, Canberra, ACT

Abstract. Paleoproductivity in the Timor Trough appears to be inversely proportional to the strength of the Indonesian Throughflow. Today, productivity in the area is inhibited by the narrow band of low-salinity surface water that moves through the Indonesian Archipelago and spreads out over the equatorial portions of the eastern Indian Ocean. During the Last Glacial Maximum, however, the reduction or absence of this low-salinity "cap" would have enhanced the possibility of upwelling and higher productivity in the region. Our results indicate that at this time, productivity was enhanced, the surface waters were being depleted of CO₂ and relative nitrate utilization was low. This suggests that the thermocline was shallow and that upwelled, nutrient-rich water was present.

1. Introduction

The Western Pacific Warm Pool (WPWP) is characterized by waters with sea surface temperatures (SST) exceeding 28°C. Its importance for climate dynamics has been recognized in recent studies, as has the need to understand long-term variations of primary production in low latitudes [e.g., *Thunell et al.*, 1994; *Ahmad et al.*, 1995; *Linsley*, 1996]. Knowledge of past variation in primary production and nutrient utilization may contribute to the understanding of past changes in the thermal structure in the region. In the Timor Trough, which is situated at the southern edge of the WPWP, variations of primary production are poorly documented.

Today, the study area is strongly influenced by the Indonesian Throughflow (ITF). The ITF (Figure 1) enters the Indian Ocean as a narrow band of low-salinity water, with a maximum water transport estimated in the range of 7-18 Sv [*Gordon and Fine*, 1996]. It is strongest in austral winter. The ITF represents the interocean transport of excess freshwater from the Pacific to the Indian Ocean through the Indonesian Seas [*Godfrey and Golding*, 1981; *Godfrey and Ridgway*, 1985]. This is caused by the necessity to maintain constant pressure around islands, such as the island continent Australia [*Godfrey*, 1989]. Water that passes the ITF flows into the Indian Ocean as the west flowing South-Java and the South Equatorial Currents and as the south flowing Leeuwin Current [*Godfrey and Ridgway*, 1985]. The latter is maintained because of the lower steric height farther south along the coast off western Australia. Southward flow is accompanied by surface cooling, and surface cooling produces continuous southward flow [*Tomczak and Godfrey*, 1994].

The dynamics of this eastern boundary current along the western Australian coast are thus different from those of the Pacific and Atlantic Oceans. In these oceans, equatorward winds produce equatorward surface current flow, poleward undercurrents, and coastal upwelling along the eastern boundaries of the ocean basins. Along the western Australian coast, however, annual mean winds do blow toward the equator, but at the surface a strong poleward flow runs against the wind, and the undercurrent is equatorward. The poleward flow is strong enough to override the wind-driven equatorward current, and the onshore geostrophic flow is strong enough to override the offshore Ekman flow. Hence the upwelling that one might expect from the equatorward winds along the western Australian coast is overwhelmed by an onshore geostrophic drift [*Smith*, 1992; *Tomczak and Godfrey*, 1994].

Today, there is no significant upwelling in the study area [*Tomczak and Godfrey*, 1994]. However, because the pressure difference from the Pacific to the Indian Ocean is the driving force for through flow [*Wyrtki*, 1987], both the volume transport of through flow and the thermal structure in the area are expected to vary during the El Niño-Southern Oscillation (ENSO) cycle. Larger than normal transport is expected during the La Niña (cold) phase, when strong easterlies along the equatorial Pacific build up high sea level in the western Pacific. Conversely, during an ENSO event, Pacific equatorial winds are anomalously westerly, and western Pacific sea level falls. This low sea level is transferred to the coast NW of Australia. As a consequence, the baroclinic pressure gradient between NW Australia and Java decreases, resulting in a weakening of the ITF [*Clarke and Liu*, 1994].

The alternation of easterly and westerly wind stress anomalies during an ENSO cycle is accompanied by a weaker reversal of anomalies in the eastern Pacific and in the equatorial Indian Ocean. The winds over the equatorial Indian Ocean determine the thermal structure on the Indonesian coast. During ENSO, when Pacific wind anomaly is westerly, Indian Ocean anomaly is easterly, resulting in a shallow thermocline along the coast of Java. This has been observed to occur simultaneously with

¹Also at Research School of Earth Sciences, Australian National University, Canberra, ACT, Australia.

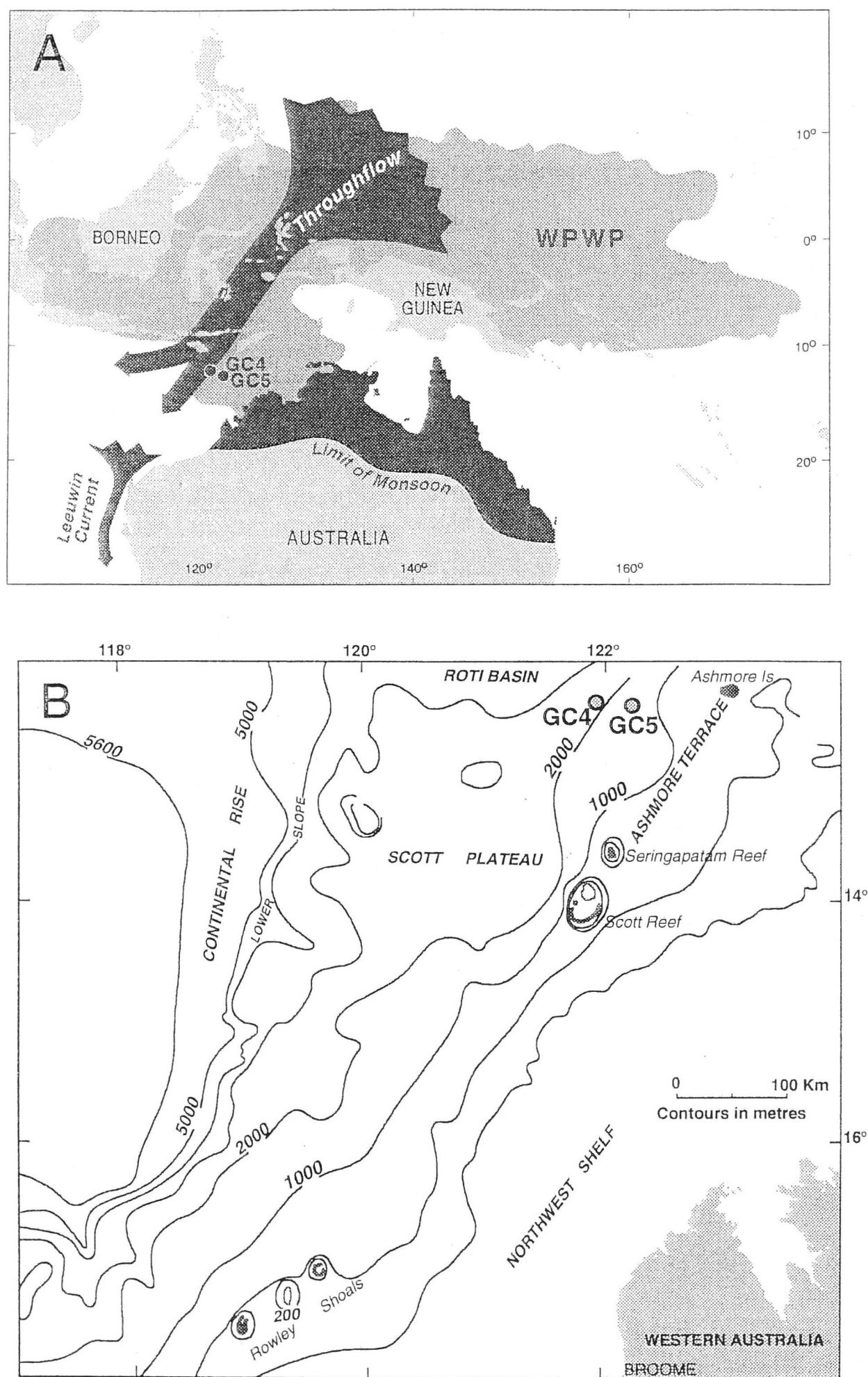


Figure 1. (a) Physiographic map showing the location of the study site, the Western Pacific Warm Pool (WPWP) (mean sea surface temperature (SST) $>28^{\circ}\text{C}$), and schematic modern ocean circulation patterns. During the Last Glacial Maximum, the WPWP and the Indonesian Throughflow were restricted, which resulted in weak upwelling in the study area. In western Australia, the Leeuwin Current was absent or considerably weaker, and a strong West Australian Current transported cooler waters equatorward on a year-round basis. (b) Bathymetric map showing the study sites.

Figure 1. (continued)

extremely cold SST, suggesting that upwelling contributes to the formation of a "cold spot". This SST anomaly is widespread during some ENSO events, extending from Timor along Java and Sumatra [Meyers, 1996].

During the Last Glacial Maximum (LGM), the circulation patterns in the Indian Ocean were significantly different from those of today. It has been suggested that a north flowing West

Australian Current, associated with a weaker or absent Leeuwin Current linked to a reduced WPWP [Martinez, 1994] and thereby weaker ITF, led to increased productivity and coastal upwelling at higher latitudes off western Australia [McCorkle et al., 1994; Wells et al., 1994]. As well, the Westerlies may have been compressed, and thus more intense, and moved north during the LGM. Part of the West Wind Drift was deflected equatorward by

Australia. Thus, in contrast to the modern pattern of weak, seasonally reversing flow, the West Australian Current was a significant eastern boundary current. This current transported cooler waters equatorward all year-round [Prell *et al.*, 1980].

In this study, geochemical results are presented from two sediment cores from the continental margin off northwestern Australia to show past changes in productivity and nutrient utilization which may be related to changes in the ITF and thermal structure in the area. We focus on LGM-Holocene contrasts because for these time periods ^{14}C dating is available in the region (B.N. Opdyke, unpublished data, 1999) in addition to the $\delta^{18}\text{O}$ record of *Globigerinoides ruber*. We will point out signals observed during isotope stages 3 and 4 for which an age model based on the $\delta^{18}\text{O}$ record of *G. ruber* has been established but will not discuss them in detail because of the lack of results from additional dating.

2. Material and Methods

Two gravity cores, GC4 (12.17°S, 121.56°W, water depth 2069 m) and GC5 (12.22°S, 122.12°W, water depth 1462 m), were taken during a R/V *Franklin* cruise in 1996. Two series of 3-cm³ syringe samples were taken at 10-cm intervals for each core. To establish a foraminiferal $\delta^{18}\text{O}$ record, organic matter was removed from the samples of one series by treatment with 5% hydrogen peroxide solution (H_2O_2). The size fraction >150 μm was separated by wet sieving. Foraminiferal specimens of *G. ruber* were hand picked from the >150- μm size fraction, washed in alcohol, and placed in an ultrasonic cleaner for <5 s. A total of 10–15 clean specimens (with a total weight between 150 and 200 μg) were selected for stable isotope analysis. Isotope analysis was carried out using an automated individual carbonate-reaction (Kiel) device coupled with a Finnigan-MAT 251 mass spectrometer. The $\delta^{18}\text{O}$ values were calculated as per mil (‰) deviations relative to Peedee belemnite (PDB) and were calibrated via the NBS-19 standard ($\delta^{18}\text{O} = -2.20$ ‰). Average reproducibility for a typical 150- μg sample was 0.05‰.

The chronostratigraphy of the cores was based on the $\delta^{18}\text{O}$ records for *G. ruber*, applying the SPECMAP timescale [Imbrie *et al.*, 1984; Martinson *et al.*, 1987] (Figure 2). An interpolation was made between $\delta^{18}\text{O}$ -age tie points, and linear sedimentation rates were derived.

For all following analyses, the samples of the second series were freeze dried, crushed, and homogenized. For stable isotope analysis ($\delta^{13}\text{C}_{\text{TOC}}$ and $\delta^{15}\text{N}$), carbonate was removed from the sediment samples by adding 2% hydrochloric acid to sediment subsamples (20-mg aliquots). This was repeated until formation of CO_2 bubbles ceased. The samples were then dried at 60°C and combusted with a CHN-analyzer (ANCA/SL) coupled to a 20/20 mass spectrometer (Europa Scientific Ltd, UK). Pure CO_2 and N_2 gases from tanks calibrated as a standard against carbonate (NBS-22) and atmospheric nitrogen [Mariotti, 1983], respectively, were used as reference gases. Isotope ratios were calculated using the following equation:

$$\delta X (\text{‰}) = (R_{\text{sample}} / R_{\text{reference}} - 1) 10^3,$$

where X and R are ^{13}C (or ^{15}N) and $^{13}\text{C}/^{12}\text{C}$ (or $^{15}\text{N}/^{14}\text{N}$), respectively.

Two secondary standards, flour for N and beet sugar for C, calibrated against IAEA-NI $(\text{NH}_4)_2\text{SO}_4$ and IAEA reference standard NBS-22, respectively, were included in the sample

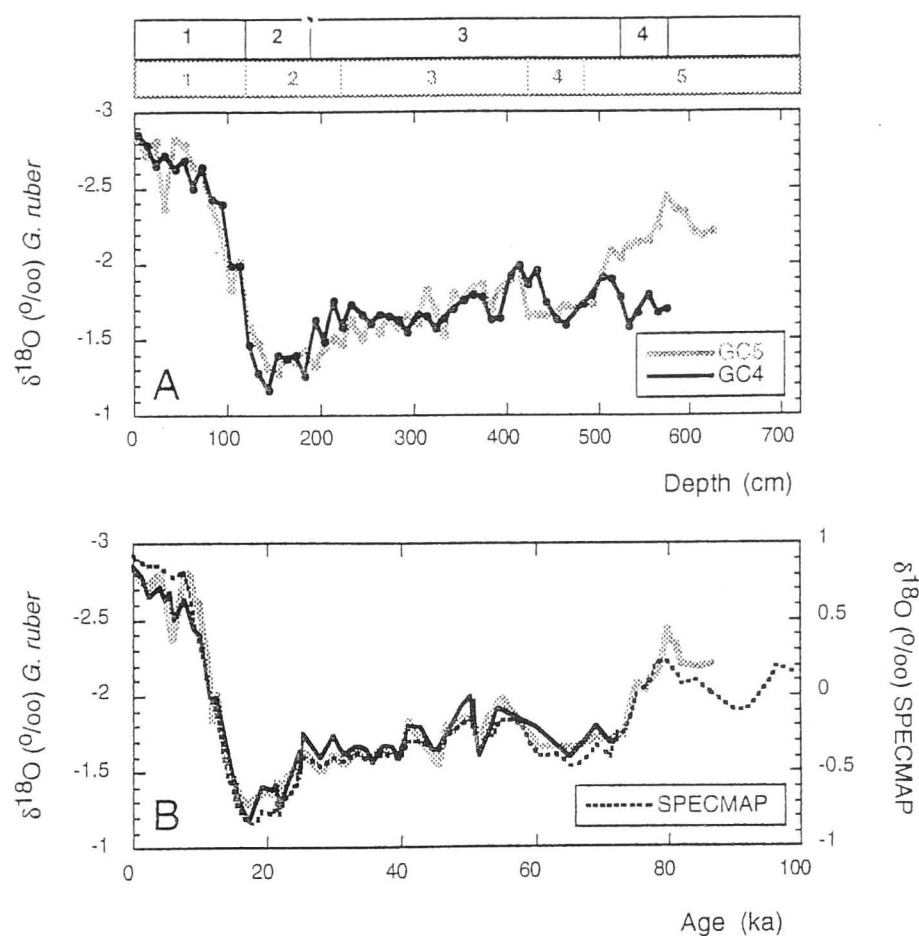


Figure 2. (a) Plot of $\delta^{18}\text{O}$ records of *Globigerinoides ruber* versus depth of cores GC4 (black) and GC5 (gray). Major isotopic events identified in the cores are indicated. (b) Plot of $\delta^{18}\text{O}$ stratigraphies of cores GC4 and GC5 compared to the SPECMAP $\delta^{18}\text{O}$ record (dotted line).

batch after every eighth sample. Values were reported relative to air nitrogen and relative to PDB. Analytical variability was checked again using a soil, homogenized as an internal standard, as a sample after every reference standard. Throughout the analysis of sets of up to 50 samples, the test standard (flour) analyzed in this way gave a standard deviation of 0.16‰ on a measured mean $\delta^{15}\text{N}$ of 3.87‰, and similar precision was obtained for the reference soil (16.56 ± 0.33 ‰). Variation between duplicates was <0.2‰. The precision of $\delta^{13}\text{C}$ analysis was better than 0.22‰, and variation between duplicates was <0.3‰. Total organic carbon (TOC) and total nitrogen (TN) values were determined simultaneously when measuring the isotope ratios, with the test standard showing a standard deviation of 0.009% for C and 0.001% for N, with duplicates having a variation <0.08% and 0.009% for C and N, respectively.

Total carbon was measured on 2-mg aliquots, weighed in aluminum capsules, with a NA 1500 NC Fisons Analyzer at 1020°C. Together with the samples, urea, soil, and one sediment sample were measured as internal standards after every sixth sample. From these measurements, the reproducibility appeared to be better than 0.06%. We reported mean values of duplicate measurements. Variation between duplicates was <0.2%. Inorganic carbon content was derived from the difference between total carbon and organic carbon, and calcium carbonate content was calculated from inorganic carbon values by multiplying the inorganic carbon content by a factor of 8.33.

For major element determination (BaO , Al_2O_3 , K_2O), samples were prepared as glass discs following the method of Norrish and Hutton [1969], with the exception that the flux used consisted of 12 parts lithium metaborate. These glass discs were measured on a PW2400 wavelength dispersive X-ray fluorescence (XRF) spectrometer. The precision of these measurements was better than 0.002% for BaO, 0.03% for

Al_2O_3 , and 0.05% for K_2O . Total barium was corrected for the nonbiogenic barium fraction using the Al content of the sediments, where Al is used as a measure of aluminosilicate contribution [Calvert, 1976; Shimmield, 1992]. Total barium content was normalized using the equation given by Dymond *et al.* [1992]: $\text{Ba}_{\text{excess}} = \text{Ba}_{\text{tot}} - (\text{Al} \times 0.0075)$.

The correction factor in the equation refers to the global $\text{Ba}/\text{Al}_{\text{aluminosilicate}}$ ratio of crustal rocks. Like Francois *et al.* [1995], we have also estimated ranges for biogenic Ba fluxes referring to the extrema in the range of Ba/Al of $0.01 < \text{Ba}/\text{Al} < 0.005$ for crustal rocks as reported by Taylor and McLennan [1985]. There is, however, a measure of imprecision with this method depending on the magnitude of the terrigenous barium fraction [Dymond *et al.*, 1992]. Because much of the terrigenous barium may be contained within feldspar, we have also calculated Ba/K ratios to normalize for variations in feldspar contents [Schneider *et al.*, 1997].

3. Results

Linear sedimentation rates range from 3.5 to 15.3 cm/kyr (Figure 3). Values are higher during the LGM than the Holocene in the shallow core GC5, but not in core GC4. It is possible that the values are influenced by syndepositional redistribution of the sediments, which may result from changes in downslope transport, possibly related to changes in sea level.

TOC concentrations are higher in the sediments from the LGM than the Holocene (Figure 3), implying higher productivity during the LGM. The organic matter fraction of the sediments is predominantly of marine origin, although a minor terrigenous

component may be present. Evidence for this is given by the TOC/N , $\delta^{13}\text{C}_{\text{TOC}}$, TOC/Al , and N/Al values (Figures 3 and 4).

The TOC/N ratios in the sediments are relatively low and point toward the dominance of a marine organic matter fraction (Figure 3) [cf. Müller, 1977, and references therein]. TOC/N ratios are higher during isotope stages 2 and 3. For the sediments from these stages, terrigenous input cannot be ruled out from the elemental composition alone.

Low TOC content (mostly $< 0.8\%$) associated with low TOC/N ratios (< 7.5) can be seen for both cores in isotope stage 1. In contrast, relatively high TOC contents ($> 0.8\%$) can be observed together with high TOC/N ratios (> 7.5) in the core section corresponding to isotope stage 2. Unlike the sediments of stage 1, the sediments of stage 2 contain an inorganic nitrogen fraction in both sediment cores (A. Müller, unpublished data, 1999). The latter is likely to be bound to illite [cf. Müller, 1977]. The TOC/Al and N/Al ratios in core GC4 show similar trends in being highest in stage 2 and lowest in stage 1 (Figure 3). These changes occur almost simultaneously with the transition from isotope stage 1 to isotope stage 2 and indicate the presence of two distinct sedimentological or stratigraphic units rather than continuous diagenetic alteration.

Higher CaCO_3 concentrations were observed in the sediments from the LGM compared with those from the Holocene (Figure 4). As with the above values, excess barium concentrations and Ba/K ratios are higher during the LGM than the Holocene (Figure 4), implying higher productivity. As TOC are relatively low in the study area compared with high-productivity regions, it seems unlikely that barite undergoes significant diagenetic mobilization and reprecipitation due to anoxic conditions in the

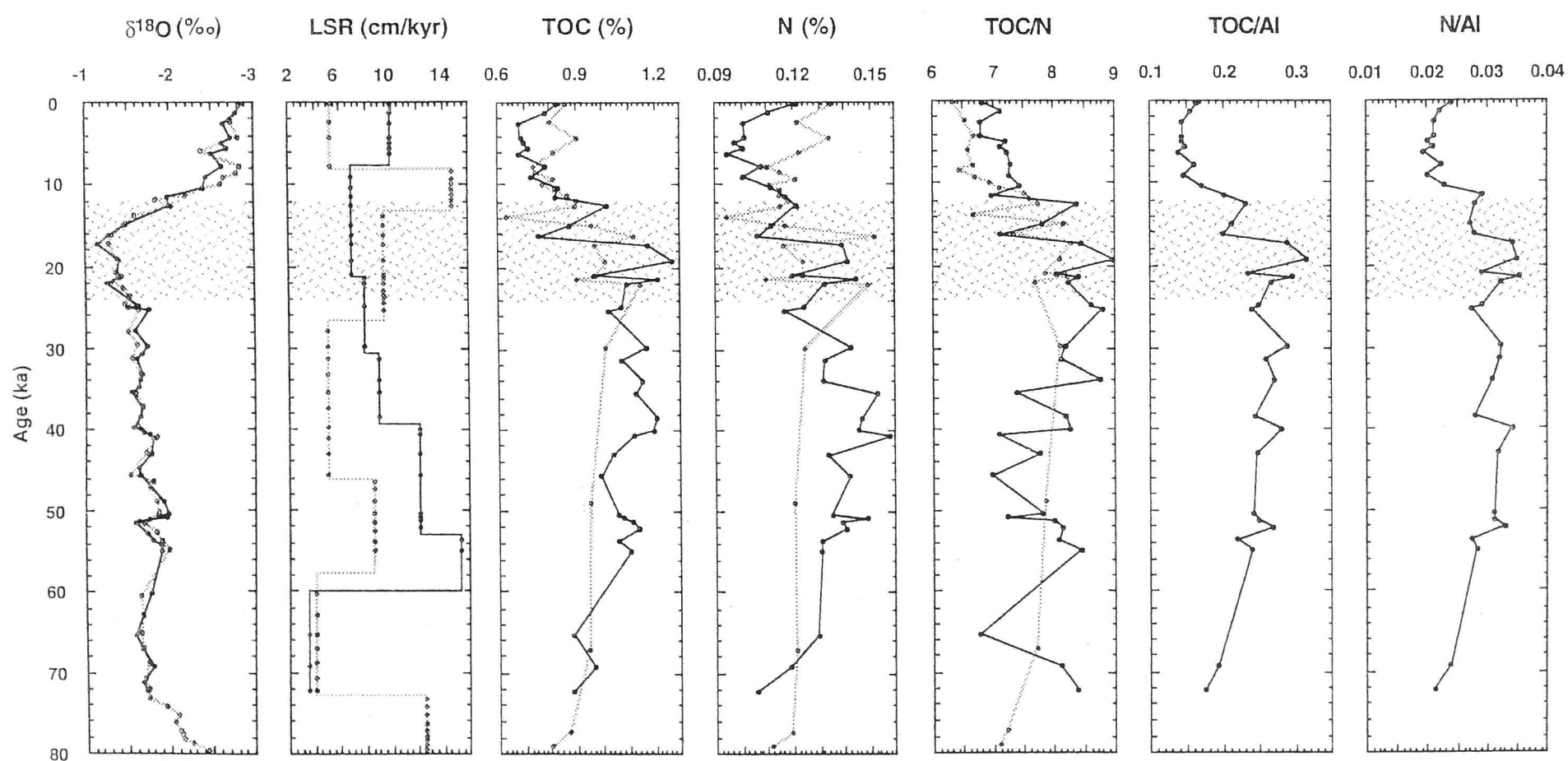


Figure 3. Linear sedimentation rates (LSR), concentrations of total organic carbon (TOC) and nitrogen (N), and TOC/N , TOC/Al , and N/Al ratios in sediment cores GC4 (black) and GC5 (gray). The $\delta^{18}\text{O}$ values of *Globigerinoides ruber* are shown to allow the temporal comparison of the records. The trends of the concentrations of nitrogen closely follow those of organic carbon. Organic carbon and nitrogen concentrations are more elevated in stage 2 than stage 1. TOC/N ratios are higher in stages 2, 3, and 4 compared with those of stage 1. The TOC/Al and N/Al ratios show similar trends. They are highest in stage 2 and lowest in stage 1.

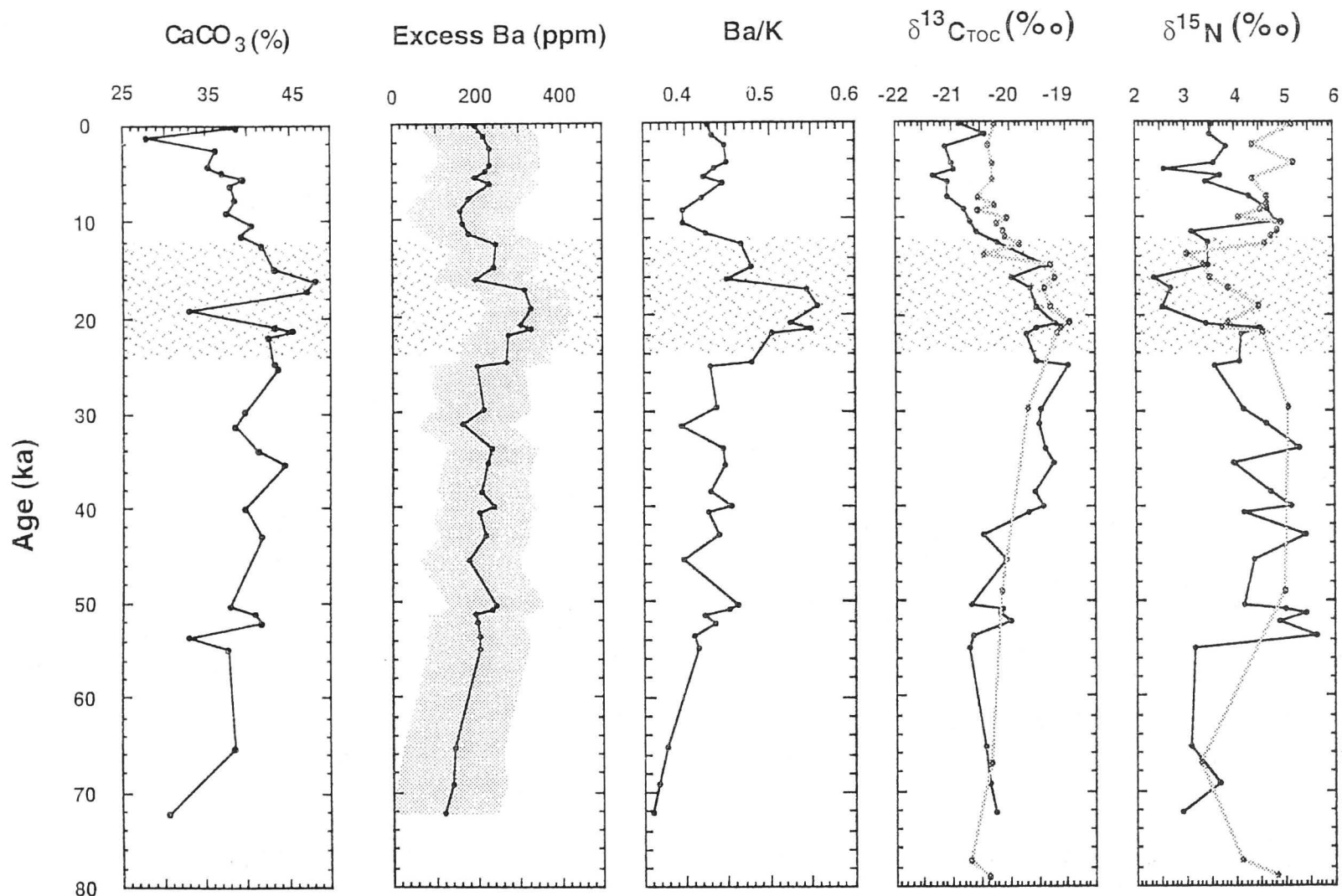


Figure 4. Calcium carbonate (CaCO_3) and excess barium (Ba) concentrations, Ba/K ratios, and stable isotope values of organic carbon ($\delta^{13}\text{C}$) and nitrogen ($\delta^{15}\text{N}$) (core GC4: black; core GC5: gray). The CaCO_3 concentrations reach maximum values in stage 2. Excess Ba concentrations in core GC4 are higher in stage 2 than stages 1 and 3. To account for a possible variation in the Ba/Al of aluminosilicates, we show the range of excess barium values (shaded) that would meet the values in the range of the Ba/Al ratios for crustal rocks given by Taylor and McLennan [1985]. Ba/K ratios in core GC4 are clearly elevated during stage 2 compared with stage 1. The changes observed in the excess barium values and Ba/K ratios in core GC4 closely follow the variations in organic carbon (Figure 3) and calcium carbonate contents for stages 1 and 2. Periods of high organic carbon content also reveal high biogenic barium content. The $\delta^{15}\text{N}$ values in both cores are clearly lower during stage 2 than stages 1 and 3. The $\delta^{13}\text{C}_{\text{TOC}}$ values of cores GC4 and GC5 are lowest in stage 1 but are elevated in stages 2 and 3.

surface sediments [von Breymann *et al.*, 1992; Torres *et al.*, 1996].

The pattern of the records of the values above and those of $\delta^{13}\text{C}_{\text{TOC}}$ and $\delta^{15}\text{N}$ show similar trends along the cores. The sediments show clearly lower $\delta^{15}\text{N}$ and higher $\delta^{13}\text{C}_{\text{TOC}}$ values during the LGM than the Holocene (Figure 4). The LGM-Holocene variation of TOC, $\delta^{13}\text{C}_{\text{TOC}}$, $\delta^{15}\text{N}$, $\text{Ba}_{\text{excess}}$, Ba/K, and CaCO_3 records show a strong relationship with the planktonic foraminiferal $\delta^{18}\text{O}$ record. As a general trend, the Holocene is characterized by low TOC, CaCO_3 , $\text{Ba}_{\text{excess}}$, Ba/K, and $\delta^{13}\text{C}_{\text{TOC}}$ and high $\delta^{15}\text{N}$ values, while the values from the LGM show the opposite. Apart from these general trends, the $\delta^{13}\text{C}_{\text{TOC}}$ and especially the $\delta^{15}\text{N}$ records appear to lag the $\delta^{18}\text{O}$, TOC, N, CaCO_3 , and barium records and reach maximum and minimum values a few thousand years later. In addition to the glacial-interglacial changes, higher-frequency fluctuations appear to be recorded in the sediment sequence. However, at this stage, the resolution and the length of our data series are not sufficient to ensure that these fluctuations are not subject to noise. We will discuss these high-frequency fluctuations in a forthcoming paper using a longer time series and a higher-resolution timescale.

4. Discussion

4.1. Glacial-Interglacial Changes in Paleoproductivity

The combined use of paleoproductivity proxies in our study has proven useful in pointing out times of elevated productivity. This proxy comparison shows generally good agreement between three different paleoproductivity indicators. Given the uncertainty of any single proxy, simultaneous application of more than one tracer strengthens the interpretation of glacial-interglacial changes in paleoproductivity. However, our results also indicate that higher glacial productivity was increased only relative to the low productivity characteristics of this region in the modern ocean. In the following, we discuss each proxy independently.

4.1.1. Organic carbon, TOC/N ratios, and possible diagenetic imprints. Evidence of higher surface ocean productivity during the LGM is given by the TOC concentrations, which are higher in the sediments from the LGM than the Holocene (Figure 3). In estimating changes in productivity from TOC values, we do not account for possible

differences in organic matter preservation due to changes in the magnitude of the sedimentation rates [Heath *et al.*, 1977; Müller and Suess, 1979]. This was done because TOC variations do not appear to show dependence on the sedimentation rates. In particular, higher TOC values during the LGM are not always associated with higher sedimentation rates which could have supported preservation of organic matter.

Sediments from northwestern Australia do not appear to contain a significant input of terrigenous organic matter. This is because the $\delta^{13}\text{C}_{\text{TOC}}$ values of the sediments are high (Figure 4), excluding significant input from C3 plant detritus. The only possible input of a terrigenous organic matter fraction would be from C4 plants. This cannot be excluded for the study area, as palynological studies have shown that the climate was drier and grassland vegetation, characterized by C4 plants, was more prevalent during the LGM in northern Australia [van der Kaars, 1991]. Increased input of C4 plant detritus, associated with increased aridity during the LGM [Prell *et al.*, 1980], could cause a shift to heavier $\delta^{13}\text{C}_{\text{TOC}}$ values in the sediments because C4 plants generally have a higher range of $\delta^{13}\text{C}$ values than C3 plants [Schidlowski *et al.*, 1983]. For example, Goñi *et al.* [1998] demonstrated in the Mississippi River drainage basin that when both C3 and C4 plant sources are equally important, land-derived organic carbon ($\delta^{13}\text{C}_{\text{terr}} = -20$ to -22‰) can be isotopically indistinguishable from marine sources ($\delta^{13}\text{C}_{\text{mar}} = -19$ to -21‰).

However, today, our study area is not affected by large river inputs as is the case for the sites of Goñi *et al.* [1998]. In addition, dust input around Australia is smaller than during the LGM [Hesse, 1994]. During the Holocene, the ranges of the $\delta^{13}\text{C}_{\text{TOC}}$, TOC/N, and $\delta^{15}\text{N}$ and the similar occurrence of higher C/N and lower $\delta^{13}\text{C}_{\text{TOC}}$ in GC4 than GC5 may reflect a terrigenous matter input from C3 plants, although the C/N values are too low to support the input having significant influence. Hydrographic transport patterns could be responsible for differences in the values between the cores from different water depths.

Because of the different geographical and climate conditions, increased input of terrigenous organic material from rivers and dust, in the form of C4 plant detritus, seems possible during the LGM. Although we cannot exclude such an input, it does not in itself appear significant enough to account for the magnitude of the shift in the TOC/N values and the isotope signals of bulk organic matter in the sediments. We therefore do not consider an increased input of C4 plants to have caused the observed shifts in the TOC/N and $\delta^{13}\text{C}_{\text{TOC}}$ values.

The cause of the glacial-interglacial variations in the TOC/N ratios may be attributed to variations in organic matter preservation rather than a source change. Variations in TOC/N ratios during diagenesis may be caused by variations in the organic matter-clay associations. This is because the sorption of organic matter to mineral surfaces (decreasing grain size meaning increasing specific surface area) in marine sediments stabilizes the component molecules and slows remineralization rates [Keil *et al.*, 1994]. Most of the sediments during isotope stage 1 contain only small amounts of organic matter ($<0.8\%$ TOC) and, consequently, have low organic matter/clay mineral (TOC/Al) ratios (Figure 3). In these sediments, the (mainly organic) nitrogen compounds protected within the interlayer spaces of

clay minerals [e.g., Müller, 1977] appear to primarily determine the lower TOC/N ratios.

In contrast, the diagenetic alteration in the sediment sequence of stage 2, with high TOC concentrations ($>0.8\%$) and higher TOC/N, is likely to be different from that occurring in the sediment sequence corresponding to isotope stage 1. This is because the effect of clay mineral assemblages on the TOC/N ratios may vary with the amount of organic matter in the sediments. Increasing TOC/N ratios are often accompanied by an increasing organic matter content [Müller, 1977; Fontugne and Calvert, 1992]. In the stage 2 sequence, a higher organic matter/clay mineral ratio (TOC/Al) can be observed (Figure 3), allowing a relatively smaller fraction of nitrogen to be preserved. We conclude that changes in the TOC/N ratios in the sediments of our study area are primarily controlled by organic matter preservation.

4.1.2. Barium. $\text{Ba}_{\text{excess}}$ and Ba/K values are higher during the LGM than during the Holocene, suggesting elevated productivity. Barium is a highly refractive element in the water column, retaining a high proportion of the original productivity signal relative to other common proxies like organic carbon and calcium carbonate [Dymond *et al.*, 1992]. Here we compare biogenic (or excess) barium concentrations [Francois *et al.*, 1997] and Ba/K ratios [Schneider *et al.*, 1997] to obtain a reliable picture of productivity changes based on barium values. The similar glacial-interglacial trends of the $\text{Ba}_{\text{excess}}$ and Ba/K ratios suggest that changes in terrigenous input do not mask the productivity signal reflected by the ratios.

4.1.3. Calcium carbonate. The CaCO_3 concentrations imply higher productivity during the LGM. Glacial-interglacial changes in CaCO_3 values have been interpreted in terms of variations in both CaCO_3 supply and dissolution intensity [Lyle *et al.*, 1988; Farrell and Prell, 1989; Archer and Maier-Reimer, 1994]. Carbonate dissolution varies as a function of water depth, bottom water chemistry, and carbonate flux [Archer, 1991]. We cannot rule out the possibility that the lower carbonate values in the Holocene section of our sediments reflect dissolution rather than low carbonate supply. However, the similarity of the CaCO_3 trends with those of TOC and barium (Figures 3 and 4) suggests that changes in the rate of CaCO_3 supply, due to variations in productivity, drive the glacial-interglacial changes in CaCO_3 concentrations. All productivity proxies in this study show elevated values during the LGM, although the degree to which they are subject to dissolution or alteration may differ between proxies.

4.2. Glacial-Interglacial Changes in $[\text{CO}_2(\text{aq})]$ in Surface Waters

The changes in the $\delta^{13}\text{C}_{\text{TOC}}$ values in the sediments of this study occur chronologically parallel to paleoproductivity changes documented by the organic carbon, calcium carbonate, and barium data. The $\delta^{13}\text{C}_{\text{TOC}}$ values suggest CO_2 depletion in the surface waters, possibly as a result of enhanced productivity, during stage 2 and during the second half of stage 3. As has been shown, phytoplankton blooms can cause rapid lowering of surface water $p\text{CO}_2$ [e.g., Watson *et al.*, 1991]. Diagenetic alteration does not appear to have caused the change in the $\delta^{13}\text{C}_{\text{TOC}}$ values. We also excluded the likelihood that a terrigenous organic matter fraction has influenced the $\delta^{13}\text{C}_{\text{TOC}}$

values of the sediment. On the basis of the assumption that changes in inorganic carbon $\delta^{13}\text{C}$ did not occur, we conclude that the shift from higher to lower marine sedimentary $\delta^{13}\text{C}_{\text{TOC}}$ across the Pleistocene-Holocene transition has resulted from an increase in ^{13}C discrimination by Holocene phytoplankton. This was associated with a widespread increase in relative $\text{CO}_{2(\text{aq})}$ availability and/or a decrease in phytoplankton carbon demand [cf. *Descolas-Gros and Fontugne, 1985; Falkowski, 1991; Rau et al., 1992*]. Alternatively, the elevated glacial $\delta^{13}\text{C}_{\text{TOC}}$ values could reflect increased phytoplankton utilization of ^{13}C -rich HCO_3^- (relative to $\text{CO}_{2(\text{aq})}$) during that time, which could also be the result of increased productivity in the surface waters [*Degens et al., 1968; Descolas-Gros and Fontugne, 1985; Falkowski, 1991*].

We document here past glacial-interglacial variations in plankton $\delta^{13}\text{C}_{\text{TOC}}$ and suggest that these variations are caused by changes in surface water CO_2 concentrations as a result of variations in surface ocean productivity. In addition, we note the magnitude of change is in agreement with those reported in association with glacial-interglacial changes in surface ocean $p\text{CO}_2$ [cf. *Rau, 1994*]. However, no empirical relationship between plankton $\delta^{13}\text{C}_{\text{TOC}}$ and $[\text{CO}_{2(\text{aq})}]$, and no detailed and sound paleo-SST estimates, have been provided for the study area so far. That is why we find it difficult to delineate local from global signals within the sedimentary record [cf. *Rau, 1994*], which may have been caused by lower atmospheric CO_2 levels during the LGM [*Barnola et al., 1987*].

4.3. Changes in Nutrient Utilization in the Surface Waters

Sedimentary nitrogen isotope ($\delta^{15}\text{N}$) records from a number of regions have been interpreted as reflecting changes in relative nitrate utilization [e.g., *Farrell et al., 1995; Francois et al., 1997; Holmes et al., 1997*]. Thereby isotopically light particulate organic matter is produced during conditions of relative nutrient depletion (low relative nutrient utilization), whereas the opposite applies for isotopically heavy organic matter (high relative nutrient utilization). As well, from several studies, it is apparent that glacial-interglacial cycles have a strong effect on $\delta^{15}\text{N}$ values in many regions when climate-induced changes in hydrography and/or upwelling intensity occur [e.g., *Altabet et al., 1995; Farrell et al., 1995; Ganeshram et al., 1995*].

We measured $\delta^{15}\text{N}$ values in the sediments of our study area in order to investigate changes in nutrient availability and productivity (Figure 4). The following discussion shows that our values do reflect these specific changes rather than having been influenced by the factors of a terrigenous organic matter input, the degradation of sedimentary organic matter, and the occurrence of denitrification in the water column of the study area.

Because the TOC/N and $\delta^{13}\text{C}_{\text{TOC}}$ data do not suggest a possible input of terrigenous organic matter into the sediments to be significant, a $\delta^{15}\text{N}$ signature of terrestrial matter in the sediments would be clearly overprinted by the signal of relative nitrate utilization. In addition, we assume that the $\delta^{15}\text{N}$ signal has not been influenced by offsets between isotope ratios of particulate organic matter sinking through the water column and underlying sediments due to particle decomposition and trophic exchange of nitrogen. Although such offsets have been observed in similar settings with low TOC concentrations in sediments

deposited under oxic conditions, their effects are usually constant and therefore not considered to be significant relative to the signals observed [*Altabet and Francois, 1994a*].

In addition, the $\delta^{15}\text{N}$ values do not appear to be affected by the occurrence of denitrification in the water column of the study area. Evidence for this comes from several sources. First, the $\delta^{15}\text{N}$ values in the sediments do not exhibit a general elevation which would indicate the occurrence of denitrification [*Cline and Kaplan, 1975*]. Moreover, O_2 concentrations today do not drop below 0.2 mL/L [*Wyrski, 1988*], the value that has been described for modern upwelling areas off Peru as being the threshold necessary for denitrification to occur [*Packard et al., 1983*]. Finally, if denitrification was an important factor affecting the $\delta^{15}\text{N}$ values in this area in the past, high sedimentary organic matter content should be associated with high sedimentary $\delta^{15}\text{N}$ values [e.g., *Schäfer and Ittekkot, 1993; Ganeshram et al., 1995*]. The highest $\delta^{15}\text{N}$ values are observed during the Holocene when TOC concentrations are low, and denitrification does not occur today. This indicates that denitrification has not occurred in the past either.

The results indicate that the sedimentary isotopic signal is primarily controlled by the degree of nutrient utilization in the surface waters and that in this region, changes in relative nutrient utilization between the LGM and the Holocene determine the variation in the $\delta^{15}\text{N}$ signal in the sediments. During the Holocene, lower paleoproductivity was concurrent with higher $\delta^{15}\text{N}$ values, which suggests higher relative nitrate utilization. In contrast, the low $\delta^{15}\text{N}$ values suggest that nitrate was less depleted during the LGM when productivity was high. Thus, although productivity was higher, relatively less of the available nitrate pool was utilized by the phytoplankton. Absolute nitrate concentrations must have been elevated to support the high rates of productivity.

Given the present-day oceanography, one plausible explanation for the higher nutrient levels during the LGM involves nutrient supply to the surface waters being more efficient. This is because of a shallower thermocline, the restriction or the absence of the low-salinity cap of the ITF, and the occurrence of upwelling in the area. Upwelled water provides a large pool of nitrate which is available for uptake during photosynthesis, leading to lower planktonic $\delta^{15}\text{N}$ values than when nitrate is more limiting [*Altabet and Francois, 1994b; Holmes et al., 1996*]. Moreover, increased productivity, associated with the presence of upwelling nutrients, has been found to correlate with low $\delta^{15}\text{N}$ values in both sinking organic matter and sediments [*Schäfer and Ittekkot, 1993; Altabet and Francois, 1994b*]. However, glacial productivity in the Timor Trough was high relative only to the low-productivity characteristics of this region in the modern ocean. There is no evidence of strong upwelling of the magnitude of that observed in the modern ocean off the western coasts of Africa and South America.

In addition to the above interpretation for the LGM decline in the $\delta^{15}\text{N}$ values, we notice that other factors must have affected the sediment $\delta^{15}\text{N}$ record. This is because the $\delta^{15}\text{N}$ values of the sediment in our study area are very low compared to those from other study areas with similar settings for which total nitrate utilization and diagenetic enrichment by $\sim 3\text{--}4\text{‰}$ has been considered. Similar to our study area, the latter areas are

characterized by low TOC in the sediments as well as high O_2 in the water column [Altabet and Francois, 1994a; Francois *et al.*, 1997]. If our values showed such a diagenetic offset, they would reflect extremely low nitrate utilization.

Alternatively, the values could be explained by the removal of nitrate not utilized by phytoplankton from the surface waters by physical processes like advection or mixing [Francois *et al.*, 1997]. At present, there is strong evidence for tidal mixing in the study area [J.S. Godfrey and J.V. Mansbridge, Ekman transports, tidal mixing, and the control of temperature structure in Australia's northwest waters, submitted to *Journal of Geophysical Research*, 1999]. Another explanation could be that nitrogen (N_2) fixation was of importance. The $\delta^{15}N$ signature of newly fixed nitrogen is $\sim 0\text{‰}$, close to the isotopic composition of N_2 in air [Wada and Hattori, 1979]. N_2 -fixing cyanobacteria of the genus *Trichodesmium* occur off northwest Australia [Capone *et al.*, 1997]. N_2 fixation provides fixed N to compensate for the deficit in nitrate relative to phosphate that results from denitrification [Falkowski, 1997].

The $\delta^{15}N$ values indicate that if N_2 fixation was of importance, it was more intense during the LGM than the Holocene. This could be for two reasons. First, the inflow of nitrate-depleted surface waters from semienclosed basins of the Indonesian Seas into the study area may have occurred during the LGM. Inflow of oxygen-depleted waters has been reported for the Indonesian Throughflow sensitive northern Indian Ocean [Véneç-Peyré *et al.*, 1995]. At that time, sea level was lower, and denitrification was likely to occur in semienclosed basins in the Indonesian Seas. Regionally, these areas were characterized by high productivity during the LGM [Linsley, 1996; Ahmad *et al.*, 1995]. Haug *et al.* [1998] showed for the Cariaco Basin that denitrification resulted in the removal of nitrate from thermocline depths. This encouraged the growth of N_2 -fixing cyanobacteria when this nitrate deficit was transferred into the surface layer by mixing. A N_2 fixation response [Haug *et al.*, 1998] to glacial-interglacial variations in denitrification on a global scale in the open ocean [Altabet *et al.*, 1995; Ganeshram *et al.*, 1995] is not likely to have occurred in our study area. The trend seen in our data does not accord with global trends of a glacial decrease in denitrification, accompanied by an increase in the oceanic nitrate reservoir, as our values suggest that N_2 fixation would have been more likely to occur during glacials in the Timor Trough.

Second, apart from the reported evidence for changes in the nutrient supply due to variations in the strength of the ITF, we cannot exclude that changes in N_2 fixation may have been influenced by other factors. Besides phosphorus, N_2 -fixing cyanobacteria need trace elements, in particular, iron and molybdenum [e.g., Capone *et al.*, 1997]. Given the lower sea level and the increase in dust flux to the study area during the LGM, metal input is likely to have been higher at that time and would not have inhibited higher levels of N_2 fixation. Further studies will be necessary to show the importance of N_2 fixation in the region.

There is still not enough information to unambiguously interpret these $\delta^{15}N$ records in more detail. However, our interpretation of upwelling in the region during the LGM is derived from a combination of factors. Primarily, the increased productivity during the LGM suggests increased nutrient supply. Previous studies have also shown that during the LGM, the WPWP was reduced in size. Moreover, the present-day

oceanography favors the occurrence of a shallow thermocline and weak upwelling during El Niño events [Meyers, 1996], when the WPWP is reduced in size [Yan *et al.*, 1992].

4.4. Fluctuations and Lags in Proxy Records

The TOC, $CaCO_3$, and $\delta^{13}C_{TOC}$ records and their correlation with the $\delta^{18}O$ record suggest that sea level variations have driven changes in the fertility of the surface waters of the study area. This is because variations in environmental parameters such as SST and surface ocean stratification can be expected to be linked to glaciation and sea level history. The parallel trend of the bulk sediment $\delta^{15}N$ variations suggests coincident changes in the nutrient cycling. However, the lag between $\delta^{15}N$ and sea level suggests that other factors were important.

The lag of the $\delta^{15}N$ record compared to the $\delta^{18}O$ record is of the magnitude of a few thousand years. Similar lags have been observed in other regions and were attributed to a significant $[NO_3]/[PO_4]$ change in the global ocean, which would take several thousand years, whereas changes on a regional scale would require less time [e.g., Haug *et al.*, 1998]. However, at present, we have no proof of a global driving force for the $\delta^{15}N$ signals.

In addition to the glacial-interglacial changes, higher-frequency fluctuations appear to be recorded in the sediment sequence. Although the resolution and the length of our present data series are not sufficient to ensure that these fluctuations are not subject to noise, we note that similar fluctuations have been observed in other areas of the northern Indian Ocean. Véneç-Peyré *et al.* [1995], on the basis of correspondence analysis of foraminiferal and radiolarian assemblages, suggested short-term events (with a duration of <5 kyr), for example, temporary deepenings of the mixed layer. These authors related these events to the rapid inflow of oxygen-depleted water through the Indonesian straits, as a result of the highest sea level rise during deglaciation. They suggested that the events reflected the reorganization of the oceanographic circulation, before the establishment of the regular interglacial through flow. Similar explanations of variable inflow by the ITF could apply in our study area.

The strong contrasts observed at isotope stage 2/1 transition can be considered to be the oceanic signature of the highest sea level rise, which caused an increased outflow of surface waters from the Indonesian basins. Similar contrasts were observed in the Indonesian Throughflow sensitive northern Indian Ocean [e.g., Véneç-Peyré *et al.*, 1997]. Evidence for highest sea level rise at that time has been given by reef terraces, which are presently emerged in the region of the Indo-Pacific Ocean [Chappell and Shackleton, 1986].

The high $\delta^{13}C_{TOC}$, TOC, and $CaCO_3$ in stage 3 prior to the clearly elevated values in stage 2 may indicate that a phytoplankton community was already established and then fertilized further. This was previously observed for the northern Indian Ocean and was thought to be related to water stratification [Véneç-Peyré *et al.*, 1995]. The more elevated values in stage 2 are linked to lowest sea level, which contributed further to shallow water, mixing, and more efficient nutrient supply to the surface waters. This is reflected by the minima seen in the $\delta^{15}N$. Although we cannot offer a detailed interpretation, we suggest that the enhanced barium levels in stage 2, which do not occur in stages 3 and 4, are also linked to lowest sea level.

5. Conclusions

Glacial-interglacial changes in productivity and nutrient utilization in the Timor Trough in the eastern Indian Ocean appear to reflect changes in the activity of the ITF and sea level. Productivity appears to be inversely proportional to the strength of the ITF. On the basis of the present-day oceanography, we infer that during the Holocene, productivity was inhibited by stratification of the water column, suppressed vertical mixing, and low nutrient concentrations in surface waters. This is because of the narrow band of low-salinity surface water that moves through the Indonesian Archipelago and spreads out over the equatorial portions of the eastern Indian Ocean.

However, higher surface ocean productivity during the LGM than the Holocene can be seen in this area; the surface waters being depleted in CO_2 and relative nitrate utilization lower. Covariation of the paleo- $\delta^{15}\text{N}$ signal with changes in paleoproductivity indicates the presence of a higher flux of nutrient-rich water to the surface during the LGM. This higher flux may be the result of a shallower thermocline and weak upwelling in the region. Our findings may reflect the restriction or the absence of this low-salinity "cap" of the ITF, which would be in agreement with previous suggestions of a considerably

weaker ITF during the LGM. In addition, thermal structure appears to have been influenced by sea level changes in the region.

Apart from the reported evidence for changes in the nutrient supply due to variations in the depth of the thermocline, we also suggest that N_2 fixation may have contributed to the N nutrition of the surface waters. Further studies will be necessary, however, to show the importance of N_2 fixation in the region. The paleorecords do not appear to be influenced by changes in the nutrient reservoir in the global ocean but reflect local changes in nutrient supply. The latter are likely to be caused by changes in sea level and the strength of the ITF.

Acknowledgments. This paper greatly benefited from constructive and thoughtful reviews by Luc Beaufort, Daniel McCorkle, and Roger Francois. Comments by Gail Craswell and discussions with Gary Meyers also helped to improve the quality of this paper. Ullrich Senff carried out XRF analyses, and Heather Lynch and Michael Gagan gave assistance during $\delta^{18}\text{O}$ isotopic analysis of foraminifera. We would like to thank the crew of the R/V *Franklin* for their help during sampling. Research was supported by the ANU, a grant by the German Academic Exchange Service (DAAD), and a grant by the Deutsche Forschungsgemeinschaft (DFG) to A.M. during parts of this study and by an ARC Large Grant (A39702412) to B.N.O.

References

- Ahmad, S.M., F. Guichard, K. Hardjawidjaksana, M.K. Adisaputra, and L.D. Labeyrie, Late Quaternary paleoceanography of the Banda Sea, *Mar. Geol.*, **122**, 385-397, 1995.
- Altabet, M.A., and R. Francois, Sedimentary nitrogen isotopic ratio as a recorder for surface ocean nitrate utilization, *Global Biogeochem. Cycles*, **8**(1), 103-116, 1994a.
- Altabet, M.A., and R. Francois, The use of nitrogen isotopic ratio for reconstruction of past changes in surface ocean nutrient utilization, in *Carbon Cycling in the Glacial Ocean*, edited by R. Zahn et al., *NATO ASI Ser., Ser. I*, **17**, 281-306, 1994b.
- Altabet, M.A., R. Francois, D.W. Murray, and W.L. Prell, Climate-related variations in denitrification in the Arabian Sea from sediment $^{15}\text{N}/^{14}\text{N}$ ratios, *Nature*, **373**, 506-509, 1995.
- Archer, D., Equatorial Pacific calcite preservation cycles: Production or dissolution?, *Paleoceanography*, **6**(5), 561-571, 1991.
- Archer, D., and E. Maier-Reimer, Effect of deep-sea sedimentary calcite preservation on atmospheric CO_2 concentration, *Nature*, **367**, 260-263, 1994.
- Barnola, J.M., D. Raynaud, D.Y.S. Korotkevich, and C. Lorius, Vostok ice core provides 160,000-year record of atmospheric CO_2 , *Nature*, **329**, 408-414, 1987.
- Calvert, S.E., The mineralogy and geochemistry of nearshore sediments, in *Treatise on Chemical Oceanography*, vol. 6, edited by J.P. Riley and R. Chester, pp. 187-280, Academic, San Diego, Calif., 1976.
- Capone, D.G., J.P. Zehr, H.W. Paerl, B. Bergman, and E.J. Carpenter, *Trichodesmium*, a globally significant marine cyanobacterium, *Science*, **276**, 1221-1229, 1997.
- Chappell, J., and N.J. Shackleton, Oxygen isotopes and sea level, *Nature*, **324**, 137-140, 1986.
- Clarke, A.J., and X. Liu, Interannual sea level in the northern and eastern Indian Ocean, *J. Phys. Oceanogr.*, **24**, 1224-1235, 1994.
- Cline, J.D., and I.R. Kaplan, Isotopic fractionation of dissolved nitrate during denitrification in the Eastern Tropical North Pacific Ocean, *Mar. Chem.*, **3**, 271-299, 1975.
- Degens, E.T., R.R.L. Guillard, W.M. Sackett, and J.A. Hellebust, Metabolic fractionation of carbon isotopes in marine plankton, I, Temperature and respiration experiments, *Deep Sea Res. Oceanogr. Abstr.*, **15**, 1-9, 1968.
- Descolas-Gros, C., and M.R. Fontugne, Carbon fixation in marine phytoplankton: carboxylase and paleoclimatological aspects, *Marine Biology*, **87**, 1-6, 1985.
- Dymond, J., E. Suess, and M. Lyle, Barium in deep-sea sediment: A geochemical proxy for paleoproductivity, *Paleoceanography*, **7**(2), 163-181, 1992.
- Falkowski, P.G., Species variability in the fractionation of ^{13}C and ^{12}C by marine phytoplankton, *J. Plankton Res.*, **13**, 21-28, 1991.
- Falkowski, P.G., Evolution of the nitrogen cycle and its influence on the biological sequestration of CO_2 in the ocean, *Nature*, **387**, 272-275, 1997.
- Farrell, J.W., and W.L. Prell, Climatic change and CaCO_3 preservation: An 800,000 year bathymetric reconstruction from the central equatorial Pacific Ocean, *Paleoceanography*, **4** (4), 447-466, 1989.
- Farrell, J.W., T.F. Pedersen, S.E. Calvert, and B. Nielsen, Glacial-interglacial changes in nutrient utilization in the equatorial Pacific Ocean, *Nature*, **377**, 514-517, 1995.
- Fontugne, M.R., and S.E. Calvert, Late Pleistocene variability of the carbon isotopic composition of organic matter in the eastern Mediterranean: Monitor of changes in carbon sources and atmospheric CO_2 concentrations, *Paleoceanography*, **7**(1), 1-20, 1992.
- Francois, R., S. Honjo, S.J. Manganini, and G.E. Ravizza, Biogenic barium fluxes to the deep sea: Implications for paleoproductivity reconstruction, *Global Biogeochem. Cycles*, **9**(2), 289-303, 1995.
- Francois, R., M.A. Altabet, E.-F. Yu, D.M. Sigman, M.P. Bacon, M. Frank, G. Bohrmann, G. Bareille, and L.D. Labeyrie, Contribution of Southern Ocean surface-water stratification to low atmospheric CO_2 concentrations during the last glacial period, *Nature*, **389**, 929-935, 1997.
- Ganeshram, R.S., T.F. Pedersen, S.E. Calvert, and J.W. Murray, Large changes in oceanic nutrient inventories from glacial to interglacial periods, *Nature*, **376**, 755-758, 1995.
- Godfrey, J.S., A Sverdrup model of the depth-integrated flow for the world ocean allowing for island circulations, *Geophys. Astrophys. Fluid Dyn.*, **45**, 89-112, 1989.
- Godfrey, J.S., and T.J. Golding, The Sverdrup relation in the Indian Ocean, and the effect of Pacific-Indian Ocean throughflow on Indian Ocean circulation and on the East Australian Current, *J. Phys. Oceanogr.*, **11**, 771-779, 1981.
- Godfrey, J.S., and K.R. Ridgway, The large-scale environment of the poleward-flowing Leeuwin Current, Western Australia: Longshore steric height gradients, wind stresses and geostrophic flow, *J. Phys. Oceanogr.*, **15**, 481-495, 1985.
- Goffi, M.A., K.C. Ruttenberg, and T.I. Eglinton, A reassessment of the sources and importance of land-derived organic matter in surface sediments from the Gulf of Mexico, *Geochim. Cosmochim. Acta*, **62**(18), 3055-3075, 1998.
- Gordon, A.L., and R.A. Fine, Pathways of water between the Pacific and Indian Oceans in the Indonesian seas, *Nature*, **379**, 146-149, 1996.
- Haug, G.H., T.F. Pedersen, D.M. Sigman, S.E. Calvert, B. Nielsen, and L.C. Peterson, Glacial/interglacial variations in production and nitrogen fixation in the Cariaco Basin during the last 580 kyr, *Paleoceanography*, **13**(5), 427-432, 1998.
- Heath, G.R., T.C. Moore, and J.P. Dauphin, Organic carbon in deep-sea sediments, in *The Fate of Fossil Fuel CO_2 in the Oceans*, edited by R.N. Anderson and A. Malahoff, pp. 605-625, Plenum, New York, 1977.
- Hesse, P.P., The record of continental dust from Australia in Tasman Sea sediments, *Quat. Sci. Rev.*, **13**, 257-272, 1994.
- Holmes, M.E., P.J. Müller, R.R. Schneider, M. Segl, J. Pätzold, and G. Wefer, Stable nitrogen

- isotopes in Angola Basin surface sediments, *Mar. Geol.*, 134, 1-12, 1996.
- Holmes, M.E., R.R. Schneider, P.J. Müller, M. Segl, and G. Wefer, Reconstruction of past nutrient utilization in the eastern Angola Basin based on sedimentary $^{15}\text{N}/^{14}\text{N}$ ratios, *Paleoceanography*, 12(4), 604-614, 1997.
- Imbrie, J., J.D. Hays, D.G. Martinson, A. McIntyre, A. Mix, J.J. Morley, N.G. Pisias, W.L. Prell, and N.J. Shackleton, The orbital theory of Pleistocene climate: Support from a revised chronology of the marine ^{18}O record, in *Milankovitch and Climate*, edited by A.L. Berger et al., NATO ASI Ser., Ser. C, vol. 126, part I, pp. 269-305, D. Reidel, Norwell, Mass., 1984.
- Keil, R.G., D.B. Montluçon, F.G. Prahl, and J.I. Hedges, Sorptive preservation of labile organic matter in marine sediments, *Nature*, 370, 549-552, 1994.
- Linsley, B.K., Oxygen-isotope record of sea level and climate variations in the Sulu Sea over the past 150,000 years, *Nature*, 380, 234-237, 1996.
- Lyle, M., D.W. Murray, B.P. Finney, J. Dymond, J.M. Robbins, and K. Brooksforce, The record of late Pleistocene biogenic sedimentation in the eastern tropical Pacific Ocean, *Paleoceanography*, 3(1), 39-59, 1988.
- Mariotti, A., Atmospheric nitrogen is a reliable standard for natural ^{15}N abundance measurements, *Nature*, 303, 680-683, 1983.
- Martinez, J.I., Late Pleistocene palaeoceanography of the Tasman Sea: Implications for the dynamics of the warm pool in the western Pacific, *Palaeogeogr., Palaeoclimatol., Palaeoecol.*, 112, 19-62, 1994.
- Martinson, D.G., N.G. Pisias, J.D. Hays, I. Imbrie, T.C. Moore, and N.J. Shackleton, Age dating and the orbital theory of the ice-ages: Development of a high-resolution 0 to 300,000-year chronostratigraphy, *Quat. Res.*, 27, 1-29, 1987.
- McCorkle, D.C., H.H. Veeh, and D.T. Heggie, Glacial-Holocene paleoproductivity off western Australia: A comparison of proxy records, in *Carbon Cycling in the Glacial Ocean*, edited by R. Zahn et al., NATO ASI Ser., Ser. I, 17, 443-479, 1994.
- Meyers, G., Variation of Indonesian throughflow and the El Niño - Southern Oscillation, *J. Geophys. Res.*, 101(C5), 12,255-12,263, 1996.
- Müller, P.J., C/N ratios in Pacific deep-sea sediments: Effect of inorganic ammonium and organic nitrogen compounds sorbed by clays, *Geochim. Cosmochim. Acta*, 41, 765-776, 1977.
- Müller, P.J., and E. Suess, Productivity, sedimentation rate and organic matter in the oceans, I, Organic carbon preservation, *Deep Sea Res., Part A*, 26, 1347-1362, 1979.
- Norrish, K., and J.T. Hutton, An accurate X-ray spectrographic method for the analysis of a wide range of geological samples, *Geochim. Cosmochim. Acta*, 33, 431-453, 1969.
- Packard, T.T., P.C. Garfield, and L.A. Codispoti, Oxygen consumption and denitrification below the Peruvian upwelling, in *Coastal Upwelling: Its Sediment Record*, part A, edited by J. Thiede and E. Suess, pp. 365-398, Plenum, New York, 1983.
- Prell, W.L., W.H. Hutson, D.F. Williams, A.W.H. Be, K. Geitzenauer, and B. Molino, Surface circulation of the Indian Ocean during the Last Glacial Maximum, approximately 18,000 yr BP, *Quat. Res.*, 14, 309-336, 1980.
- Rau, G.H., Variations in sedimentary organic $\delta^{13}\text{C}$ as a proxy for past changes in ocean and atmospheric CO_2 concentrations, in *Carbon Cycling in the Glacial Ocean*, edited by R. Zahn et al., NATO ASI Ser., Ser. I, 17, 307-321, 1994.
- Rau, G.H., T. Takahashi, D.J. Des Marais, D.J. Repeta, and J.H. Martin, The relationship between $\delta^{13}\text{C}$ of organic matter and $[\text{CO}_2(\text{aq})]$ in ocean surface water: Data from a JGOFS site in the northeast Atlantic Ocean and a model, *Geochim. Cosmochim. Acta*, 56, 1413-1419, 1992.
- Schäfer, P., and V. Ittekkot, Seasonal variability of $\delta^{15}\text{N}$ in settling particles in the Arabian Sea and its palaeochemical significance, *Naturwissenschaften*, 80, 511-513, 1993.
- Schidlowski, M., J.M. Hayes, and I.R. Kaplan, Isotopic inferences of ancient biochemistries: Carbon, sulfur, hydrogen, and nitrogen, in *Earth's Earliest Biosphere: Its Origin and Evolution*, edited by J.W. Schopf, pp. 149-186, Princeton Univ. Press, Princeton, N.J., 1983.
- Schneider, R.R., B. Price, P.J. Müller, D. Kroon, and I. Alexander, Monsoon related variations in Zaire (Congo) sediment load and influence of fluvial silicate supply on marine productivity in the east equatorial Atlantic during the last 200,000 years, *Paleoceanography*, 12(3), 463-481, 1997.
- Shimmield, G.B., Can sediment geochemistry record changes in coastal upwelling paleoproductivity? Evidence from northwest Africa and the Arabian Sea, in *Upwelling Systems: Evolution Since the Early Miocene*, edited by C. Summerhayes, W. Prell, and K.-C. Emeis, *Geol. Soc. Spec. Publ.*, 64, 29-46, 1992.
- Smith, R.L., Coastal upwelling in the modern ocean, in *Upwelling Systems: Evolution Since the Early Miocene*, edited by C.P. Summerhayes, W.L. Prell, and K.-C. Emeis, *Geol. Soc. Spec. Publ.*, 64, 9-28, 1992.
- Taylor, R.S., and S.M. McLennan, *The Continental Crust: Its Composition and Evolution*, 312 pp., Blackwell Sci., Cambridge, Mass, 1985.
- Thunell, R., D. Anderson, D. Gellar, and Q. Miao, Sea-surface temperature estimates for the tropical western Pacific during the last glaciation and their implications for the Pacific Warm Pool, *Quat. Res.*, 41, 255-264, 1994.
- Tomczak, M., and J.S. Godfrey, *Regional Oceanography: An Introduction*, 422 pp., Pergamon, Tarrytown, N.Y., 1994.
- Torres, M.E., H.J. Brumsack, G. Bohrmann, and K.C. Emeis, Barite fronts in continental margin sediments: A new look at barium remobilization in the zone of sulfate reduction and formation of heavy barites in diagenetic fronts, *Chem. Geol.*, 127, 125-139, 1996.
- van der Kaars, W.A., Palynology of eastern Indonesian marine piston-cores: A late Quaternary vegetational and climatic record for Australasia, *Palaeogeogr., Palaeoclimatol., Palaeoecol.*, 117, 55-72, 1991.
- Vénec-Peyré, M.-T., J.P. Caulet, and C.V. Grazzini, Paleohydrographic changes in the Somali Basin (5°N upwelling and equatorial areas) during the last 160 kyr, based on correspondence analysis of foraminiferal and radiolarian assemblages, *Paleoceanography*, 10(3), 473-491, 1995.
- Vénec-Peyré, M.-T., J.P. Caulet, and C.V. Grazzini, Glacial/interglacial changes in the equatorial part of the Somali Basin (NW Indian Ocean) during the last 355 kyr, *Paleoceanography*, 12(5), 640-648, 1997.
- von Breyman, M.T., K.C. Emeis, and E. Suess, Water depth and diagenetic constraints on the use of barium as a palaeoproductivity indicator, in *Upwelling Systems: Evolution Since the Early Miocene*, edited by C.P. Summerhayes, W.L. Prell, and K.-C. Emeis, *Geol. Soc. Spec. Publ.*, 64, 273-284, 1992.
- Wada, E., and A. Hattori, Natural abundances of ^{15}N in particulate organic matter in the North Pacific Ocean, *Geochim. Cosmochim. Acta*, 40, 249-251, 1979.
- Watson, A.J., C. Robinson, J.E. Robinson, P.J. Williams, and M.J.R. Fasham, Spatial variability in the sink for atmospheric carbon dioxide in the North Atlantic, *Nature*, 350, 50-53, 1991.
- Wells, P.E., G.M. Wells, J. Cali, and A. Chivas, Response of deep-sea foraminifera to late Quaternary climate changes, southeast Indian Ocean, offshore Western Australia, *Mar. Micropaleontol.*, 23, 185-229, 1994.
- Wyrki, K., Indonesian Throughflow and the associated pressure gradient, *J. Geophys. Res.*, 92(C12), 12,941-12,946, 1987.
- Wyrki, K., *Oceanographic Atlas of the International Indian Ocean Expedition*, 531 pp., Nat. Sci. Found., Washington, D. C., 1988.
- Yan, X.-H., C.-R. Ho, Q. Zheng, and V. Klemas, Temperature and size variabilities of the Western Pacific Warm Pool, *Science*, 258, 1643-1645, 1992.

A. Müller and B. N. Opdyke, Department of Geology, Australian National University, Canberra, ACT, Australia. (amuller@geology.anu.edu.au; bno@basins.anu.edu.au).

(Received January 5, 1999;
revised August 24, 1999;
accepted August 26, 1999.)

Early marine diagenesis in corals and geochemical consequences for paleoceanographic reconstructions

Anne Müller^{1,2}, Michael K. Gagan², Malcolm T. McCulloch²

Abstract. Detecting the potential geochemical consequences of early marine diagenesis is essential for establishing the validity of past climate reconstructions from coral. We present coral skeletal $\delta^{18}\text{O}$ and Sr/Ca data for two long coral cores spanning 1839-1994 AD at Ningaloo Reef, Western Australia, one of which includes significant secondary precipitation of marine inorganic aragonite. Long-term trends in reconstructed sea surface temperatures (SSTs) for the well preserved coral correlate strongly with instrumental SST records spanning the 20th century. In contrast, the $\delta^{18}\text{O}$ and Sr/Ca for the diagenetically altered coral give identical cool SST anomalies of 4-5°C, as a consequence of the addition of secondary aragonite enriched in ^{18}O and Sr. Our results indicate that cross-checking of paleoclimate reconstructions with two supposedly independent paleothermometers may not be valid, and that coral records showing cooler SSTs in the past need to be interpreted with caution. Furthermore, modern coral records with long-term trends in $\delta^{18}\text{O}$ indicating recent warming and freshening of the ocean can be potentially explained by early marine diagenesis.

Introduction

Sea surface temperatures (SSTs) are an important quantity for understanding past climate dynamics, and estimates of SSTs are an essential boundary condition used in general circulation models of past and future climate (Graham 1995, Bush 1999). Large negative SST anomalies of 4 to 6.5°C have been reconstructed for the last deglaciation and the last glacial maximum (LGM) using $\delta^{18}\text{O}$ and Sr/Ca measurements in scleractinian corals (Guilderson et al. 1994, Beck et al. 1997). The tropical sea surface temperatures recorded from fossil coral for the LGM (Guilderson et al. 1994), however, are much lower than those recorded from other marine proxies. These proxies, which include foraminifera speciation (CLIMAP 1981, Mix et al. 1986), foraminiferal oxygen isotopes (Broecker 1986, Birchfield 1987) and alkenone results (Lyle et al. 1992, Rostek et al. 1993, Sikes and Keigwin 1994), suggest a cooling of no more than 3°C. At present, it is not clear if this difference reflects regional differences in the extent of cooling, or if one group of proxies is misleading (Broecker 1996). Another surprising finding is the large warming and/or freshening trends for the ocean surface over the last 200 years

indicated by many recent coral $\delta^{18}\text{O}$ records (reviewed by Gagan et al. 2000). These long-term trends generally exceed those of 20th century instrumental records (Cane et al. 1997) and suggest that tracers in corals may overestimate cooling of the ocean in the past.

Recent studies indicate that anomalously low SST estimates given by Sr/Ca thermometry may be produced by early marine diagenesis including recrystallization and secondary aragonite precipitation in live coral. Secondary inorganic aragonite has a significantly higher Sr/Ca ratio than primary coral aragonite (Enmar et al. 2000). Marine aragonite may be common in corals that are only decades old. Few studies have investigated the geochemical implications of early marine diagenesis; thus our understanding of these for paleoenvironmental and paleoclimatic reconstructions is limited.

A common approach used to address the issue of diagenesis is independent geochemical tracers to cross-check the results of coral records. For example, the large cooling for the last glacial maximum and the mid-stages of the last deglaciation has been justified because SSTs reconstructed from both coral $\delta^{18}\text{O}$ and Sr/Ca showed the same large negative temperature anomalies (Guilderson et al. 1994, Beck et al. 1997, McCulloch et al. 1999). In this paper, we show that cool artefacts in coral records can be produced by early marine diagenesis because secondary aragonite is enriched in $\delta^{18}\text{O}$ and Sr/Ca relative to the coral skeleton. In our study area, the cool artefacts given by $\delta^{18}\text{O}$ and Sr/Ca are identical in magnitude.

Procedures

Cores were drilled from live coral colonies at two different locations in Ningaloo Reef Marine Park, Western Australia. One was located in Tantabiddi Lagoon (21°54.3'S, 113°57.9'E) and the other off South Muiron Island (21°41.9'S, 114°18.8'E) (Fig.1).

5-year sample increments were chosen using X-ray prints, gamma densitometry data and UV fluorescence light. Aliquots of powder from every second increment were analyzed for $\delta^{18}\text{O}$ and Sr/Ca. $\delta^{18}\text{O}$ analysis was carried out using an automated individual carbonate-reaction (Kiel) device coupled with a Finnigan-MAT 251 mass spectrometer. The $\delta^{18}\text{O}$ values were calculated as per mil (‰) deviations relative to VPDB, and were calibrated via the NBS-19 standard ($\delta^{18}\text{O} = -2.20\text{‰}$). Average reproducibility for a typical 150-μg sample was $\pm 0.04\text{‰}$ (2σ , $n=14$), which is equivalent to about $\pm 0.2^\circ\text{C}$ if $\delta^{18}\text{O}$ is controlled by temperature alone. Sr/Ca ratios were measured by isotope dilution on a Finnigan MAT 261 thermal ionisation mass spectrometer (TIMS), following the method described in Alibert and McCulloch (1997). A power law was used to correct for the instrumental fractionation relative to $^{43}\text{Ca}/^{42}\text{Ca} = 0.960269$ (the spike composition) and $^{86}\text{Sr}/^{88}\text{Sr} = 0.1194$. The reproducibility of Sr/Ca was 0.00005 (2σ) which is equivalent to $<0.2^\circ\text{C}$.

¹ Department of Geology, Australian National University, Canberra, ACT, Australia

² Research School of Earth Sciences, Australian National University, Canberra, ACT, Australia

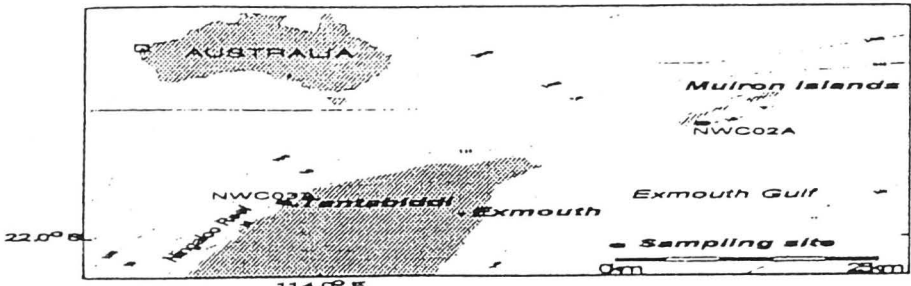


Figure 1. Location of the coral study sites in Ningaloo Reef Marine Park, Western Australia. Bathymetric lines show water depth in m.

Results

While XRD results show that the coral cores do not contain any detectable amounts of calcite, petrographic investigations indicate that secondary aragonite is present within the coral skeleton toward the base of core NWC02A (S. Muiron Isl.) (Fig.2A). The formation of secondary aragonite fibres in corals, as seen in skeletal pores in Fig.2, has previously been suggested to occur under marine conditions (Sansone et al. 1988, Tribble et al. 1990). Secondary aragonite could not be seen in core NWC03A (Tantabiddi) (Fig.2B).

The presence of the secondary aragonite is reflected by the dramatic shift in the $\delta^{18}\text{O}$ and Sr/Ca values toward the base of the core. The $\delta^{18}\text{O}$ and Sr/Ca values for the pristine coral show little change over time (Fig.3A). However, higher $\delta^{18}\text{O}$ and Sr/Ca values can be seen in the cemented bottom part of core NWC02A (S. Muiron Isl.) and are linked to the presence of the secondary aragonite (Fig.4A). Our findings for Sr/Ca are in agreement with those of Enmar et al (2000), who also reported higher Sr/Ca in early marine inorganic aragonite cements than in pristine *Porites* skeletons. A change in growth rate does not account for the anomalous skeletal chemistry at the basal part of this core because extension rates were the same at the base of the core as those elsewhere.

The results suggest that, in this case, the $\delta^{18}\text{O}$ and Sr/Ca values do not reflect the true SSTs for the altered coral core. We have calculated SSTs from $\delta^{18}\text{O}$ using the mean slope of five established equations for the temperature dependence of oxygen isotope fractionation in coral aragonite (Fig.3B, 4B): $T = (4.854 \pm 0.773)\delta^{18}\text{O}$ (McConnaughey 1989, Leder et al. 1996, Quinn et al. 1996, Wellington et al. 1996, Gagan et al. 1998). Similarly, we have used the mean slope of five published Sr/Ca-SST relationships using TIMS measurements of Sr/Ca to calculate a change in degree Celsius ($^{\circ}\text{C}$) per unit change in Sr/Ca (Fig.3B, 4B): $T = (17242 \pm 3506)\text{Sr/Ca}$ (Beck et al. 1992, Min et al. 1995, Shen et al. 1996, Alibert and

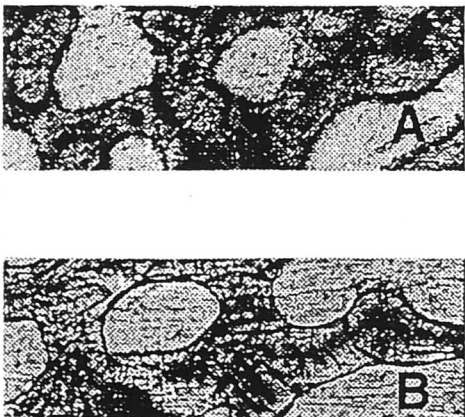


Figure 2. Microscopic images of: (A) Diagenetically altered coral skeleton in basal part of core NWC02A at South Muiron Island. (B) Pristine coral aragonite of core NWC03A at Tantabiddi.

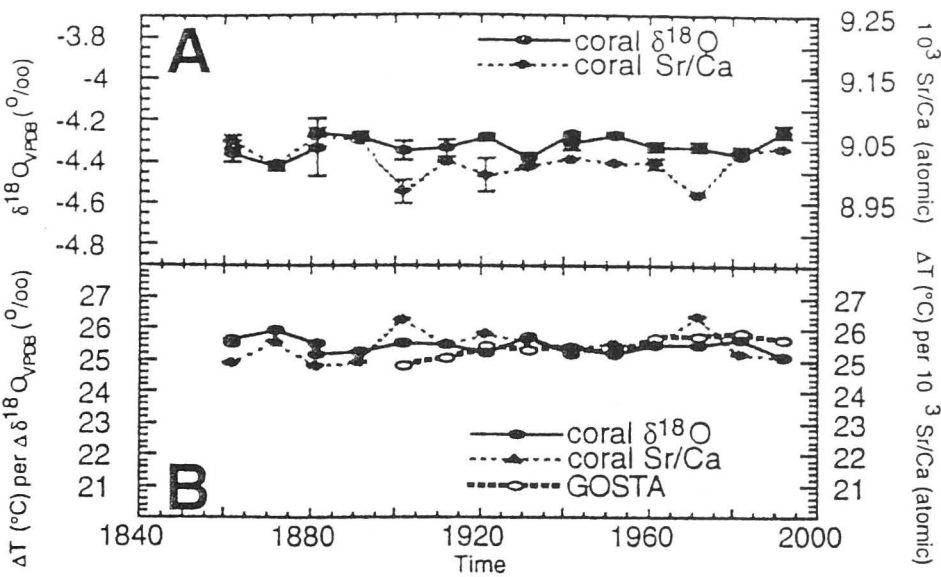


Figure 3. (A) $\delta^{18}\text{O}$ (circles) and Sr/Ca values (squares) in the pristine coral core NWC03A at Tantabiddi. Error bars show standard deviation (2σ) for duplicate measurements. (B) Sea surface temperature (SST) units reconstructed from $\delta^{18}\text{O}$ (circles) and Sr/Ca (squares) values. The GOSTA instrumental SST data set (open circles) is shown for comparison.

McCulloch 1997, Gagan et al. 1998). To simplify our calculations and since we are only interested in the slope of the relationship of each tracer to temperature, we have only used the mean slope of the five equations considered for each tracer and we have ignored the offset. Consequently, rather than true SSTs we have calculated the relative SST change per unit in $\delta^{18}\text{O}$ and Sr/Ca respectively. This simplification is possible because the least-square approximation for these linear equations shows that the slope would be the same whether the offset was included or not.

For both cores, the means of the reconstructed $\delta^{18}\text{O}$ -SST and Sr/Ca-SST unit values have been aligned with the mean value of the GOSTA instrumental SST data (Parker et al. 1995) for the period 1900-1994 AD (Fig. 3B, 4B). A comparison of the SST unit data with the GOSTA data shows that the $\delta^{18}\text{O}$ and Sr/Ca based SST trends in the pristine coral core correspond reasonably well with those of the GOSTA instrumental SST

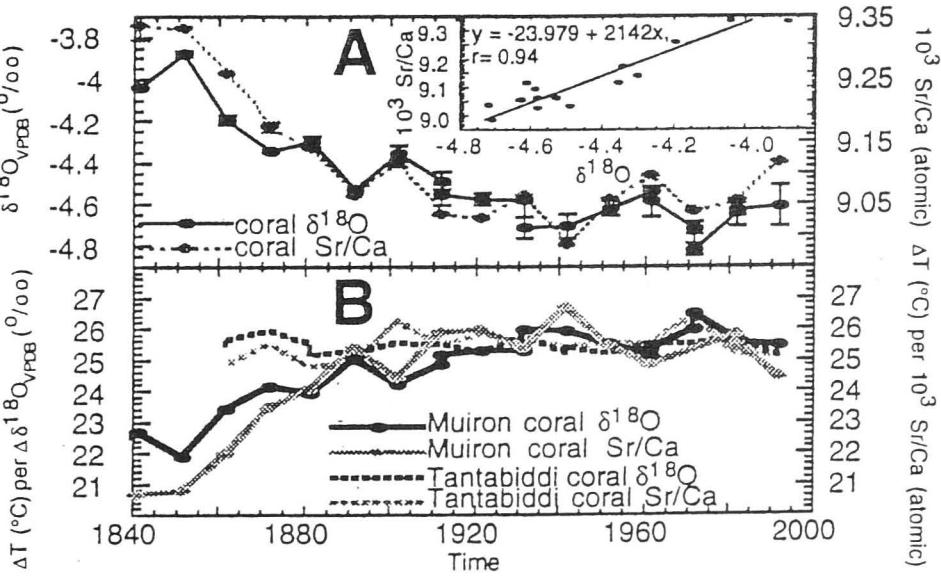


Figure 4. (A) $\delta^{18}\text{O}$ (circles) and Sr/Ca values (squares) in the diagenetically altered coral core NWC02A at South Muiron Island. Error bars show standard deviation (2σ) for duplicate measurements. (B) Reconstructed sea surface temperature (SST) units, calculated from $\delta^{18}\text{O}$ and Sr/Ca values. We compared the GOSTA aligned reconstructed SST unit data from both coral cores. This approach was chosen to eliminate the influence of differences in chemistry between the two coral cores in the absence of diagenesis.

data set (Fig.3B). A comparison of the aligned SST unit data from the pristine and the altered core, however, indicates a large difference of 4–5°C in the data from the basal parts of the two cores (Fig.4B). Both the $\delta^{18}\text{O}$ and Sr/Ca based values record cooler temperatures for the altered core. Interestingly, our coral shows a similar magnitude of decrease in SSTs for $\delta^{18}\text{O}$ and Sr/Ca based reconstructions. The trend for $\delta^{18}\text{O}$ to rise from older to younger regions of the core resembles that of other records which were interpreted to reflect warming/freshening trends of the ocean (Gagan et al. 2000). In contrast, no such trend of decreasing $\delta^{18}\text{O}$ can be seen in the pristine core.

There is a strong correlation of $\delta^{18}\text{O}$ and Sr/Ca in the altered core NWC02A off S. Muiron Island. ($r=0.94$, $n=16$) (insert in Fig.4A). This indicates simultaneous enrichment of $\delta^{18}\text{O}$ and Sr/Ca, as determined by kinetic behaviour, with the addition of secondary aragonite. The relationship between $\delta^{18}\text{O}$ and Sr/Ca in this core is such that it yields nearly equal SST changes for both tracers regardless of the degree of diagenesis. The slope of the regression line shows that a change in $\delta^{18}\text{O}$ of 0.2‰ (equal to a change of 1°C) would be accompanied by a change in Sr/Ca of 0.8 (equal to a change of 1.3°C). The correlation coefficient in the unaltered upper half of the core is lower ($r=0.57$, $n=8$) than in the altered lower half ($r=0.95$, $n=8$). This suggests that the kinetic behaviour in the coral skeleton is moderately masked by environmental conditions, such as changes in environmental temperature and composition, which can modify $\delta^{18}\text{O}$ (McConnaughey 1989) and Sr/Ca values (Alibert and McCulloch 1997). In contrast, $\delta^{18}\text{O}$ and Sr/Ca values in the unaltered core from Tantabiddi show poor correlation ($r=0.34$, $n=14$), most likely due to changes in isotopic composition of sea water because of high rates of evaporation in the lagoon.

Discussion

Both the skeletal aragonite and the secondary aragonite compositions deviate from equilibrium in that they show depleted compositions in ^{18}O (McConnaughey 1989) and Sr (cf Kinsman and Holland 1969). The cement shows values closest to what would represent equilibrium carbonate precipitation. The correlation in the altered coral core, and particularly in its basal part, suggests a simultaneous depletion of $\delta^{18}\text{O}$ and Sr/Ca for the cement. The simultaneous depletion of ^{18}O and Sr/Ca relative to equilibrium reflects the kinetic effects which have been previously credited with much of the ^{13}C depletion and all of the ^{18}O depletion, relative to isotopic equilibrium (McConnaughey 1989).

As expected, we reconstructed the same temperature from $\delta^{18}\text{O}$ and Sr/Ca values at the top of the core (Fig.4B). This was because we used the $\delta^{18}\text{O}$ and Sr/Ca equations which have been set up for pristine coral from known seawater temperatures and isotopic compositions. These calibrations consider the specific departure of coral from equilibrium (McConnaughey 1989).

We did not, however, expect to find that both tracers would show the same temperature at the base of the core, which proved to be the case (Fig.4B). In our coral both tracers show a downcore change in the status of kinetic disequilibrium with seawater, with the cement having a different kinetic disequilibrium status than the coral skeleton. The difference in kinetic disequilibrium can be caused by differences in the composition of the solution from which the aragonite crystals

of the coral and the cement were precipitated. Another reason for the difference could be a difference in precipitation rate of the aragonite crystals. We might expect from this difference in kinetic disequilibrium that the temperature equations would not be applicable to the cement and that temperature reconstructions based on these equations would result in different temperatures being reconstructed from each tracer.

The offset between the pristine top and the altered base of the core in Fig.4B is 4–5°C SST units for both $\delta^{18}\text{O}$ and Sr/Ca. This simultaneous anomaly can be explained by mechanisms of crystal growth. Contrary to what would be expected, in the secondary aragonite of our coral, both distribution coefficient of Sr and isotope fractionation of ^{18}O are a function of the rate of crystal growth as well as the composition of the layer of solution in the vicinity of the crystal surface. It has previously been shown experimentally that the distribution coefficient of Sr can be a function of the rate of crystal growth as well as the composition of this layer of solution (Kinsman and Holland 1969). This study showed that coprecipitation of Sr^{2+} with aragonite can depend upon surface phenomena rather than upon equilibrium between the solution and the interior of aragonite crystals. The value of the distribution coefficient for Sr would depend upon surface phenomena under certain conditions. One such condition is a high rate of crystal growth. The rate of crystal growth needs to be greater than the rate of diffusion of Sr^{2+} and Ca^{2+} between the solution and the interior of growing aragonite crystals. A second condition is that the rate of crystal growth is sufficiently slow to allow the Sr/Ca ratio in the younger regions of the crystal to adjust itself accordingly by reaction with the solution. In this situation the growth region of the crystal is moved away from older regions before the older regions have time to equilibrate with the precipitating solution. It then follows that the offset is similar for both $\delta^{18}\text{O}$ and Sr/Ca because their distribution in both the coral skeleton and the secondary aragonite is largely controlled by kinetic effects, which are determined by similar mechanisms of crystal growth controlled by surface phenomena.

The covariation in $\delta^{18}\text{O}$ and Sr/Ca in our coral shows that these two measurements do not give an independent evaluation of SSTs and that they cannot reliably be used as cross checks. This implies that chemical cross checks with two tracers may not be sufficient to verify coral records and that textural studies using petrographic observations or scanning electron microscopy must be included to detect potential secondary overgrowths.

Our finding of cold Sr/Ca artefacts produced by diagenesis adds to previous suggestions of potential misinterpretations of SST reconstructions from coral Sr/Ca. For example, it has also been shown that increases in the Sr/Ca ratio of seawater due to large shelf recrystallization fluxes during glacial maxima would produce up to 1.5° errors in paleotemperatures calculated from Sr/Ca ratios in *Porites* since the LGM (Stoll and Schrag 1998).

The magnitude of the "temperature" drop observed in our altered coral is nearly 5°C. This cold artefact is larger than that observed in previous investigations of diagenetic effects on Sr/Ca (Enmar et al. 2000). The magnitude of the decrease in temperature in our coral exceeds that of some observed differences in reconstructed SSTs among different paleoproxies, as pointed out above. Consequently, secondary aragonite in fossil corals must be carefully considered for records suggesting SSTs are cooler than today. Also,

interpretation of warming or freshening trends in coral records can be affected by early marine diagenesis. Nearly all published coral $\delta^{18}\text{O}$ records show warming/freshening trends toward the present over the last 200 years. It is possible that many of these trends are in fact related to secondary aragonite accumulating over 10s of years, beginning at the older base of the corals. Clearly, these trends have to be critically assessed, and care taken in drawing conclusions from $\delta^{18}\text{O}$ trends on the role of the tropical oceans in the hydrological cycle.

Acknowledgments. This study was supported by the Australian National Greenhouse Advisory Committee. A.M. was supported by the ANU and the DFG (Deutsche Forschungsgemeinschaft).

References

- Alibert, C. and M.T. McCulloch, Strontium/calcium ratios in modern *Porites* corals from the Great Barrier Reef as a proxy for sea surface temperature: Calibration of thermometer and monitoring of ENSO, *Paleoceanography* 12, 345-363, 1997.
- Beck, J.W., R.L. Edwards, E. Ito, F.W. Taylor, J. Recy, F. Rougerie, P. Joannot and C. Henin, Sea surface temperature from coral skeletal strontium/calcium ratios, *Science* 257, 644-647, 1992.
- Beck, J.W., J. Récy, F. Taylor, R.L. Edwards and G. Cabioch, Abrupt changes in early tropical sea surface temperature derived from coral records, *Nature* 385, 705-707, 1997.
- Birchfield, G.E., Changes in deep-ocean water $\delta^{18}\text{O}$ and temperature from the Last Glacial Maximum to the present, *Paleoceanography* 2, 431-442, 1987.
- Broecker, W.S., Oxygen isotope constraints on surface ocean temperatures, *Quaternary Research* 26, 121-134, 1986.
- Broecker, W.S., Glacial climate in the tropics, *Science* 272, 1902-1904, 1996.
- Bush, A.B.G., Assessing the impact of mid-Holocene insolation on the atmosphere-ocean system, *Geophysical Research Letters* 26, 99-102, 1999.
- Cane, M.A., A.C. Clement, A. Kaplan, Y. Kushnir, R. Murtugudde, D. Podzdnayakov, R. Seager and S.E. Zebiak, 20th century sea surface temperature trends, *Science* 275, 957-960, 1997.
- CLIMAP project members, Seasonal reconstructions of the Earth's surface at the last glacial maximum, *Geol.Soc.Am. Map chart ser.* MC36, 1-18, 1981.
- Enmar, R., M. Stein, M. Bar-Matthews, E. Sass, A. Katz and B. Lazar, Diagenesis in live corals from the Gulf of Aqaba. I. The effect on paleo-oceanography tracers, *Geochimica et Cosmochimica Acta* 64, 3123-3132, 2000.
- Gagan, M.K., L.K. Ayliffe, D. Hopley, J.A. Cali, G.E. Mortimer, J. Chappell, M.J. and Head, Temperature and surface-ocean water balance of the mid-Holocene tropical western Pacific, *Science* 279, 1014-1018, 1998.
- Gagan, M.K., L.K. Ayliffe, J.W. Beck, J.E. Cole, E.R.M. Druffel, R.B. Dunbar and D.P. Schrag, New views from tropical paleoclimates from corals, *Quaternary Science Reviews* 19, 45-64, 2000.
- Graham, N.E., Simulation of recent global temperature trends, *Science* 267, 666-671, 1995.
- Guilderson, T.P., R.G. Fairbanks and J.L. Rubenstone, Tropical temperature variations since 20,000 years ago: Modulating interhemispheric climate change, *Science* 263, 663-665, 1994.
- Huber, M. and L.S. Sloan, Climatic responses to tropical sea surface temperature changes on a „greenhouse“ Earth, *Paleoceanography* 15, 443-450, 2000.
- Kinsman, D.J.J. and H.D. Holland, H.D., The co-precipitation of cations with CaCO_3 - IV. The co-precipitation of Sr^{2+} with aragonite between 16°C and 96°C, *Geochimica et Cosmochimica Acta* 33, 1-17, 1969.
- Leder, J.J., P.K. Swart, A. Szmant and R.E. Dodge, The origin of variations in the isotopic record of scleractinian coral: I. Oxygen, *Geochimica et Cosmochimica Acta* 60, 2857-2870, 1996.
- Lyle, M.W., F.G. Prahl, and M.A. Sparrow, Upwelling and productivity changes inferred from a temperature record in the central equatorial Pacific, *Nature* 355, 812, 1992.
- McConnaughey, T.A., C and O isotopic disequilibrium in biological carbonates, I, Patterns, *Geochimica et Cosmochimica Acta* 53, 151-162, 1989.
- McCulloch M.T., A.W. Tudhope, T.M. Esat, G.E. Mortimer, J. Chappell, B. Pillans, A.R. Chivas, A. Omura, Coral record of equatorial sea-surface temperatures during the penultimate deglaciation at Huon Peninsula, *Science* 283, 202-204, 1999.
- Min, R.G., R.L. Edwards, F.W. Taylor, J. Recy, C.D. Gallup and J.W. Beck, J.W., Annual cycles of U/Ca in coral skeletons and U/Ca thermometry, *Geochimica et Cosmochimica Acta* 59, 2025-2042, 1995.
- Mix, A.C., W.F. Ruddiman and A. McIntyre, Late Quaternary paleoceanography of the tropical Atlantic, 2; The seasonal cycle of sea surface temperatures, 0-20,000 years B.P., *Paleoceanography* 1, 339-353, 1986.
- Quinn, T.M., F.W. Taylor, T.J. Crowley and S.M. Link, Evaluation of sampling resolution in coral stable isotope records: A case study using monthly stable isotope records from New Caledonia and Tarawa, *Paleoceanography* 11, 529-542, 1996.
- Parker, D.E., M. Jackson and E.B. Horton, The GISST2.2 sea surface temperature and sea-ice climatology, CRTN63, Hadley Centre, Met. Office, Bracknell, U.K., 35 pp., 1995.
- Rostek F., G. Ruhland, F.C. Bassinot, P.J. Müller, L.D. Labeyrie, Y. Lancelot and E. Bard, Reconstructing sea surface temperature and salinity using $\delta^{18}\text{O}$ and alkenone records, *Nature* 364, 319-321, 1993.
- Sansone, F.J., G.W. Tribble, C.C. Andrews and J.P. Cajnton, Anaerobic diagenesis within Recent, Pleistocene, and Eocene marine carbonate frameworks, *Sedimentology* 37, 887-1009, 1990.
- Shen, C.-C., T. Lee, C.-Y. Chen, C.-H. Wang, C.-F. Dai and L.-A. Li, The calibration of D [Sr/Ca] versus sea surface temperature relationship for *Porites* corals, *Geochimica et Cosmochimica Acta* 60, 3849-3858, 1996.
- Sikes E.L. and L.D. Keigwin, Equatorial Atlantic sea surface temperature for the last 30-kyr - a comparison of Uk^{37} , $\delta^{18}\text{O}$ and foraminiferal assemblage temperature, *Paleoceanography* 9, 31-45, 1994.
- Stoll, H.M. and D.P. Schrag, D.P., Effects of Quaternary sea level cycles on strontium in seawater, *Geochimica et Cosmochimica Acta* 62, 1107-1118, 1998.
- Tribble, G.W., F.J. Sansone and S.V. Smith, Stoichiometric modeling of carbon diagenesis within a coral reef framework, *Geochimica et Cosmochimica Acta* 54, 2439-2449, 1990.
- Wellington, G.M., R.B. Dunbar and G. Merlen, Calibration of stable oxygen isotope signatures in Galapagos corals, *Paleoceanography* 11, 467-480, 1996.

M.K. Gagan, M.T. McCulloch, Research School of Earth Sciences, Australian National University, Canberra, ACT 0200, Australia

A. Müller, Department of Geology, Australian National University, Canberra, ACT 0200, Australia (amuller@geology.anu.edu.au)

(Received April 19, 2001; Revised August 7, 2001; Accepted August 16, 2001)